Dissertation

Studying *Helicobacter pylori* as a manipulator of the NKG2D stress and tumor surveillance system

submitted by
Margit ANTHOFER, MSc

for the Academic Degree of
Doctor of Philosophy (PhD)

at the
Medical University of Graz

Institute of Pathology

under the Supervision of
Assoz. Prof. Priv.-Doz. Dr.med.univ. Gregor GORKIEWICZ

2024

Statutory Declaration

I hereby declare that this thesis is my own original work and that I have fully acknowledged by name all of those individuals and organisations that have contributed to the research for this thesis. Due acknowledgement has been made in the text to all other material used. Throughout this thesis and in all related publications I followed the “Guidelines of the Medical University of Graz on Good Scientific Practice“.

January 2024.

Disclosures

Parts of this thesis have been published in

Anthofer M[1], Windisch M[1], Haller R[1], Ehmann S[1], Wrighton S[1], Miller M[1], Schernthanner L[1], Kufferath I[1], Schauer S[1], Jelušić B[1], Kienesberger S[2,3], Zechner EL[2,3], Posselt G[4], Vales-Gomez M[5], Reyburn HT[5], Gorkiewicz G[1,3]. Immune evasion by proteolytic shedding of natural killer group 2, member D ligands in Helicobacter pylori infection. Front Immunol. 2024. doi: 10.3389/fimmu.2024.1282680

[1]Institute of Pathology, Medical University of Graz, Graz, Austria

[2]Institute of Molecular Biosciences, University of Graz, Graz, Austria

[3]BioTechMed-Graz, Graz, Austria

[4]Department of Biosciences and Medical Biology, Paris Lodron University of Salzburg, Salzburg, Austria

[5]Department of Immunology and Oncology, Spanish National Centre for Biotechnology, Madrid, Spain

All co-authors have agreed to the inclusion of their published data in this dissertation.

Acknowledgements

PhD student Margit Anthofer received funding from the Austrian Science Fund FWF (W1241) and the Medical University of Graz through the PhD Program DK-MOLIN.

Many thanks to my advisor Gregor for your support throughout my PhD studies: For the inspiring and dynamic discussions, for the encouragement to think outside the box and create novel hypotheses, for sharing your profound medical and biological understanding and for your never-ending enthusiasm and the regular motivation-boosts.

To my thesis committee members Sabine and Ellen: Thank you for your support during the application for this PhD position and for providing in depth feedback and productive discussions, which were very helpful in the development of the project and the final publication.

I would like to acknowledge the Medical University of Graz and the PhD program DK-MOLIN that offered a fantastic range of opportunities to grow as a young scientist, including courses, lectures and retreats, access to cutting-edge technology, and the possibility to participate in international conferences and a research stay abroad.

My research stay in Madrid was one of the top experiences during my PhD studies. Special thanks to Mar and Hugh and all the lovely lab members (especially Ane, Carmen, Gloria, Maren and Yaiza) for making me feel welcome and as part of a family from day one. The experience of having worked in your lab is invaluable.

Countless people helped me along the way, taking their time to provide information and productive discussions. Special thanks to the super helpful people from the Institute of Pathology (especially Silvia and Christina). To Iris Kufferath for performing visualization of exosomes by electron microscopy and to Sylvia Eidenhammer for performing immunohistochemistry stainings. Many thanks to the lovely staff of ZMF and to all the colleagues who helped me with my research (particularly Ana, Barbara, Bettina, Leon, Lorenz, Marija, Markus, Matthew, Michael, Nandhitha, Onur, Philipp, Rosa, Sandra and Sebastian).To my dear colleagues and friends: Thank you from the bottom of my heart for the wonderful times inside and outside of the lab, for the fun lunches that were usually the highlight of my day and for being there for me during the difficult phases. I could not have done it without you.

Finally, big thanks go to my family for all the support you have shown me during these years. To my parents, who have supported me in my education throughout my life and who encouraged me to take on the challenge of a doctoral thesis. And to my husband, who was my tower of strength on this rocky road, thank you for your comfort and patience.

Table of Contents

Abbreviations and Definitions

α-MICA/B (anti-MICA/B neutralizing antibody)

ADAM (a disintegrin and metalloprotease)

AGS-MICA (AGS cell line transfected to express MICA)

C. acnes (*Cutibacterium acnes*)

cag (cytotoxin-associated genes)

CagA (cytotoxin-associated gene A)

CagL (cytotoxin-associated gene L)

CTL (cytotoxic T lymphocyte)

ELISA (enzyme-linked immunosorbent assay)

ER (endoplasmic reticulum)

EV (extracellular vesicle)

GPI anchor (glycosylphosphatidylinositol anchor)

H. pylori (*Helicobacter pylori*)

HpG (*H. pylori* gastritis)

IF (immunofluorescence)

IHC (immunohistochemistry)

IL (interleukin)

Isotype (isotype control antibody)

LAMP-1 (lysosomal-associated membrane protein 1)

MIC (MHC class I polypeptide-related sequence)

MICA (MHC class I polypeptide–related sequence A)

MICB (MHC class I polypeptide-related sequence B)

MIF (macrophage migration inhibitory factor)

MMP (matrix metalloprotease)

NK (natural killer)

NKG2D (natural killer group 2, member D)

NKG2D-L (NKG2D ligand)

PAI (pathogenicity island)

PD-L1 (programmed cell death 1 ligand 1)

qPCR (quantitative reverse-transcription PCR)

SCFA (short-chain fatty acid)

SFFV (spleen focus forming virus)

siRNA (small interfering RNA)

sMICA/B (soluble MICA/B protein)

T4S (type IV secretion)

TGF-β (transforming growth factor beta)

Th (T helper)

TLR (Toll-like receptor)

TM domain (transmembrane domain)

Tregs (regulatory T cells)

ULBP (UL16 binding protein)

VacA (Vacuolating cytotoxin A)

Abstract in German

Helicobacter pylori (*H. pylori*) ist ein karzinogenes Bakterium, das bei der Hälfte der Weltbevölkerung den Magen besiedelt. Das Bakterium nutzt zahlreiche Strategien, um die Immunität in der Schleimhaut zu dämpfen und so seine Persistenz im Magen zu erleichtern. Diese Persistenz-Strategien scheinen mit der Karzinogenese verknüpft zu sein, denn eine geschwächte Immunität kann Krebsentstehung begünstigen, indem transformierte Zellen der Immunerkennung entgehen und sich ungehindert zu einer Malignität entwickeln können. In diesem Zusammenhang hat unsere Forschungsgruppe zuvor Hinweise darauf gefunden, dass *H. pylori* das NKG2D System, ein wichtiges System zur Erkennung von Schleimhautstress, manipulieren könnte. NKG2D-Liganden werden von Epithelzellen während einer Infektion oder malignen Transformation exprimiert und können über den Rezeptor NKG2D von natürlichen Killerzellen (NK) und zytotoxischen T-Lymphozyten (CTLs) erkannt werden. Die Rezeptor-Liganden-Bindung aktiviert die Zytotoxizität der Lymphozyten, was zur Eliminierung der Liganden-exprimierenden Zellen führt. Ziel dieser Studie war es herauszufinden, ob und wie *H. pylori* das NKG2D-System beeinflusst. Die Analyse von menschlichem Magengewebe zeigte, dass NKG2D-exprimierende Zelltypen bei *H. pylori*-Gastritis trotz starker Immuninfiltration nicht induziert wurden. Bei Gastritis war auch die Genexpression des Rezeptors NKG2D geringer, während die Gen- und Proteinexpression von NKG2D-Liganden im Vergleich zum gesunden Zustand erhöht war, was auf eine Fehlregulation des NKG2D-Systems hinweist. Verschiedene Zellkultur-Experimente ergaben, dass *H. pylori* die Transkription und proteolytische Freisetzung von NKG2D-Liganden in Magenepithelzellen induziert und, dass diese Effekte mit den *H. pylori*-Virulenzfaktoren CagA und VacA verbunden sind. Schließlich konnte durch die Verwendung einer NK-Zelllinie gezeigt werden, dass die löslichen NKG2D-Liganden, welche von *H. pylori*-infizierten Zellen freigesetzt werden, tatsächlich die zytotoxische Aktivität von Effektor-Immunzellen dämpfen. Zusammenfassend beschreibt diese Studie eine bisher unerkannte Methode der Immun-Manipulation durch *H. pylori*. Diese Immun-Umgehungs-Strategie könnte die bakterielle Persistenz erleichtern und darüber hinaus die Entstehung von Magenkrebs begünstigen. Diese Ergebnisse liefern neue Einblicke in die Wechselwirkungen von Schleimhaut-Pathogenen mit dem Immunsystem des Wirts und erweitern unser Verständnis der Immun-Umgehungs-Mechanismen von Tumoren, was die Entwicklung von zukünftigen Immuntherapie-Ansätzen vorantreiben könnte.

Abstract in English

Helicobacter pylori employs numerous strategies to dampen mucosal immunity in order to facilitate its persistence in the stomach. Impaired immunity can also favor cancer development since transformed cells might escape immune recognition and grow unimpeded to overt malignancy. *H. pylori* is a carcinogen, whose persistence strategies and gastric carcinogenesis are likely interlinked. In this context, our research group previously found indications that *H. pylori* might modulate the natural killer group 2, member 2 (NKG2D) system, an important mucosal stress-detection system. NKG2D ligands are expressed by epithelial cells during infection or malignant transformation and can be detected by natural killer (NK) cells and cytotoxic T lymphocytes (CTLs) via the receptor NKG2D. Receptor-ligand binding activates lymphocyte cytotoxicity, resulting in the elimination of ligand-expressing cells. Interestingly, a range of immune evasion strategies to avoid recognition via the NKG2D system were found in cancers and in virus infections. Here we aimed to identify, whether and how *H. pylori* might affect the NKG2D system. By analysing human stomach tissues, we found that NKG2D-expressing cell types were not induced in *H. pylori* gastritis, despite major immune infiltration. In these tissues, gene expression of the receptor NKG2D was lower, while gene and protein expression of NKG2D ligands were elevated in gastritis, compared to the healthy state, indicating a dysregulation of the NKG2D system. Using cell-culture assays, we found that *H. pylori* induced the transcription and proteolytic shedding of NKG2D ligands in stomach epithelial cells and those effects were associated with the *H. pylori* virulence factors CagA and VacA. Finally, the use of an NK cell line allowed us to demonstrate, that soluble NKG2D-ligands released by *H. pylori*-infected epithelial cells, dampened the cytotoxic activity of effector immune cells. In conclusion, this study describes a so far unrecognized method of immune manipulation by *H. pylori*. NKG2D-evasion by *H. pylori* might contribute to the chronic infection by facilitating bacterial persistence. In addition, this mechanism might drive the development of stomach cancer by enabling transformed cells to persist. These results provide new insights into the interactions of mucosal pathogens with the host immune system and advance our understanding of tumor immune escape mechanisms, which may fuel the development of future immunotherapy approaches.

1. Introduction

1.1. Helicobacter pylori

Helicobacter pylori (*H. pylori*) is a gram-negative, spiral-shaped, flagellated, microaerophilic bacterium (1). Its preferred habitat is the human gastric mucosa (2) and the earliest occurrence in humans could be traced back to about 100.000 years ago (3). Today, around half of the world's population are colonized, with varying prevalences in different countries and a general decline in prevalence in younger generations (4). Transmission commonly occurs early in life within families, especially from mother to child (5–7) and *H. pylori* typically persists in the gastric mucosa life-long (8).

1.1.1. Impact of *H. pylori* on human health and disease

H. pylori has both pathogenic and symbiotic features (9) (Figure 1). Around 10-20 % of infected persons develop gastric or duodenal ulcer disease at one point in their life and 1-2 % of infected individuals develop one of two types of gastric cancer – gastric adenocarcinoma or gastric mucosa-associated lymphoid tissue (MALT) lymphoma (10). Gastric carcinoma is the fifth most common tumor disease and the third deadliest of all tumor diseases worldwide (11). *H. pylori* is considered a major risk factor for stomach cancer and was classified as a human class-I carcinogen (10). The risk of gastric adenocarcinoma decreases after eradication treatment (12) where commonly a triple therapy is used consisting of two antibiotics and a proton pump inhibitor drug (10). However, antibiotic-resistances are becoming increasingly common and lower the efficacy of *H. pylori* eradication severely (13). In addition, recurrence is possible, either due to incomplete clearance of the infection or due to re-infection (14).

Aside from its harmful effects, *H. pylori* co-exists asymptomatically in the stomach of most infected individuals and is considered a member or the commensal microbiota (9). Although asymptomatic carriers show altered gastric histology with increased leucocyte infiltration, there is no clinical manifestation (9). The variability in clinical outcome in different individuals seems to be due to several parameters including host genetics, bacterial genetics, environmental factors and age of acquisition (15,16).

Moreover, *H. pylori* seems to act protective against a range of diseases and has been described as a late-life pathogen that may benefit humans earlier in life (17). Inverse associations were found between *H. pylori* infection and gastroesophageal reflux disease (18), Barrett esophagus (19), gastro-intestinal infections (20), allergic diseases such as hay fever (21), cutaneous allergies (21), atopic dermatitis (21), food allergy (22), early childhood asthma (16) and celiac disease (23) as well as the 2 major forms of inflammatory bowel disease – Crohn's disease (21) and ulcerative colitis (21). Concerning inflammatory bowel diseases, there is experimental data from mouse models confirming *H. pylori's* protective role, with *H. pylori* infection and regular doses of *H. pylori* extracts protecting against severe disease (24). With respect to asthma, experimental data from mouse models confirmed that *H. pylori* infection efficiently protects from allergic airway inflammation via the induction of highly suppressive regulatory T cells (Treg) in the lung (16). The *H. pylori* virulence factor vacuolating cytotoxin A (VacA) was shown to be important for creating a tolerogenic environment that facilitates Treg differentiation (25). Interestingly, the age of *H. pylori* acquisition was relevant, since only neonatal infection, but not infection of adult mice, resulted in protection against asthma (16).

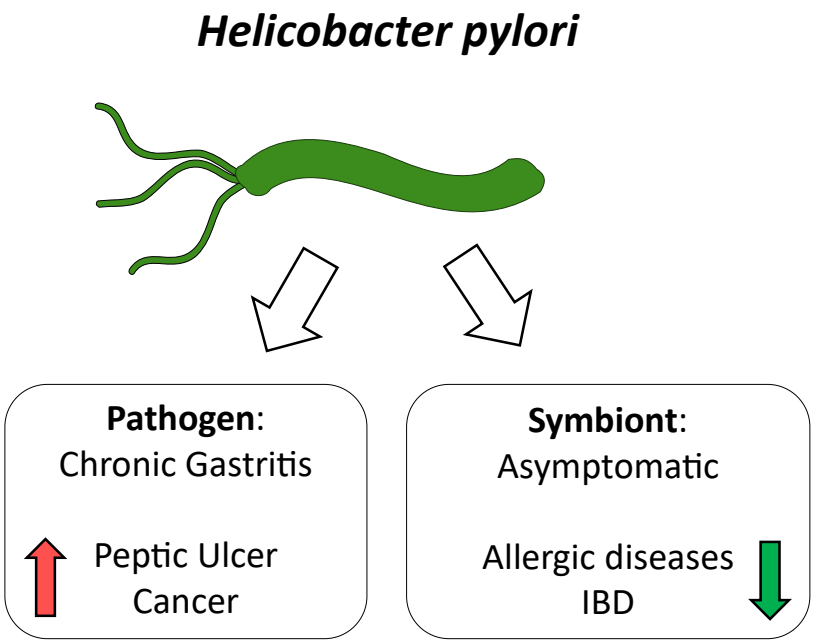

Figure 1. The two-sided role of *H. pylori* in human health and disease. *H. pylori* is considered a pathogen since it causes chronic gastritis (=infiltration of leucocytes into the gastric lamina propria) in all infected individuals and is a major risk factor for developing peptic ulcers and stomach cancer. On the other hand, chronic gastritis remains asymptomatic life-long in most infected persons and infection

protects from a range of diseases including allergic diseases and inflammatory bowel diseases (IBDs). This image was created with Microsoft PowerPoint and contains elements from Servier Medical Art (https://smart.servier.com/), adapted with permission through the Creative Commons Attribution licence CC-BY, version 4.0 (https://creativecommons.org/licenses/by/4.0/).

1.1.2. Infection process, virulence factors and strains

To escape the acidic environment of the stomach lumen, *H. pylori* penetrates the mucous layer. For this process, *H. pylori* uses its flagella, that confer extraordinary mobility (26) and the specific *H. pylori* enzyme, urease, that hydrolyzes urea into ammonia and carbon dioxide and thereby neutralizes the pH in the area surrounding the bacterium (27). *H. pylori* colonizes directly at the surface of the stomach epithelium where it adheres with a large range of adhesins and produces several virulence factors that modulate host cells (2). A great number of *H. pylori* virulence factors are known. CagA and VacA are the two best studied virulence factors and the risk for cancer development is mainly associated with the presence and allelic variant of these two virulence factors (10,28). Various *H. pylori* strain types exist across the world and they are mainly distinguished by the presence and allele type of the major *H. pylori* pathogenicity factors VacA and CagA (29).

1.1.3. Vacuolating cytotoxin A (VacA)

The vacuolating cytotoxin A (VacA) is secreted by *H. pylori* and inserted into host cells by a pinocytic-like mechanism (30). VacA is a pore-forming toxin – it inserts into lipid bilayers and forms anion-selective membrane channels (31). The typical phenotype caused by VacA is vacuolation of *H. pylori*-infected cells which is believed to be a result of swelling of intracellular endosomes due to an osmotic imbalance after channel-formation by VacA (32). In addition, this function leads to the release of cytochrome c from mitochondria which induces cell apoptosis (33). VacA also contributes to epithelial barrier disruption (34) and binds to cell-membrane receptors which leads to the initiation of a pro-inflammatory response (33). Notably, VacA was also shown to directly affect lymphocytes. It inhibits activation and proliferation of T helper cells and B cells and thereby helps to escape the adaptive immune response (35,36). Overall VacA is associated with severe clinical outcomes, such as peptic ulcer and gastric cancer (37). All *H. pylori* strains carry the *vacA* gene, indicating its relevance for infection, but

differently pathogenic *vacA* alleles exist. Genetic variations were found in the signal region (genotypes s1 and s2) and in the mid region (genotypes m1 and m2) and in the intermediate region (genotypes i1 and i2). The alleles s1, m1 and i1 are associated with an increased risk for gastric carcinoma (38–41).

1.1.4. Cytotoxin-associated gene A (CagA) and the *cag*-pathogenicity island (PAI)

The cytotoxin-associated gene A (CagA) is encoded in the *cag*-pathogenicity island (PAI), a 40-kilobase genomic region, and is translocated into host cells by a type IV secretion system (T4SS) that is encoded in the same PAI (28). The typical phenotype caused by CagA is the hummingbird phenotype, which is an elongated shape of *H. pylori*-infected cells (42). CagA also affects tight junctions, cellular polarity, cell motility, proliferation and differentiation, cell scattering, cell signaling and pro-inflammatory cytokine secretion (2,43,44–51,52–54). Additionally, CagA supresses apoptosis, which is frequently used by epithelia as a defence mechanism against infections (55) Thereby CagA contributes to establishing chronic *H. pylori* persistence. Notably, CagA was directly linked to tumor formation (56) and therefore the *cagA* gene is considered an oncogene.

The *cag*-PAI with the *cagA* gene may be absent or present in *H. pylori* strains. Strains encoding the *cag*-PAI and CagA are more prevalent in East Asian countries (28) and are more virulent. CagA-positive individuals have more severe courses of gastric inflammation and gastroduodenal ulcer disease and develop gastric adenocarcinoma more frequently (29). In addition, differently virulent *cagA* alleles exist with variations in copy number and sequence of the EPIYA motifs (28) and East-Asian-type CagA is more virulent than Western-type CagA (57). Interestingly, the *cagA* positive strains are also most strongly related to protection against diseases. For instance, infection with *H. pylori*, especially *cagA* positive strains, was inversely related to asthma and allergic rhinitis, especially for childhood onset, in a study using data from more than 7000 adults (58). In another study of approximately 500 adults, colonization with *cagA* positive *H. pylori* strains was also inversely associated with asthma and was associated with an older age of asthma onset (59). The authors hypothesize, that the protective effects associated with *cagA* positive strains are due to the fact that these strains interact most strongly with the human host (60). This would be in accordance with the ‘hygiene hypothesis’ in that extensive contact with microbes during early childhood may modulate the equilibrium of T

helper cell responses and drive the induction of immunoregulatory lymphocytes that prevent immune hyperreactivity states (58).

Cag-PAI-associated pathogenicity is not only conferred by CagA but also by the other PAI-encoded proteins – for instance, by CagL, the protein at the tip of the T4SS. CagL binds to the host transmembrane receptor α5β1 integrin (61). This interaction is critical for CagA translocation (61), but also induces aberrant signaling within host cells (62), induces pro-inflammatory cytokine secretion (63), and activates the metalloprotease A disintegrin and metalloprotease 17 (ADAM17), contributing to transient hypochlorhydria (64).

1.1.5. Impact of *H. pylori* on the immune system

H. pylori colonizes directly at the surface of the stomach epithelium, underneath the protective mucous-layer (2). This close contact with the epithelial cells triggers a strong immune response with heavy leucocyte infiltration in the lamina propria (2). The infiltrate consists of abundant plasma-, B- and both pro-inflammatory CD4+ T cells (e.g., T helper cells Th1, Th17) and anti-inflammatory CD4+ T cells (e.g., Tregs). Individual compositions of these leucocytes affect disease courses (65,66) – as human asymptomatic carriers and mice infected during the neonatal period show high numbers of Tregs and low numbers of Th1 and Th17 while patients with clinically overt peptic ulcer disease and mice infected at an adult age show low numbers of Tregs and enhanced numbers of Th1 and Th17 cells (67–69). Higher Treg numbers were associated with lower gastric immunopathology (67–69) and the Treg-derived cytokines interleukin 10 (IL-10) and transforming growth factor β (TGFβ) were critical for preventing T-effector cell driven immunopathology (69). Despite the profound inflammatory response, the immune system is usually unable to clear the infection, because *H. pylori* employs an arsenal of immune evasion strategies (2). For instance, *H. pylori* produces pathogen-associated molecular patterns (PAMPs) that have evolved to avoid recognition by Toll-like receptors (TLRs). These PAMPs include *H. pylori* lipopolysaccharide (LPS), which is not detected by TLR4 due to specific lipid A modifications (70) and *H. pylori* flagellin, which is resistant to detection by TLR5 due to mutations in the TLR5 binding site (71). *H. pylori* DNA is enriched in the sequence 5'TTTAGGG that induces anti-inflammatory signaling via TLR9 (72). In fact, *H. pylori* DNA may be applied therapeutically for in mice, oral administration of purified DNA alleviated experimentally induced inflammatory bowel disease, and this effect was attributed to the unique immunoregulatory sequence stretch (73,74). *H. pylori* also survives

phagocytosis by neutrophils and macrophages, modifies the expression of immunomodulatory proteins (e.g. Programmed death-ligand 1, PD-L1 and TGFβ) in stomach epithelial cells and modulates the activation, proliferation and differentiation of certain lymphocytes (2,10,75). With this collection of immune escape strategies, *H. pylori* ensures its own survival and chronic persistence at the surface of the stomach epithelium (2,76). In addition to promoting bacterial persistence, anti-inflammatory mechanisms can also protect from immunological diseases, as it was shown for instance for asthma (2,21). Moreover, immunosuppression by *H. pylori* may also facilitate cancer development, since transformed cells may escape immune surveillance and outgrow to overt malignancy. The major effector cell types for the early detection and eradication of transformed cells are natural killer (NK) cells and cytotoxic T lymphocytes (CTLs). The role and modulation of these cell types in *H. pylori* gastritis is not well understood so far (65).

1.2. NK cells

NK cells represent 5–20% of peripheral blood lymphocytes and their life cycle takes several weeks wherein they differentiate from highly proliferative cytokine producers towards less proliferative cytolytic effectors. They act at the interface between innate and adaptive immunity and are well-established for their essential role in the control of tumor development and virus infections (77,78). CTLs are the most extensively studied and best understood anti-tumor effectors and the major target of current anti-tumor immunotherapies. However, NK cells are emerging as novel promising targets for the next wave of immunotherapies. In contrast to CTLs, NK cells do not require antigen-presentation via major histocompatibility complex (MHC) class-I for their activation but rather detect the absence or presence of self-proteins by a range of different receptors (79) (explained in more detail in section 1.2.3.). Thus, unlike CTLs, NK can kill MHC class-I-deficient tumors. In addition, NK cell-derived cytokines and chemokines promote tumor inflammation and CTL infiltration (78).

To kill target cells, NK cells release the contents of lytic granules, which contain effector proteins such as perforin, granzymes and granulysin, in a directed manner towards their target cell. Perforin binds to the target cell membrane and forms pores which allow the entry of granzymes. Granzymes are a family of closely related serine proteases that induce caspase activation, mitochondrial dysfunction, or caspase-independent apoptosis. Granulysin has pore-

forming activity, which alters membrane permeability and results in osmotic lysis and mitochondrial damage. Together these effects rapidly lead to apoptosis of the target cell (80).

1.2.1. NK cells in bacterial infection

Accumulating evidence demonstrates that, beside their well-established role in anti-tumor and anti-virus immunity, NK cells are also important in the fight against bacterial infections by detecting bacterial infection, by contributing to inflammation via secreting interferon gamma (IFN-γ), by activating monocytes and macrophages and by killing bacteria-infected cells and bacteria directly (81–84). For instance, mice depleted of Thy1+NK cells showed reduced IFN-γ production and increased bacterial burden during *Salmonella typhimurium* infection. In contrast, repopulating mice lacking T, B and NK cells with IFN-γ competent NK cells improved control of *S. typhimurium* infection (85). In pulmonary *Staphylococcus aureus* infection of mice, NK cells were elevated and increased phagocytosis of *S. aureus* by lung macrophages while mice depleted of NK cells were more susceptible to staphylococcal infection (86). *In vitro,* NK cells killed *Mycobacterium tuberculosis*-infected monocytes (87) as well as mycobacteria directly (88). Direct killing of mycobacteria was contact dependent and mediated by perforin and granulysin that disrupted mycobacterial cell-wall integrity. The process was mediated via NKG2D and NCRs (NKp30, NKp44, and NKp46), suggesting that NK cells use similar cellular mechanisms to kill both bacterial pathogens and target host cells (88). NK cells can detect bacterial products via TLRs (79). In addition, it was recently discovered that the activating NK cells can be activated to degranulation via the NK cell receptor KIR2DS4 that recognizes a highly conserved sequence motif in bacterial recombinase A (RecA) from multiple human pathogens, including *Helicobacter pylori* (89).

1.2.2. *H. pylori's* effect on NK cells

H. pylori is known to impair macrophages, dendritic cells and T- and B-cells (2,76,90). However, little is known about the activity and killing potential of NK cells during *H. pylori* infection and whether *H. pylori* modulates NK cell function. The response of NK cells to *H. pylori* appears to be either positive or negative, depending on the type of antigenic challenge. Direct stimulation of NK cells with live *H. pylori* or different *H. pylori* preparations (lysate,

glycine extract, glutaraldehyde-fixed) increases the production of IFN-γ, granzyme B (GrB) and perforin (PRF1) (91), augments NK cell cytotoxicity (92), and induces the expansion of CD25+ NK cells (93). *H. pylori* lipopolysaccharide (LPS), however, downregulates IFN-γ expression (93), and perforin production by NK cells (94), and cytotoxicity of peripheral blood mononuclear cells (PBMC) (93,95). The indirect modulation of NK cells via *H. pylori*-stimulated monocytes or dendritic cells may be either activating (96), or inhibiting (97). *In vivo*, *H. pylori* infection was associated with either unchanged (91), or increased (98) numbers of NK cells in the gastric mucosa and a reduced natural cytotoxic activity of peripheral lymphocytes (95). In summary, the role of NK cells in *H. pylori* gastritis is not well understood and further research is required.

1.2.3. Activation and inhibition of NK cells

In contrast to T cells, NK cells are not regulated by one central activation complex, such as the T cell receptor (TCR), but instead integrate signals from multiple receptors. The balance of these signals leads to either inhibition or activation of an NK cell, wherein activating signals tend to overcome inhibitory signals (79). Inhibitory NK cell receptors, detect classical and non-classical MHC-I molecules and inhibit cytotoxicity. A loss of MHC-I expression, which frequently occurs in tumors, abrogates this inhibition, and allows self-reactivity (so-called 'missing-self' induced activation). Inhibitory NK cell receptors include the killer-cell immunoglobulin-like receptors (KIRs) of the immunoglobulin superfamily (Ig-SF) and NK group 2 member A (NKG2A) of the C-type-lectin-domain family (CTLD). Activating NK cell receptors detect ligands which are absent from healthy cells but induced on stressed, infected or transformed cells (so-called 'induced-self or 'altered-self'). Detection of these ligands activates cytokine secretion and/or NK cell degranulation, which is a polarized release of the contents of lytic granules toward target cells for direct killing. The best studied activating NK cell receptors are natural cytotoxicity triggering receptor 1 (NCR1/NKp46), natural cytotoxicity triggering receptor 2 (NCR2/NKp44) and natural cytotoxicity triggering receptor 3 (NCR3/NKp30), that belong to the immunoglobulin superfamily (IgSF) and the NK group 2 member D (NKG2D) receptor, that belongs to the C-type lectin domain (CTLD) family (77,79,99).

In addition to these NK-cell receptors, NK cells express toll-like receptors (TLRs) for the detection of bacterial or viral products and the Fc fragment of IgG, low affinity IIIa, receptor

(CD16a) to recognize immunoglobulin G (IgG) antibodies and trigger antibody-dependent cell-mediated cytotoxicity (ADCC) (79).

Under pathological conditions NK cells may induce the expression of immune checkpoints such as programmed cell death protein 1 (PD-1), T cell immunoreceptor with Ig and ITIM domains (TIGIT), T-cell immunoglobulin and mucin-domain containing-3 (TIM-3) and lymphocyte-activation gene 3 (LAG3) (78,79). Tumor cells often express ligands for these immune checkpoints and thereby inhibit T- and NK cells, favoring immune escape. Another strategy of tumors and viruses to impair NK cell function is the soluble release of ligands for activating NK cell receptors. In contrast to cell-associated ligands, these soluble ligands decrease NK cell function. This immune evasion strategy was demonstrated for the cluster of differentiation 226 (CD226/DNAM-1) ligand CD155 (100), and for the NKp30 ligands BAG6 (101) and B7-H6 (102,103), and was most extensively studied for the ligands of the receptor NKG2D (104).

1.3. NKG2D/NKG2D-L axis

NKG2D is one of the best characterized activating NK cell receptors. It is expressed on the surface of most human natural killer (NK) cells and also on γδ T cells and CD8+ αβ T cells (105,106). The receptor is highly conserved and recognizes an extensive repertoire of NKG2D ligands (NKG2D-Ls), that are MHC class I-related proteins (107). NKG2D-Ls are absent or expressed intracellularly in healthy tissues (108,109). Especially in the gastric, small intestinal and large intestinal mucosa relatively strong NKG2D-L expression was found in biopsies from healthy individuals and was confined to surface and glandular epithelial cells (108). NKG2D-Ls are upregulated and expressed at the cell surface in stressed conditions such as microbial infection (106,110,111) and oncogenic transformation (112). Binding of the NKG2D receptor to cell-surface NKG2D-Ls activates NK cell cytotoxicity that results in the killing of the ligand expressing cells (105). In CTLs, the binding of NKG2D to cell-associated NKG2D-Ls co-stimulates TCR-mediated cytotoxicity (106,110,113) (Figure 2A). NKG2D-deficient mouse models spontaneously develop cancer, much more than wild type mice (114), and in colorectal cancer patients, high NKG2D-L expression is associated with better prognosis (115). Thus, the NKG2D/NKG2D-L axis is an effective stress- and tumor surveillance system (104).

1.3.1. Regulation of the NKG2D receptor by cytokines

NKG2D receptor expression levels are upregulated in the presence of the cytokine interleukin 15 (IL-15) (104). IL-15 is produced by macrophages, monocytes and non-lymphoid cells and triggers excessive lymphocyte activation (104). Two alternatively spliced transcript variants of IL-15 have been reported, the long signal peptide isoform (IL-15 LSP) and the short signal peptide isoform (IL-15 SSP) (116) – their precise roles are so far unknown. In addition, expression of the NKG2D receptor was also shown to be regulated by other cytokines: IL-2, IL-7, IL-12, and type I interferons (IFNs) were found to increase NKG2D surface expression, whereas IL-21, IFN-γ, and TGFβ were shown to reduce NKG2D expression (107,117). However, the main regulators of NKG2D expression are NKG2D ligands (118).

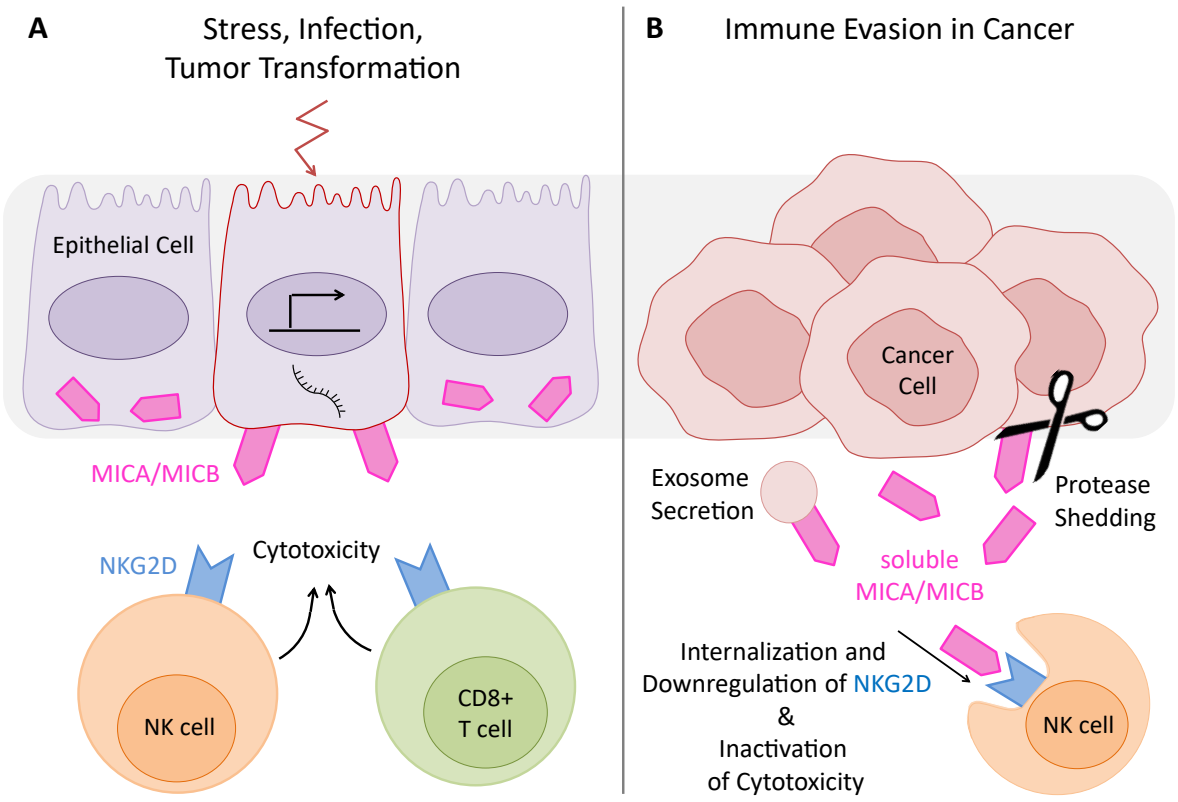

Figure 2. Scheme representing the NKG2D/NKG2D-L axis. (A) Activation of the NKG2D/NKG2D-L axis: During conditions of stress such as viral infection, certain bacterial infections or tumor transformation, epithelial cells upregulate expression of ligands for the natural killer group 2 member D (NKG2D) receptor and express them at their cell surface. NKG2D is typically expressed by NK cells and CD8+ T-cells. Interaction between receptor and ligand triggers a cytotoxic response of the effector cells that results in the degradation of ligand expressing cells. (B) Evasion of the NKG2D/NKG2D-L

axis in cancer: Cancer cells often evade NKG2D-mediated immunity by releasing NKG2D-Ls as soluble proteins, via proteolytic shedding or via exosomes. Binding of soluble NKG2D-Ls to the NKG2D receptor leads to internalization of NKG2D, downregulation of NKG2D expression and overall functional impairment of NK cells and CTLs. This image was created with Microsoft PowerPoint and contains elements from Servier Medical Art (https://smart.servier.com/), adapted with permission through the Creative Commons Attribution licence CC-BY, version 4.0 (https://creativecommons.org/licenses/by/4.0/).

1.3.2. NKG2D Ligands (NKG2D-Ls)

Human NKG2D ligands are grouped into two families: The cytomegalovirus UL16-binding protein (ULBP) family of which there are 6 variants (ULBP1-6) and the MHC class I polypeptide related sequence protein family of which there are two variants – the MHC class I polypeptide-related sequences A (MICA) and the MHC class I polypeptide-related sequences B (MICB) (104). ULBP genes are clustered on chromosome 6 and are gene orthologues of the mouse NKG2D-Ls including five different isoforms of retinoic acid early inducible-1 (RAE-1) proteins, one murine UL16-binding protein-like transcript 1 (MULT1) protein, and three different isoforms of H60 proteins (119).

1.3.3. MICA and MICB genes

The genes for MICA and MICB are located 40 and 110 kb centromeric to HLA-B (major histocompatibility complex, class I, B) (120) in the MHC-class I locus of the 3.6 megabase human MHC region on the short arm of chromosome 6 (121). The MHC region contains numerous polymorphic and multicopy genes (122). Seven MIC genes have been identified, of which only MICA and MICB genes encode expressed transcripts, whereas MICC, MICD, MICE, MICF and MICG are pseudogenes (120,123). MICA and MICB are closely related, sharing 91% identity in their coding sequences (120) and originate from a gene duplication event that occurred 14.1 million years ago, similar to MHC-B and MHC-C, which are a product of a duplication event that occurred 22.3 million years ago (124). Gene duplication is common and is proposed to generate evolutionary advantage by the acquisition of new and diversified functions (125). MIC genes are highly conserved, and are present in humans, primates, dogs, goats, cows and pigs, but not in mice or rats (120). Similar to MHC-class-I

genes, MICA and MICB are highly polymorphic (126) with 531 and 244 distinct sequence alleles currently assigned for MICA and MICB, respectively (http://hla.alleles.org/alleles/classo.html, March 2023). MIC polymorphism was shown to affect transcriptional regulation (127), NKG2D-binding affinity (128), as well as protein trafficking and secretion (129,130) and was associated with genetic predisposition for multiple diseases such as autoimmune diseases including celiac disease (131) and ulcerative colitis (132) and multiple types of cancer, including gastric adenocarcinoma (122).

1.3.4. MICA and MICB proteins

MIC proteins are membrane-bound polypeptides of about 383 amino acids, with a relative molecular mass of about 43 kDa (120). MIC proteins show homology with MHC class I chains and have a similar domain structure, including three extracellular domains (α1–3), a transmembrane domain and a cytoplasmic tail (120). Unlike MHC class I chains, which bind an intracellular peptide-antigen in a deep groove between the α1 and α2 domains, MIC proteins do not bind a peptide (133) and the groove between the α1 and α2 domains is too narrow (134). Nevertheless, the top surface of the α1α2 domain platform interacts directly with NKG2D, analogous to the interaction seen in T cell receptor-MHC class I protein complexes (128,135). ULBP proteins also contain the two domains analogous to α1 and α2 of MHC I proteins but do not contain an α3-like domain (119).

1.3.5. Regulation of MICA and MICB protein expression

On normal, healthy tissues, MIC proteins are either absent or expressed intracellularly, for example in epithelial cells of the gastrointestinal-, respiratory- and urinary tract (108,109,136). In the gut, the expression of NKG2D-ligands seems to be kept in check by the commensal microbiota (137). Stressed conditions such as microbial infections (106,110,111) and oncogenic transformation (112) induce the *de novo* expression or upregulation of MIC proteins. The molecular mechanisms leading to this induction are versatile and far from being completely understood. Infection and tumorigenesis trigger cellular stress response mechanisms such as oxidative stress (138), heat shock (139), and DNA-damage response (140,141). MIC expression was shown to be induced by cellular response mechanisms to

oxidative stress (142,143), heat shock (133) and DNA damage (144,145), as well as by increased cellular proliferation (143) and the detection of viral RNA (146). These mechanisms affect either MIC transcription (133,143), via binding sites for the transcription factors HSF1, Sp1 (133,143), E2F1 (145) and NFκB (147) in the MIC promoter, MIC mRNA stability (148), via modulation of RNA-binding proteins (148,149) and micro-RNAs (150), or cell surface localization of MIC proteins (136). Interestingly, there are some differences between MICA and MICB sequences, which result in differential regulation. The promoter regions of MICA and MICB harbor several different elements (143), and a frequent polymorphism in the MICB promoter diminishes binding of the transcription factor Sp1 and consequently decreases MICB gene expression (127). Also, at the level of mRNA stability, MICA and MICB mRNA are regulated differentially. The mRNA of MICB has a 1000 nucleotide longer 3'untranslated region (UTR), which is an important site for RNA regulation (151). Several RNA-binding proteins (149), cellular miRNAs (152,153) and viral miRNAs (154,155) were shown to affect only the expression of MICB. In contrast, the 3'UTR of MICA can switch from a short to a long version via alternative polyadenylation, affecting MICA mRNA stability (156). Differences between MICA and MICB were also observed at the level of cell surface localization and membrane turnover (157,158). It is common that expression levels of different NKG2D ligands differ within one cell line (157,159).

1.3.6. Evasion of the NKG2D axis

The stress-induced expression of NKG2D ligands is critical for antimicrobial and antitumor immunity (104). However, due to selective pressure, tumors undergo immunoediting (160) and often evolve mechanisms to avoid recognition by NKG2D (161), like the selection of tumor cell clones with reduced NKG2D-L surface expression (114,162). Also, pathogens have evolved various mechanisms to escape NKG2D-mediated immunity, most importantly the herpesviruses human cytomegalovirus (HCMV) (154,163–165), Epstein–Barr virus (EBV) (155) and Kaposi's sarcoma-associated herpesvirus (KSHV) (155,166), the hepatitis viruses hepatitis B virus (HBV) (167) and hepatitis C virus (HCV) (168) as well as the human immunodeficiency virus (HIV) (169) and severe acute respiratory syndrome coronavirus type 2 (SARS-CoV-2) (170). Evasion strategies aim at the reduction of MIC cell surface expression, either by retention inside the cell (171) or by soluble release of MICA (172,173) and MICB (174,175). Retention inside the cell is modulated by microRNAs (154,155) and proteins

(164,165) that bind MIC mRNA or proteins. Soluble release is achieved by proteolytic cleavage of the extracellular domain of MICA (173,176) or MICB (175) by metalloproteases, or by the release via exosomes (130).

1.3.7. Effects of the soluble release of MICA/B

The soluble release of MIC proteins has two effects. Firstly, it reduces the cell surface expression of MIC proteins (173) and thereby diminishes the immunological visibility of these cells (177). Secondly, soluble MIC proteins act as repressors of NKG2D. Their binding to the receptor results in the internalization and degradation of NKG2D and thereby reduces NKG2D-mediated immunity of NK cells (178) and CTLs (172) (see Figure 2B). In addition, chronic exposure to MICA reduces the responsiveness of the TCR and the activating NK cell receptors CD16, NKp46, and NKp30 through degradation of T-cell surface glycoprotein CD3 zeta chain (CD3ζ), a key intracellular signaling component in NK and T cells (179). As a result, soluble MIC release does not only protect the individual MIC-expressing cell from eradication, but leads to a profound functional impairment of NK and CD8+ T cell activity. Thus, NKG2D has been proposed as a master regulator of NK and CD8+ T cells responsiveness (180). Soluble MIC proteins are detected in the sera of patients with virus infection (181,182), premalignant disease (183,184) and cancer (172,173,181,183,185–189) and frequently correlate with certain allelic variants (181,187). In cancer, high sMICA/B levels correlate with a systemic reduction of NKG2D expression and a reduction of NK and T cells function (172,183,186,188,189) and also correlate with higher cancer stage and metastasis (185) and poorer prognosis (187). Currently, several efforts are underway in the development of cancer immunotherapies in order to overcome NKG2D-evasion strategies and exploit the NKG2D-axis as an efficient tool for cancer eradication (151,190–192).

1.3.8. Proteolytic shedding of MICA/B

Proteolytic release of soluble MICA and MICB was attributed to proteases of the A disintegrin and metalloproteinase (ADAM) family and the matrix metalloproteinase (MMP) family. ADAMs are membrane-anchored multidomain proteins that are zinc-dependent and proteolytically cleave a large range of target proteins spanning adhesion molecules,

extracellular matrix proteins, growth factors and cytokines. ADAM proteases are involved in numerous cellular processes including signaling, adhesion and migration. 22 functional ADAMs have been identified in humans, of which 12 have proteolytic activity (193). MMPs are also zinc-dependent proteases and are classified into two groups – the soluble MMPs and the membrane-attached MMPs. The proteolytic targets of MMPs include extracellular matrix proteins and cell surface bound proteins. Their functional repertoire covers processes as diverse as cell proliferation, differentiation, migration, adhesion, apoptosis, tissue repair and host defense as well as pathological processes such as morphogenesis, angiogenesis and metastasis. The MMP family in humans consists of 23 members (194).

Regarding the release of soluble MICA and MICB, the metalloproteases MMP9 (195,196), MMP14 (197), ADAM9 (198), ADAM10 (199–201) and ADAM17 (175,199,200) have been implicated. Which one of these metalloproteases is responsible seems to vary depending on cell line, tissue type and stimulus. The most frequently identified and best studied metalloproteases, in the context of MICA and MICB shedding, are ADAM10 and ADAM17. These two metalloproteases are essential during early development which is reflected by the embryonic lethality in knock-out mice. In addition, ADAM10 and ADAM17 play important roles in inflammation and tumorigenesis, including migration and proliferation in metastatic tumors (202,203).

MIC shedding requires that endoplasmic reticulum protein 5 (Erp5) associates with MIC at the cell surface and induces a conformational change that enables proteolytic cleavage (204). The binding site for Erp5 is a six-amino acid motif in the α3 domain of MIC that is conserved among all MICA and MICB alleles (205). Cleaved MIC encompasses the three extracellular domains (173,206). The site of MIC cleavage is the stalk region between the α3 domain and the transmembrane domain. Proteases do not recognize a specific sequence motif but rather are sensitive to shortenings of the stalk region (199). Further details and a graphical scheme describing MIC shedding are provided in section 3.8 and Figure 22.

1.3.9. Extracellular vesicle release of MICA

Extracellular vesicles (EVs) are cell-derived membranous structures. The ability to release membrane vesicles is conserved through evolution and all types of cells are believed to secrete them (207–209). Formerly, these vesicles were thought to serve to eliminate unneeded

waste from the cells. However, we know now that cells can actively tune the secretion of EVs, depending on their physiological condition and release vesicles with a defined cargo (210). EVs may contain proteins, lipids and genetic material and serve as a means of intercellular communication in normal cell homeostasis and in pathological processes (210–212). Several subtypes of EVs exist, differing in their subcellular origin, means of release, size and composition. The two main types are exosomes and microvesicles (213). Exosomes are 30-150 nm in diameter (214), and originate from the endosomal system through inward budding of endosomal membranes leading to the formation of multivesicular endosomes (MVEs). Exosomes are released when multivesicular endosomes fuse with the cell surface (213). Microvesicles typically have a size of 100 nm up to 1 μm (214), but are sometimes even larger (up to 10μm) (213). These vesicles are formed directly at the cell surface through outward budding of the membrane (213).

MICA and MICB are not released on EVs except for one particular MICA allele: MICA*008 which is found in 20-55% of humans with varying frequencies in different populations (126,215–218). This frequent MICA allele does not have a transmembrane (TM) domain like all other known MICA and MICB alleles, but is truncated due to a single nucleotide insertion in the exon encoding the TM region, resulting in a frame shift, leading to an early stop codon (215). Unlike other MICA alleles, this allele is synthesized in the endoplasmic reticulum (ER) as a soluble protein that attaches to the membrane via a glycosylphosphatidylinositol (GPI) anchor, similar to the NKG2D ligands ULBP1-3 and 6 (215,219). It is not susceptible to metalloprotease-mediated shedding, but is released on EVs, specifically on exosomes (130). Exosome-associated MICA*008 reduces NKG2D expression and effector cell cytotoxicity more effectively than soluble MICA (215). Several other differences between MICA*008 and full-length MICA alleles were identified: While full-length MICA is found at the basolateral side, MICA*008 is associated with the apical membrane of polarized cells, which might affect signaling processes. MICA*008 is not susceptible to several pathogen evasion strategies that target MICA and MICB, suggesting that this allelic version might have expanded in response to these evasion strategies (215). Curiously, additional evasion strategies specifically target MICA*008, indicating the complex co-evolution of pathogens and immunosurveillance mechanisms (220). There are also differences between MICA*008 and full-length MICA alleles concerning several diseases: For instance, in systemic lupus erythematosus, celiac disease, insulin-dependent diabetes mellitus and Addinson's disease MICA*008 was associated with greater risk of disease while the MICA alleles A6 and A9 (both full-length alleles)

appeared to be protective (221). Taken together, NKG2D-L polymorphism and the differential means of ligand release are associated with numerous aspects of human health and disease.

1.4. Hypothesis: *H. pylori* and the NKG2D axis

H. pylori is a cancerogenic microbe that has adapted extremely well to life in the human host and has developed numerous immune evasion strategies. The NKG2D/NKG2D-L axis is important for mucosal immunity and immunosurveillance but is a frequent target of immune evasion strategies. Little is known about the regulation of the NKG2D/NKG2D-L axis during *H. pylori* infection and chronic gastritis. Only one research group, beside ours, has analyzed the regulation of NKG2D-Ls in *H. pylori* infection: Hernández et al. recently demonstrated that heat-killed *H. pylori* upregulates NKG2D ligand expression on gastric adenocarcinoma cells (222). In a previous study, our group observed an induction of NKG2D ligands in the gastric mucosa of *H. pylori* gastritis patients. However, a corresponding induction of NKG2D expression was lacking in these patients (223). This observation prompted us to hypothesize, that *H. pylori* might induce an NKG2D-evasion strategy. This could contribute to the hypofunctional immunity in the stomach mucosa during *H. pylori* infection which allows for chronic bacterial persistence and facilitates tumor development in *H. pylori*-infected persons.

NKG2D-evasion by pathogens and tumors is often achieved by the release of soluble NKG2D-Ls. Researching the existing literature we found that *H. pylori* was shown to activate the metalloprotease ADAM17 at the cell surface via an interaction of CagL – the protein at the tip of the bacterial Type-4-Secretion-System – with human integrin β1 (64). ADAM17 is one of the proteases that were shown to shed the NKG2D ligand MICA (176) and activity of ADAM17 was connected to a prolonged half-live of MICA mRNA (148). Thus, we hypothesized that a possible strategy by which *H. pylori* might evade the NKG2D/NKG2D-L axis might be the induction of shedding of NKG2D-Ls via activation of the protease ADAM17.

1.5. Aim of this study

The aim of this work was to investigate the impact of *H. pylori* infection on the NKG2D/NKG2D-L axis, to identify a potential NKG2D-evasion strategy and to analyse the resulting consequences in *H. pylori*-associated pathologies. In specific, our objectives were to

determine whether *H. pylori* induces the release of soluble NKG2D-Ligands from infected gastric epithelial cells, to elucidate the underlying molecular mechanisms and the involved human and bacterial factors and to assess potential immunomodulatory effects of these soluble NKG2D-Ls on effector immune cells.

2. Materials and Methods

2.1. Human stomach biopsies

The use of human tissues was approved by the institutional review board of the Medical University of Graz (EK-23-212ex10/11). We used formalin-fixed and paraffin-embedded (FFPE) tissue samples from the Institute of Pathology at the Medical University of Graz (Appendix 1). Warthin–Starry staining (224) and immunohistochemistry (IHC) with an anti-*H. pylori* antibody (clone SP48; Ventana) were performed to detect *H. pylori* in these tissues.

2.2. Immunohistochemistry

For Hematoxylin and eosin (H&E) staining a standard protocol was performed. For immunohistochemistry, 2 µm thick tissue sections were prepared. The staining of CD45 and CD8 was performed on a Dako Omins machine. The EnVision FLEX staining system was used with EnVision FLEX TRS, High pH for 30 min at 97°C Antigen-Retrieval for CD45 and with EnVision FLEX TRS, Low pH for 24 min at 95°C Antigen-Retrieval for CD8 detection. For Blocking the EnVision FLEX Peroxidase-Blocking-Reagent was incubated for 3 min. The primary antibodies CD45 (Clones 2B11 + PD7/26, Cat# GA75161-2, Agilent Technologies, RRID: AB_2661839), CD8 (Clone C8/144B, Cat# GA62361-2, Agilent Technologies) were incubated at 36°C for 20 min. Finally, detection was performed with the EnVision FLEX HRP and the EnVision FLEX Mouse Linker.

CD56 and NKp46 staining was performed with the Ventana system. For CD56 CC1 Standard (Ventana) was used at 95°C for 32 min, for NKp46 CC1 Standard (Ventana) was used at 95°C for 64 min. The CD56 antibody (clone MRQ42; 760-4596, Ventana Medical Systems) did not require dilution and was incubated for 16 min at 36°C. The NKp46 antibody (clone 195314, MAB1850, R and D systems, RRID: AB_2149153) was diluted 1:100 and incubation

was performed for 1 h at 36°C. The ultraView Universal DAB Detection Kit (Ventana) was used for the detection of CD56 and NKP46.

For MICA/B staining, we performed antigen retrieval in sodium citrate buffer, pH 6.0, (Gatt-Koller) for 40 min in a microwave. To inhibit endogenous peroxidase activity, we incubated the section for 15 min in 3% H_2O_2 in methanol. The UltraVision LP Detection System HRP Polymer (Ready-to-use) (TL-060-HL; Thermo Scientific) was used for blocking of nonspecific protein binding and for detection. The primary MICA/B antibody (clone F-6; dilution 1:100; Santa Cruz Biotech, RRID: AB_2143751) was incubated at RT for 1 h. MICA/B staining was also performed with snap-frozen (2-methylbutane) stomach biopsy sections.

For counterstaining Mayer's hemalum solution (Merck) was used and as a mounting medium Entellan (Merck) was used. All IHC stainings, except for MICA/B, were performed by Sylvia Eidenhammer from the Institute of Pathology. Evaluation and scoring of all immunohistochemistry stainings was performed by Gregor Gorkiewicz. The lymphocyte markers (CD45, CD8, CD56 and NKP46) were scored as positive cells per 1 mm2 of the tissue section. For MICA/B, the staining intensity in epithelial cells and in the lamina propria was scored (0= absent, 0.5= very weak, 1= weak, 1.5= weak to medium, 2= medium, 2.5= medium to strong, 3= strong).

2.3. qPCR

For isolating RNA from FFPE samples (7 sections, each 5 µm thick) we used Deparaffinization Solution (Qiagen) and the RNeasy FFPE kit (Qiagen) (including a DNase treatment step). The NucleoSpin® RNA extraction kit (Machery-Nagel) or TRIzol reagent (Invitrogen), were used for the isolation of RNA from cell cultures. We used the NanoDrop™ 2000c (Thermo Fisher Scientific) for spectrophotometric determination of RNA quality and quantity. Subsequently, we performed reverse transcription using the High Capacity cDNA Reverse Transcription kit (Applied Biosystems) with the RNAase inhibitor (Applied Biosystems), according to the manufacturer's instructions. A CFX384 qPCR thermocycler (BioRad) and the SYBR® Green PCR Master Mix (Applied Biosystems) were used to perform qPCR with the following protocol: 10 min at 95°C, 39 cycles of 15 sec at 97°C and 1 min at 60°C, then 15 sec at 60°C and a melting step until 95°C. Appendix 2 shows the oligonucleotide primers that were used for qPCR in this study. We used Glycerinaldehyd-3-phosphat-

fehydrogenase (GAPDH) as a housekeeping gene. In Figures 5 and 7A, the results of qPCR are reported as –ΔCt, in all other figures the data are presented as relative expression ratio, which was calculated according to Pfaffl's method (equation 1) (225). For the calculation of the relative expression ratio we used cells harvested at time point 0 h as control group in Figures 6, 7B, 8, 9, 10, 14B, 31 and 32. In Figure 29A we used the mean of all healthy control biopsies as control group and in Figures 29B-D we used non-infected cells harvested simultaneously with *H. pylori*-infected cells as control group for the calculation of the relative expression ratio.

2.4. Cell lines

As models for human stomach epithelial cells, we used the cell lines AGS and MKN28. AGS cells (female, ATCC Number: CRL-1739, RRID: CVCL_0139) were obtained from Cell Lines Service (Eppelheim, Germany), MKN28 cells (female, RRID:CVCL_1416) were a gift from Dr. Silja Wessler (Department of Biosciences and Medical Biology, Paris Lodron University of Salzburg, Austria) and were originally obtained from the Japanese Collection of Research Bioresources (JCRB; http://cellbank.nibio.go.jp/). We cultivated both stomach epithelial cell lines in RPMI 1640 medium (Gibco), with 2 mmol/L L-glutamine (Gibco), 5 mmol/L HEPES (Gibco) and 10% fetal bovine serum (FBS) (Gibco).

For the NK cell assays we used the human natural killer cell line NKL and the chronic myeloid leukemia cell line K562. NKL cells (male, RRID: CVCL_0466) were kindly provided by Dr. Francisco Borrego (Biocruces Bizkaia Health Research Institute, Barakaldo, Spain). K562 cells (female, RRID: CVCL_0004) were obtained from ATCC (cat # CCL-243). Both cell lines were cultured in RPMI 1640 medium with 0,1 mmol/L nonessential amino acids (Gibco), 1 mmol/L sodium pyruvate (Gibco), 58 µmol/L 2-mercaptoethanol (Sigma Aldrich), 100 units/ml penicillin and 100 mg/ml streptomycin (Gibco). Additionally, NKL cells received 50 units/ml recombinant human IL-2 (Peprotech), 5% human normal serum (MP Biomedicals™) and 5% FBS (Gibco). K562 cells additionally received 10% FBS (Gibco). We incubated all cell lines in this study at 37°C in a water-saturated atmosphere with 5% CO2.

2.5. Transfection of AGS cells

AGS cells expressing MICA*019 (A5) (denoted AGS-MICA cells), were generated using

the lentiviral vector pHRSIN (226) which was a gift from Prof. Paul Lehner (Cambridge Institute for Medical Research, Cambridge, United Kingdom). This vector expresses MICA*019 under control of the spleen focus-forming virus (SFFV) promoter that provides constitutive, high-level gene expression. The MICA allelic version *MICA**019 encodes a full-length MICA protein which is expected to be prone to proteolytic shedding (215). For the generation of lentiviruses, 293T cells were transfected with three plasmids in parallel: pHRSIN, pCMVR8.91 and pMD2G and cultivated for 2 days. Subsequently, the culture media of these cells, now containing lentivirus particles, were then harvested, filtered and frozen at −80°C. For the transfection of AGS cells, we mixed 0,75 ml of lentivirus preparation with 0.3×10^6 cells and added 1 µmol/L of the TBK1 inhibitor BX795 (InvivoGen) and 8 µg/mL Polybrene (Sigma-Aldrich). The cells were seeded into one well of a 6-well plate (BD Biosciences) and the plate was centrifuged for 1 h at 33°C at 800 revolutions per minute (rpm). Afterwards, we incubated the plate for 4-6 h followed by another centrifugation for 1 h at 33°C at 800 rpm. Then the cell culture medium was replaced by fresh medium and cells were cultivated and passaged for two weeks. Finally, AGS-MICA transfectants were sorted by FACS using the Alexa Fluor® 647 anti-human MICA/MICB Antibody (BioLegend Cat# 320914, RRID: AB_2266419).

2.6. Bacteria

Dr. Silja Wessler (Department of Biosciences and Medical Biology, Paris Lodron University of Salzburg, Austria) kindly provided the *H. pylori* P12 wild type strain (expressing Western *cagA* EPIYA-ABCC, and with a *vacA* s1/m1 genotype) (227,228) and isogenic mutant strains P12 Δ*cagA*, *ΔcagL* and *ΔvacA*. For the cultivation of *H. pylori*, we used agar plates containing 10% horse serum and cultivated the bacteria at 37°C under microaerophilic conditions using GENbag Microaer (Biomérieux).

As a control we used the bacterium *Cutibacterium acnes* PA-2.2 that was kindly provided by Baltasar Mayo (Instituto de Productos Lácteos de Asturias, CSIC, Spain). *C. acnes* bacteria were cultivated on Columbia agar + 5% sheep blood (Biomérieux) plates and incubated at 37°C under anaerobic conditions using GENbag Anaer (Biomérieux) (223).

2.7. Infection assay, butyrate treatment and metalloprotease inhibition

For all infection assays in this study, cells were cultivated and treated in a similar way, followed by various methods of analysis (Figure 3). We cultivated AGS, AGS-MICA and MKN28 cells for 48 h to reach approximately 70% confluence. In parallel, we cultivated *H. pylori* strains on agar plates for 48 h. Prior to infection, we harvested the bacteria from the agar plates with cotton swaps and suspended them in fresh cell culture media. We then diluted these suspensions to a certain optical density (OD_{600}) that corresponds to an MOI of 50 and used these diluted suspensions for infection of the cells.

For infection with *C. acnes*, we cultured the bacteria for 72 h on agar plates, then inoculated a liquid culture to an OD_{600} of 0.1 and cultivated this liquid culture for 24 h. Subsequently, we used the liquid culture for infection of the cells.

As a control treatment, we used butyrate (Sigma Aldrich) at 2 mmol/L, that was shown to induce *MICA/B* expression (223,229).

For the inhibition of metalloproteases, we used batimastat (BB94 (Sigma Aldrich), a well-known broad-spectrum inhibitor of MMPs and ADAMs. We diluted batimastat at 10 µmol/L in DMSO (175) and applied it simultaneous with *H. pylori* infection or butyrate treatment. DMSO was added alone to cultures as a solvent control.

After infection and/or treatment, cells were cultivated for up to 72 h and samples were taken at 24 h, 48 h or 72 h, depending on the experiment.

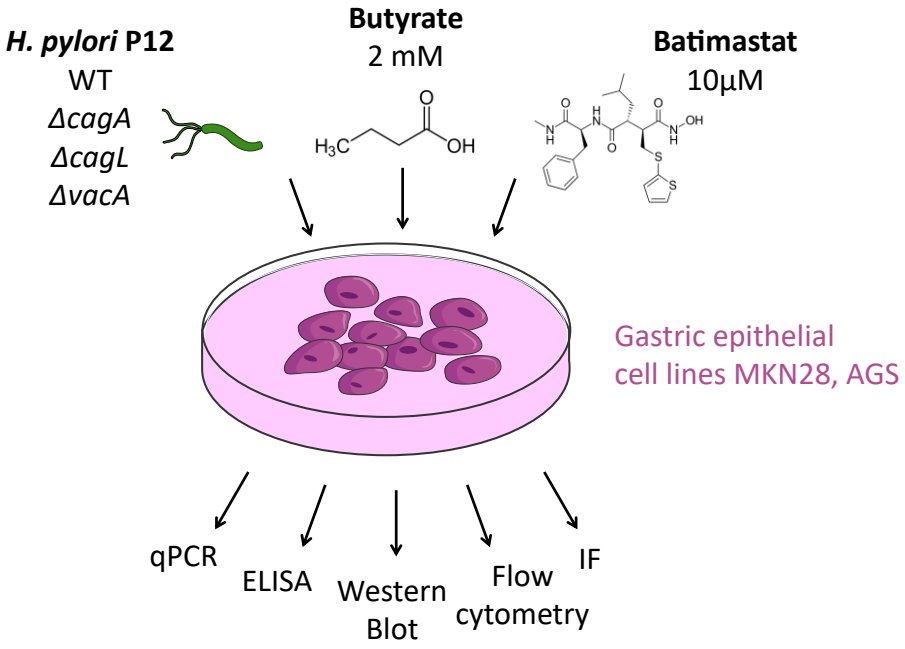

Figure 3. Experimental setup for infection assays performed in this study. Gastric epithelial cell lines MKN28 and AGS were challenged with different stimuli: *H. pylori* P12 WT or mutant strains *ΔcagA, ΔcagL, ΔvacA*, butyrate or batimastat. After a certain time period, cells or cell culture supernatant were sampled for analysis by qPCR, ELISA, western blot, flow cytometry or immunofluorescence (IF) staining. This image was created with Microsoft PowerPoint and contains elements from Servier Medical Art (https://smart.servier.com/), adapted with permission through the Creative Commons Attribution licence CC-BY, version 4.0 (https://creativecommons.org/licenses/by/4.0/).

2.8. ELISA

Prior to ELISA we sterilized cell culture supernatants with 0.22 µM sterile filters. In addition, we concentrated supernatants with Amicon® Ultra-2 mL Centrifugal Filters (MerckMillipore), when needed. Subsequently we processed supernatants using the Human MICA Duoset ELISA kit (R&D) and the Human MICB Duoset ELISA kit (R&D), according to the manufacturer's protocol and quantified the results with a SPECTROstar Omega Plate reader.

2.9.Immunofluorescence staining of MICA/B

For immunofluorescence, we cultivated cells on adhesive slides (QPath) with flexiPERM®

(Sarstedt) and performed infection assays as described above. We then fixed the cells in 4% formaldehyde (Thermo Scientific #28906), used 0,1% saponin for permeabilization and incubated cells with the Alexa Fluor® 647 anti-human MICA/MICB antibody (BioLegend Cat# 320914, RRID: AB_2266419, 1:100 dilution). For counterstaining we used 4',6-Diamidin-2-phenylindol (DAPI). The Zeiss LSM510 Meta Confocal Microscope was used to assess fluorescence staining and quantification of fluorescence intensity per cell was performed with the aid of the Nikon software NIS-Elements General Analysis (GA3).

2.10. Analysis of MICA/B expression by Flow cytometry

For flow cytometry, we harvested stomach AGS-MICA cells with Accutase® (Thermo Fisher Scientific) to prevent loss of surface proteins. Subsequently we stained cells at 4°C for 1 h with Alexa Fluor 647 anti-human MICA/B antibody (BioLegend, Cat# 320914, RRID: AB_2266419). A CytoFLEX S flow cytometer (Beckman Coulter) was used to perform flow cytometry and the data were analyzed using the software CytExpert (Beckman Coulter). Flow cytometry data are shown as median fluorescence intensity (MFI).

2.11. *VacA* genotyping

We obtained *H. pylori* strains isolated from several of the patients, whose tissue samples were used in our immunohistochemical and qPCR analyses. To determine the *vacA* genotypes of these *H. pylori* strains, we cultured them on agar plates as described above and then performed Colony PCR. Colonies were taken from agar plates and lysed in 100 µl MilliQ water, depending on colony size. The lysates were heated at 100°C for 10 min, centrifuged (1 min, 13.000 rpm) and 5 µl of the supernatants were applied in the PCR reactions. Primers and references are listed in Table 1. PCR was performed with Dream Taq Polymerase (Thermo Fisher Scientific, EP0705) using the following thermal cycling conditions: initial heating for 3 min at 95°C, then 35 cycles of 30 sec at 94°C, 1 min at 53°C and 1 min at 72°C, followed by a final step for 5 min at 72°C. Subsequently, PCR products were subjected to agarose gel electrophoresis. Gels were prepared to a final concentration of 2,5% (w/v) agarose with 1xTAE buffer and supplemented with GelRed (Millipore, SCT123). 1x TAE buffer was used as running buffer and gels were run at 4-10 V/cm. *VacA* genotypes were identified based on PCR product

size, as described previously (40,230–232). *H. pylor*i strains with known *vacA* genotypes (P12: s1/m1, PMSSI: s2/i2) (223,228) were used as controls.

Table 1. Oligonucleotide primers for the genotyping of the *vacA* s, m and i alleles.

PCR reaction	Primers	Sequences (5'-3')	Expected size of PCR product	Reference
1	VA1-F	-ATGGAAATACAACAAACACAC	259 bp (s1)	(230–232)
	VA1-R	-CTGCTTGAATGCGCCAAAC	286 bp (s2)	
	VAG-F	-CAATCTGTCCAATCAAGCGAG	567 bp (m1)	
	VAG-R	-GCGTCAAAATAATTCCAAGG	642 bp (m2)	
2	VacF1	-GTTGGGATTGGGGGAATGCCG	426 bp (i1)	(40)
	C1R	-TTAATTTAACGCTGTTTGAAG		
3	VacF1	-GTTGGGATTGGGGGAATGCCG	432 bp (i2)	(40)
	C2R	-GATCAACGCTCTGATTTGA		

2.12. Analysis of NKG2D expression by Flow cytometry

For analyzing the effect of soluble MICA/B in cell culture supernatants of stomach epithelial cells on NK cells, we infected AGS-MICA cells with *H. pylori*, as described above for 24 h. As controls we used not-infected cells. We then harvested the cell culture supernatants, sterilized them using 0.22 µM sterile filters and concentrated them using centrifugal filters (Amicon Ultra-15, PLGC Ultracel-PL Membran, 10 kDa, Merck Millipore), according to the manufacturer's instructions. After that, we treated NKL cells with these cell culture supernatants for 24 h and additionally added the human MICA/B antibody (R and D Systems Cat# MAB13001, RRID: AB_2143621) or the mouse IgG2A isotype control (R&D Systems Cat# MAB003, RRID: AB_357345) at 5 µg/ml. Next, we stained these NKL cells at 4°C for 30 min with the human NKG2D/CD314 antibody (R&D Systems Cat# MAB139, RRID: AB_2133263), followed by staining with the goat F(ab')2 anti-mouse IgG - (Fab)'2 (PE), pre-adsorbed (Abcam Cat# ab5889, RRID: AB_955482). Alternatively, we stained NKL cells with the FITC anti-human CD94 antibody (BioLegend Cat# 305504, RRID: AB_314534). Flow cytometry results of these experiments are shown as median fluorescence intensity (MFI).

2.13. Analysis of cytotoxic degranulation of NK cells by Flow cytometry

For the analysis of cytotoxic degranulation, we pre-treated NKL cells with supernatants from AGS-MICA cells, as it was described above and then co-cultured them with K562 cells for 2 h at 37°C. Subsequently, we stained these cultures with the FITC anti-human CD94 antibody (BioLegend Cat# 305504, RRID: AB_314534) to distinguish NKL cells from K562 cells, and with the APC anti-human CD107a (LAMP-1) antibody (BioLegend Cat# 328620, RRID: AB_1279055) as a marker for cytotoxic degranulation (233). Antibody stainings were performed at 4°C for 30 min. The flow cytometry results of these experiments are presented as % of the LAMP-1+ cells, out of all CD94+ cells.

2.14. MICA genotyping

We performed genotyping of the microsatellite repeat polymorphism in the transmembrane region of the *MICA* gene as it was described by Gonzalez et al. (234). For the determination of the fragment sizes, we used the Peak Scanner v1.0 software (Applied Biosystems). As controls we used cell lines with known *MICA* genotypes: Jurkat (A5.1/A6), J82 (A5.1/A6), RT4 (A5.1) and RT112 (A4).

2.15. Isolation of exosome-enriched preparations

Prior to the isolation of exosome-enriched preparations, we prepared extracellular vesicle (EV)-free FBS and HBS buffer by sequential ultra-centrifugation at 10.000 g for 30 min and at 100.000 g overnight (355618 tubes, Optima L-90K ultracentrifuge, Ti 70 rotor, Beckman coulter). We cultured AGS and MKN28 cells in T145 dishes for 48 h, then washed the cells with PBS and infected them with *H. pylori* as described above, using medium containing 1% of EV-free FBS. As controls, cells were not infected but received fresh medium containing 1% of EV-free FBS. After 48 h, we harvested the cell culture supernatants and started a sequential centrifugation protocol (130,235,236) with all centrifugations performed at 4°C: First we centrifuged the cell culture supernatants two times at 200 g for 5 min and two times at 500 g for 10 min, in order to pellet cell debris. Next, we centrifuged the supernatants for 30 min at

10,000 g (UniCen HR, 6.50 TF Rotor) in order to pellet larger vesicles. The supernatants of this centrifugation step were sterile filtered with 0.22 µm filters (Corning) and centrifuged at 100.000 g for 2 h in an Ultracentrifuge (LE-80 Ultracentrifuge, SW28 rotor, Beckman Coulter) using ultracentrifugation tubes (326823, Beckman Coulter). Finally, we solubilized the pellets of this ultracentrifugation step in EV-free HBS buffer (10 mmol/L HEPES pH 7.6, 150 mmol/L NaCl) and stored these exosome-enriched preparations at -80°C.

2.16. Isolation of soluble proteins from exosome-free supernatants

The term 'exosome-free supernatant' is used in this study for the supernatants that remained after the final ultracentrifugation step of the exosome-enrichment protocol. To isolate proteins from these exosome-free supernatants we performed Trichloroacetic acid (TCA) precipitation. We added TCA (Sigma Aldrich) to the samples to a final concentration of 20% and incubated them overnight at -20°C. Then we thawed the samples and centrifuged them for 30 min at 12,000 g at 4°C (UniCen HR, 6.50 TF Rotor). Next, we washed the pellets once with PBS and two times with acetone and let the samples air dry at RT. Finally, we solubilized the dry pellets in 8 mol/L urea in PBS and stored the samples at -80°C.

2.17. Visualization of exosomes by electron microscopy

Note: Iris Kufferath (Institute of Pathology, Medical University of Graz) performed visualization of exosomes by electron microscopy.

For the visualization of exosomes via electron microscopy, we dropped exosome-enriched preparations on a piece of parafilm and put a grid on it for 1 min. Then we removed the superfluous fluid and let the samples air-dry. After that, we placed the grid on a drop of 2% uranylacetate in 70% methanol and incubated this at RT for 20 min. Next, we prepared several beakers: one of each with 15 ml methanol, 10 ml methanol, 5 ml methanol and fresh molecular-biology grade (MBG) water (Fresenius). Then we placed the grid eight times in every beaker and removed the superfluous liquid. After that we dried the grid at RT for 5 min, then placed a drop of lead citrate (ready to use, Science Services) on the grip and incubated it at RT for 1 min. Next, we prepared four beakers with fresh MBG water and placed the grid 8x in each beaker. We then removed the superfluous liquid and let the grids air-dry. For visualization, a

ZEISS EM 900 electron microscope was used.

2.18. Western blot analysis of MICA and MICB

For protein isolation from cultured cells, we used RIPA buffer (Merck Millipore) with protease inhibitors cOmplete Mini EDTA-free, 0.1 mmol/L Pefabloc, PhosSTOP and 1 mmol/L DTT (Roche). The BioRad Protein Assay Dye Reagent (BioRad Laboratories) was used for determining protein concentrations. We used 20 µg of protein per slot from cell lysates and from TCA precipitated soluble proteins. For exosome-enriched preparations, we quantified the particle counts via the NanoSight device NS300 and the software NTA 3.3, according to the manufacturer's instructions and applied a defined number of particles per slot. Where needed, we digested samples with PNGase F (New England Biolabs) for deglycosylation, following to manufacturer's protocol. Then, we mixed samples with loading buffer (Laemmli buffer, Biorad; diluted 1:9 with β-mercaptoethanol, Sigma-Aldrich), incubated them at 95°C for 10 min, loaded them on 12,5 % (v/v) (SDS)-polyacrylamide gels and performed electrophoresis. Next, we blotted the proteins to PVDF membranes (Immobilon-P, Merck Millipore). To check blotting efficiency, we performed Ponceau S staining (Sigma Aldrich). Subsequently, we blocked non-specific binding by incubation with 5% (w/v) non-fat dry milk (Bio-Rad Laboratories) in tris-buffered saline (TBS) with 0.1% (v/v) Tween 20 (Merck Millipore) for 1 h. Then we incubated the membranes overnight at 4°C with GAPDH antibody (Cell Signaling Technology #2118, 1:1000). The next day, the membranes were incubated for 1 h at RT with rabbit IgG HRP linked F(ab′)2 (Merck, GENA9340-1ML, 1:5000 dilution). To detect immunolabeling, we used the ECL™ Select Western Blotting Detection Reagent (Merck, GERPN2235) and the ImageQuant™ LAS 500. After detection of the loading control, we stripped the membranes (Thermo Fisher, Restore™ Western blot Stripping Buffer) for 45 min at RT, blocked again and incubated them overnight at 4°C with the primary antibodies: MICA biotinylated antibody (R&D Systems Cat# BAF1300, RRID: AB_355943, 1:2000) or MICB biotinylated antibody (R&D Systems Cat# BAF1599, RRID: AB_356059, 1:2000). Next, the membranes were incubated at RT for 1 h with streptavidin-HRP (R&D Systems DY998, 1:5000). Immunolabeling was detected as described above. Quantification of band intensities in Figure 14C was performed using Image Lab Software (Bio-Rad).

2.19. siRNA transfection

For the knock-down of *MMP9* and *ADAM17* by siRNA transfection, we tested a set of four different targeting siRNAs for each protease in order to identify the siRNA with the best knockdown efficiency, as recommended by the manufacturer. For *MMP9* we tested the set LQ-005970-00-0005 (ON-TARGET plus siRNAs, Dharmacon, Horizon Discovery), for *ADAM17* we tested the set LQ-003453-00-0002 (ON-TARGET plus siRNAs, Dharmacon, Horizon Discovery). We identified the *MMP9*-targeting siRNA #4 (5'GAACCAAUCUCACCGACAG-3,) and the *ADAM17*-targeting siRNA #3 (5'-UAUGGGAACUCUUGGAUUA-3') as most efficient in our experimental setup (Figures 30 and 31). As non-targeting control, we used the non-targeting siRNA D-001810-01-05 (5'-UGGUUUACAUGUCGAUAA-3, Horizon Discovery). For the transfection, siRNAs were added to AGS cells at 50 nmol/L, together with DharmaFECT 1 transfection reagent (T-2001-01, Horizon Discovery) and cultivated for 24 h. Subsequently, we washed the cells, added fresh medium, and cultured them for another 24 h. After that, we infected the cells with *H. pylori* as described above and monitored the downregulation of the protease by qPCR and/or western blot.

2.20. Western Blot analysis of ADAM17 and ADAM10

We performed protein isolation and western blotting as described above. As primary antibodies we used the ADAM17 antibody #3976 (Cell Signaling Technology Cat# 3976, RRID: AB_2242380, 1:2000 dilution), the ADAM10 antibody #14194 (Cell Signaling Technology Cat# 14194, RRID: AB_2798420, 1:500 dilution) and the GAPDH antibody #2118 (Cell Signaling Technology Cat# 2118, RRID: AB_561053, 1:1000 dilution). Primary antibodies were incubated at 4°C overnight followed by incubation with the Rabbit IgG HRP Linked F(ab′)2 (Merck, GENA9340-1ML, 1:5000 dilution) for 1 h at RT. In between, membranes were stripped using Restore™ Western blot Stripping Buffer (Thermo Fisher) for 45 min at RT.

2.21. Statistical analysis

We used parametric tests to determine statistically significant differences between groups for all data from cell-culture assays: To compare the mean of one group to a theoretical mean

of one, we used a one-sample t-test (Figure 29A-C). To compare two independent groups we used an unpaired, two-tailed Student's t-test (Figures 15B,C and 28). To compare three or more groups, we applied one-way analysis of variance (ANOVA), together with Dunnett's multiple comparisons test in order to compare the mean of each group with the mean of one single control group (Figures 6, 8, 9, 10, 12, 29D, 32) or together with Tukey's multiple comparisons test in order to compare the mean of each group with the mean of every other group (Figures 13, 14B,D,E, 20D, 21B). When analyzing data from patient biopsies we tested for normality using the Shapiro-Wilk test. For normally distributed sample sets we then performed statistical analysis by ANOVA and Tukey's test (Figure 5). For nonparametric analyses we applied Mann Whtiney test to compare two independent groups (Figure 18B) or Kruskal Wallis test together with Dunn's multiple comparisons test, in order to compare the mean rank of each group with the mean rank of every other group of three or more groups (Figures 4B, 17B, 18A). In all analyses we considered a of $P<0.05$ as significant (* $P<0.05$; ** $P<0.01$; *** $P<0.001$; **** $P<0.0001$). We used GraphPad Prism 9 software for statistical analyses.

3. Results

3.1. Cytotoxic T Lymphocyte (CTL) and NK cell numbers are unaffected in *H. pylori* gastritis, despite major leukocyte infiltration

NKG2D is mainly expressed by NK cells and cytotoxic T lymphocytes (CTLs). *H. pylori* infection is known to trigger a strong immune infiltration, but the involvement of NKG2D-expressing cell types, is poorly understood. To investigate this, we analyzed gastric specimens from healthy controls, from patients with *H. pylori* gastritis (HpG) and gastric adenocarcinoma (cancer), which is the sequel of chronic *H. pylori* gastritis. We determined cellular infiltration status by H&E staining and we comparatively assessed numbers of total infiltrating leucocytes (CD45), CTLs (CD8) and NK cells (CD56/NKp46) by immunohistochemistry staining of the respective markers (Fig. 4A, B). As expected, total leucocytes were greatly induced in HpG and were also significantly induced in cancer (consisting mainly of B cells, plasma cells and neutrophilic granulocytes), compared to healthy controls. Notably, the numbers of CTLs and NK cells were unchanged in HpG, compared to healthy controls. In cancer, CTLs were reduced while NK cells were induced. Overall, the numbers of CTLs and especially of NK cells were very low in relation to the total leukocyte count. Taken together, these data demonstrate that

despite a strong overall immune infiltration, the major NKG2D-expressing cell types (NK and CTLs) do not accumulate in *H. pylori*-associated pathologies. This observation supports the notion that activation of these cytotoxic effector cells might be inhibited by *H. pylori*.

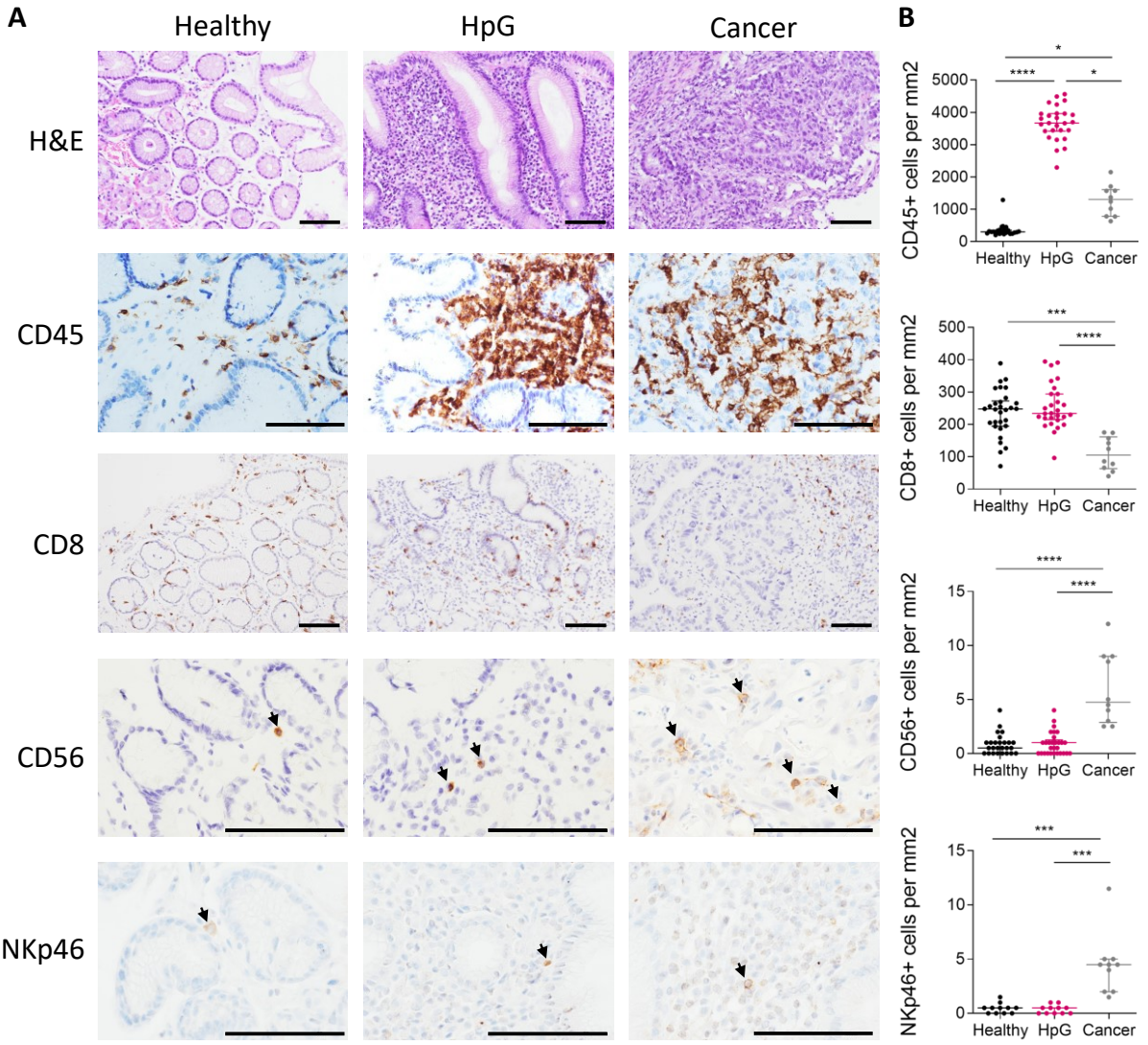

Figure 4. Cytotoxic T Lymphocytes and NK cells are not induced in *H. pylori* gastritis. Stomach biopsies (FFPE) of healthy controls, *H. pylori* gastritis (HpG) and gastric adenocarcinoma (Cancer) (n= 10-30 per group) were subjected to H&E staining and Immunohistochemical staining of CD45 (leucocytes), CD8 (T cells), CD56 and NKp46 (NK cells). (A) Representative images, scale bars: 100 µm. (B) Quantification of positive cells per mm^2 of tissue, the data do not follow normal distribution, median ± interquartile range, Kruskal-Wallis test and Dunn's test. (IHC staining was performed by Sylvia Eidenhammer and scoring was done by Gregor Gorkiewicz, both from the Institute of Pathology.) Reproduced with modifications from Anthofer et al., Front Immunol, 2024 with permission through the Creative Commons Attribution licence CC-BY, version 4.0.

3.2. The NKG2D axis is dysregulated in *H. pylori* gastritis and gastric adenocarcinoma

To identify whether *H. pylori* infection affects the NKG2D axis, we comparatively assessed gene expression of *NKG2D* and the NKG2D-Ls *MICA* and *MICB* in gastric specimens from healthy controls, from patients with *H. pylori* gastritis (HpG) and gastric adenocarcinoma (cancer). Both, HpG and cancer showed significantly reduced tissue expression of *NKG2D*, compared to healthy controls. *MICA* gene expression was unchanged in HpG and reduced in cancer while *MICB* gene expression was significantly induced in both pathologies, compared to healthy controls (Figure 5). Taken together, these data demonstrate that despite an induction of the NKG2D-L *MICB*, expression of the receptor *NKG2D* is reduced in *H. pylori*-associated pathologies. This reduction in NKG2D expression, coupled with our previous finding showing that NK cells and CTLs are unaltered in HpG, suggests evasion of the NKG2D axis in *H. pylori* gastritis.

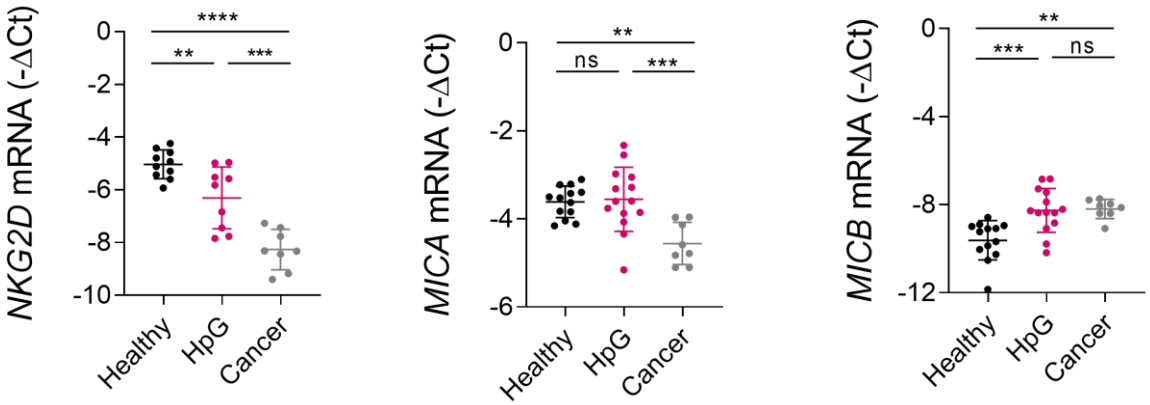

Figure 5. The NKG2D axis is dysregulated in *H. pylori* gastritis and gastric adenocarcinoma. Stomach biopsies (FFPE) of healthy controls, *H. pylori* gastritis (HpG), and gastric adenocarcinoma (Cancer) (n= 8-14 per group) were subjected to analysis of mRNA expression of *NKG2D*, *MICA* and *MICB*. The results are presented as -ΔCt. The data passed Shapiro-Wilk normality test, mean ± SD, one-way ANOVA and Tukey's test. Reproduced with modifications from Anthofer et al., Front Immunol, 2024 with permission through the Creative Commons Attribution licence CC-BY, version 4.0.

3.3. *H. pylori* induces *MICA* and *MICB* gene expression in gastric epithelial cells

Evasion of the NKG2D-axis occurs usually either by suppression of NKG2D-L expression or by release of soluble NKG2D-Ls from the cancer cells or the infected cells (161). To identify the mechanism of NKG2D-axis dysregulation in *H. pylori* infection, we performed *in vitro* infection experiments with gastric epithelial cells, which are the main target of *H. pylori* infection. We infected gastric epithelial cell lines MKN28 and AGS with the *H. pylori* P12 WT strain and isogenic mutants of the major *H. pylori* virulence factors VacA (*ΔvacA*) and CagA (*ΔcagA*). VacA and CagA are soluble toxins that enter host cells and are the main drivers of *H. pylori's* pathogenicity (2). We also used an isogenic mutant for CagL *(ΔcagL)*. The *H. pylori* protein CagL is essential for CagA injection into host cells. Additionally, CagL activates host metalloproteases at the cell membrane (2,64). Metalloproteases are important for the release of soluble NKG2D-Ls (104), therefore we hypothesized, that CagL might induce the release of soluble NKG2D-Ls in *H. pylori* infection. As control treatments we used butyrate and the bacterium *Cutibacterium acnes* (*C. acnes*), which were shown to induce *MICA/B* gene expression in epithelial cells (223,229).

To identify an effect on NKG2D-L expression we measured *MICA* and *MICB* gene expression by qPCR, after 24 h and 48 h of challenge. In MKN28 cells, both control treatments induced *MICB* expression and butyrate additionally induced *MICA* expression (Figure 6A). *H. pylori* WT infection also resulted in increased *MICA* and *MICB* gene expression and the effect increased over time. *MICB* was induced higher than *MICA*, which corresponds to the higher induction of *MICB* gene expression in HpG tissues (see Figure 5). Interestingly, also butyrate had a much stronger effect on the induction of *MICB* gene expression, compared to *MICA*. This suggests that *MICB* is generally more reactive and more inducible than *MICA*, in this cell line. Infection with the isogenic mutants *ΔcagA* and *ΔcagL* induced similar levels of *MICA* and *MICB* gene expression as the WT. Infection with the isogenic mutant *ΔvacA*, however, completely lacked an induction of *MICA* and *MICB* gene expression. This indicates that the virulence factor VacA is essential for induction of *MICA* and *MICB* gene expression in *H. pylori* infection. In AGS cells, *H. pylori* infection had no considerable effect on *MICA* and only a minor effect on *MICB* gene expression (Figure 6B).

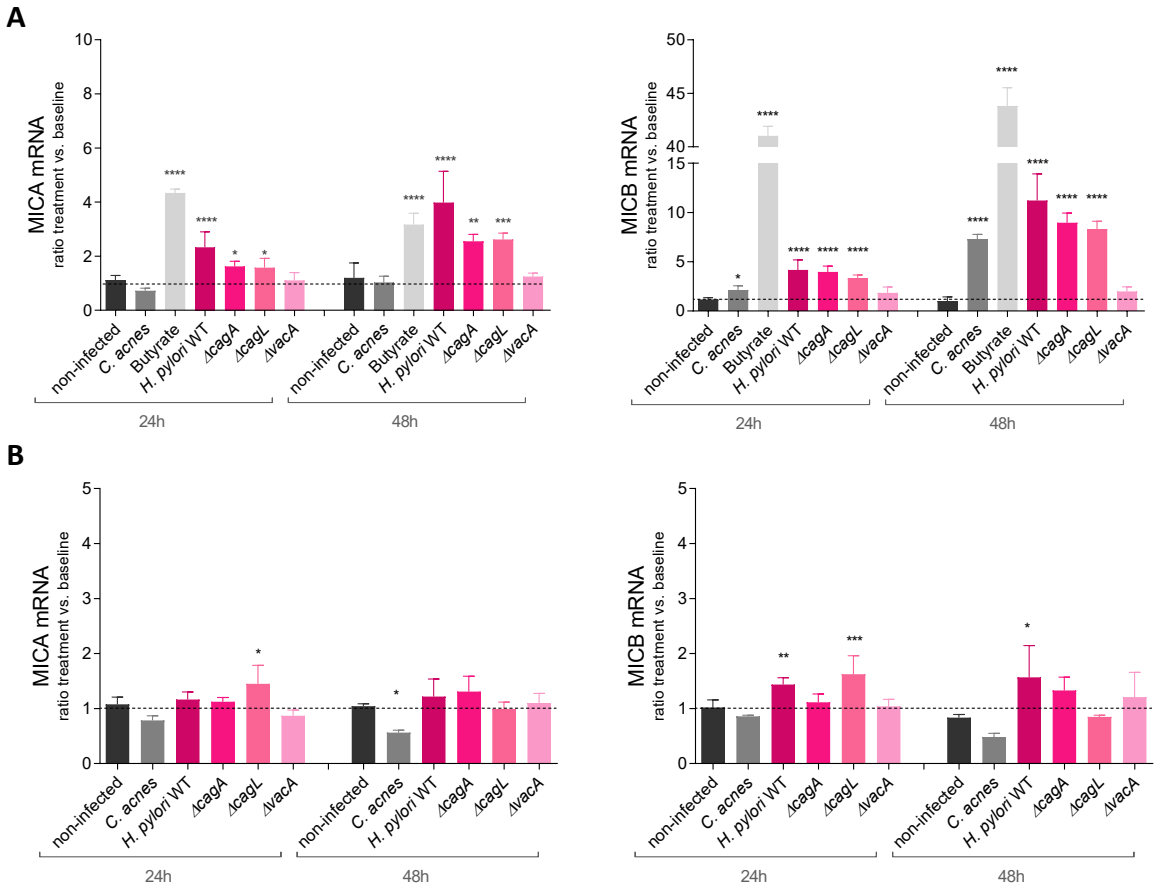

Figure 6. *H. pylori* induces *MICA* and *MICB* gene expression in gastric epithelial cell lines MKN28 and AGS. Stomach epithelial cell lines MKN28 (A) and AGS (B) were infected with *C. acnes*, treated with 2 mM butyrate, or infected with *H. pylori* WT or the isogenic mutants *ΔcagA, ΔcagL*, *ΔvacA* for 24 h and 48 h. *MICA* and *MICB* mRNA levels were determined by qPCR analysis. The results are presented as the ratio of expression after treatment versus baseline expression (prior to treatment). Asterisks indicate statistically significant differences of treated cells compared to non-infected cells at the corresponding timepoint. Mean +/- SD, One-way ANOVA and Dunnett's test.

We next aimed to better understand the differences of *MICA* and *MICB* gene expression in the two different cell lines in response to *H. pylori* infection. For this purpose, we compared baseline gene expressions of *MICA* and *MICB* in the two cell lines (Figure 7A). The highest expressed gene was *MICA* in AGS cells, followed by *MICB* in AGS cells, *MICA* in MKN28 cells and *MICB* in MKN28 cells. Next, we compared the fold-change of *MICA* and *MICB* gene expression in the two cell lines, after 48 h of *H. pylori* infection (Figure 7B). In AGS cells, where baseline *MICA/B* gene expression was high, *H. pylori* WT caused only a minor induction. In MKN28 cells, where baseline *MICA/B* gene expression was low, *H. pylori* WT caused a

strong induction. Next, we correlated the baseline gene expression and the fold-change of gene expression after 48 h of *H. pylori* infection of *MICA* and *MICB* in both cell lines (Figure 7C). The fold-change of gene expression after *H. pylori* infection significantly correlated inversely with the level of baseline gene expression (Pearson's r = -0,7363; p = 0,0005). Thus, differential inducibility of *MICA* and *MICB* gene expression is connected to internal variations in baseline gene expression in MKN28 and AGS cells. To identify the specific causes of this variation in baseline gene expression, a detailed analysis of the genetic context of *MICA* and *MICB* in these two cell lines would be required. *MICA* and *MICB* are highly polymorphic genes and several different allelic variations exist that can affect gene expression (143,149,151–153,156,237). The cell line AGS was reported to be MICA-protein deficient due to a single point mutation in the *MICA* gene that prevents proper protein folding (238). Potentially, the high levels of *MICA* gene expression in this cell line are connected to this lack of mature protein – for instance due to a lack of feedback regulation or as a result of an overcompensation mechanism. Importantly, this analysis showed that differential inducibility of *MICA* and *MICB* gene expression is connected to internal variations in baseline gene expression, which suggests that *H. pylori* plays no role in this differential induction of *MICA* and *MICB* gene expression.

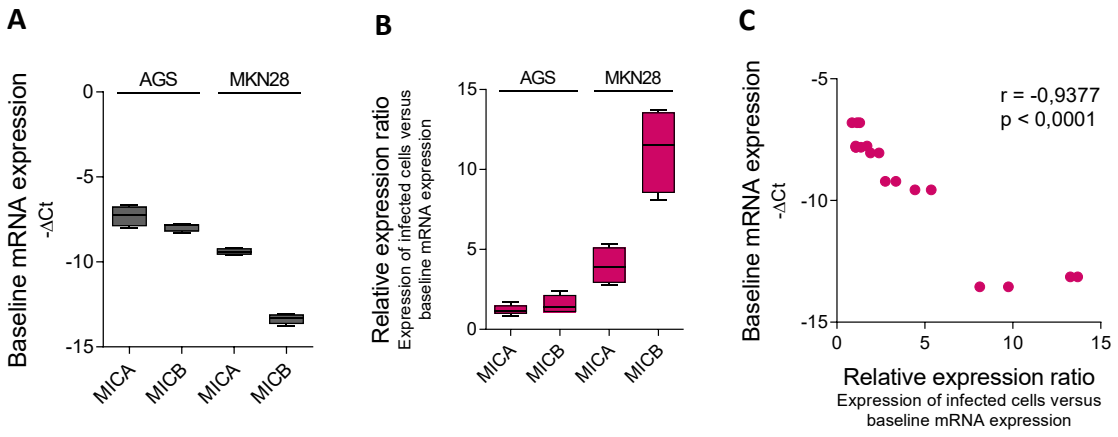

Figure 7. Inducibility of *MICA* and *MICB* gene expression correlates with the level of baseline gene expression in AGS and MKN28 cells. (A) *MICA* and *MICB* mRNA expression levels of the cell lines MKN28 and AGS prior to any treatment (=baseline) were determined by qPCR analysis. The results are presented as -ΔCt, Box and Whiskers Min to Max. (B) MKN28 and AGS cells were infected with *H. pylori* WT for 48 h, *MICA* and *MICB* mRNA levels were determined by qPCR analysis. The results are presented as the relative expression ratio of infected cells versus baseline mRNA expression, Box and Whiskers Min to Max. (C) Correlation of the baseline gene expression and the relative expression ratio after infection for 48 h, Pearson correlation. Reproduced from Anthofer et al., Front

In conclusion we found that *H. pylori* can greatly induce *MICA* and *MICB* gene expression in gastric epithelial cells, and the pathogenicity factor VacA appears to be essential for this induction. The intensity of induction of gene expression depends on the level of baseline gene expression of the respective gene in the respective cell line.

3.4. Gene expression analysis of the mediators of NKG2D suggests overall activation of the NKG2D axis in *H. pylori* infection

NKG2D is not only regulated by MICA and MICB, but also by a range of cytokines and by the other NKG2D-Ls – the UL16 binding proteins (ULBPs) (118). To assess the overall regulation of the NKG2D axis in *H. pylori* infection, we measured gene expression of the NKG2D-Ls *ULBP1*, *ULBP2* and *ULBP3* and of interleukin 15 (*IL-15*), which is an activator of NKG2D expression (239). For *IL-15*, two alternatively spliced transcript variants exist – the long signal peptide isoform (*IL-15 LSP*) and the short signal peptide isoform (*IL-15 SSP*) that both produce a mature protein but differ in their cellular trafficking and extracellular delivery (116). In addition to these activators of NKG2D, we measured gene expression of the cytokines transforming growth factor β (*TGF*-β) and macrophage migration inhibitory factor (*MIF*), which are repressors of NKG2D expression (240). We measured gene expression of these regulators of NKG2D in MKN28 cells and AGS cells after 24 h and 48 h of infection with the *H. pylori* WT and the isogenic mutant *ΔvacA*. In some analyses we additionally treated cells with the isogenic mutants *ΔcagA* and *ΔcagL* and the controls butyrate and *C. acnes*. In MKN28 cells, *H. pylori* WT greatly induced *ULBP1* by about 7-fold and significantly induced *ULBP2* expression (Figure 8A). In AGS cells, *ULBP1* gene expression was not detectable but *H. pylori* WT infection greatly induced *ULBP2* by about 8-fold and significantly induced *ULBP3* (Figure 8B). VacA might play a role in the induction of some of the *ULBPs*. The *IL-15* isoforms LSP and SSP were induced upon *H. pylori* WT infection by 10- and 4-fold in MKN28 cells (Figure 9A) and by 5- and 4-fold in AGS (Figure 9B), respectively. VacA seemed to play no role in the induction of *IL-15* and butyrate and *C. acnes* did not considerably affect *IL-15* expression. *TGF*-

β was induced by about 2-fold in MKN28 (Figure 10A) and AGS cells (Figure 10B) and *MIF* remained unaffected by *H. pylori* infection.

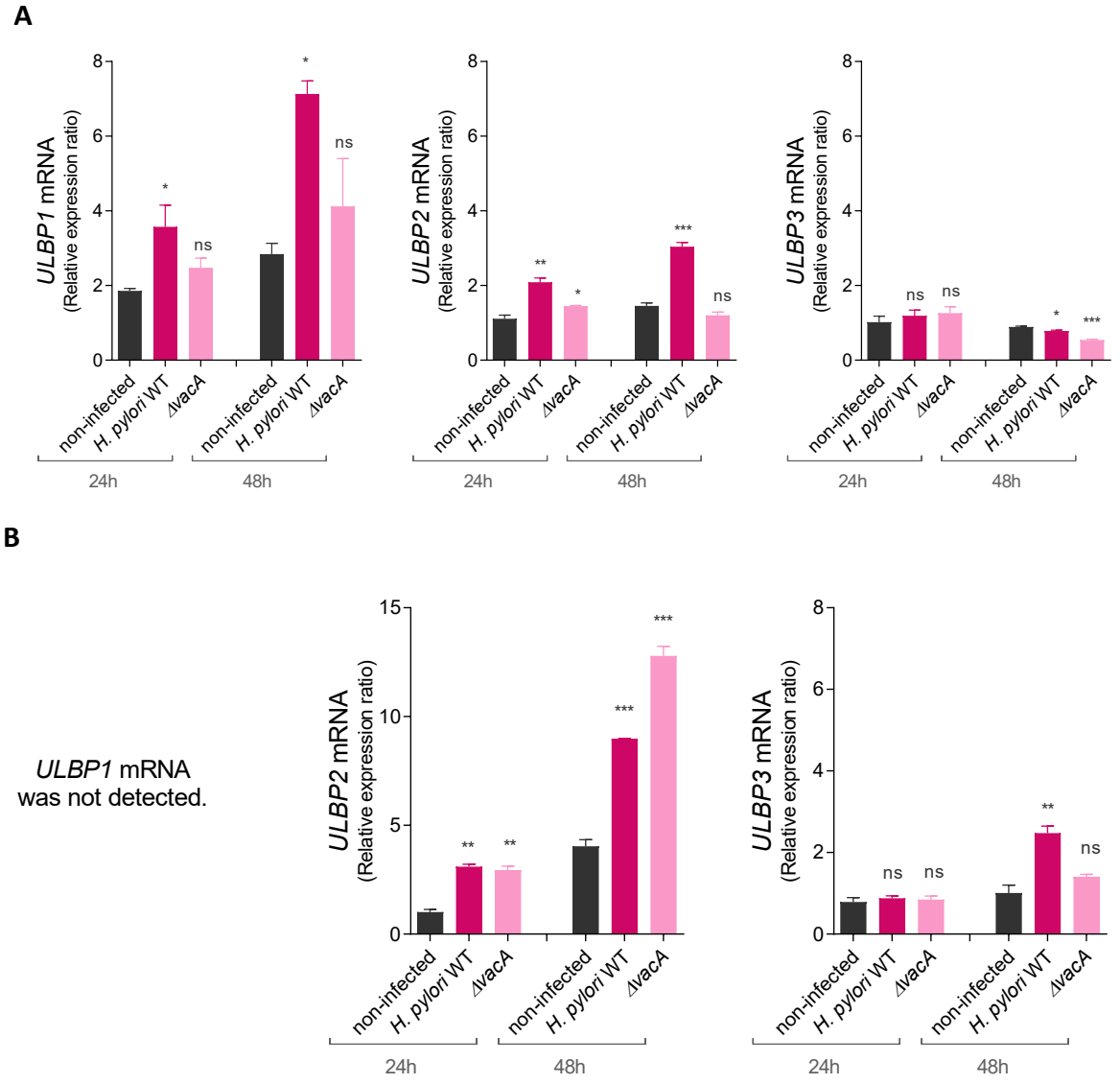

Figure 8. Gene expression analysis of *ULBP1*, *ULBP2* and *ULBP3*. Gastric epithelial cell lines MKN28 (A) and AGS (B) were infected with *H. pylori* wild-type (WT) or isogenic mutant *ΔvacA* for 24 h and 48 h. Gene expression was determined by qPCR analysis. The results are presented as the relative expression ratio of gene expression after treatment versus baseline gene expression (pre-treatment). Mean +/- SD. Asterisks indicate statistically significant differences of treated cells compared to control cells at the corresponding timepoint. One-way ANOVA and Dunnett's test. Reproduced with modifications from Anthofer et al., Front Immunol, 2024 with permission through the Creative Commons Attribution licence CC-BY, version 4.0.

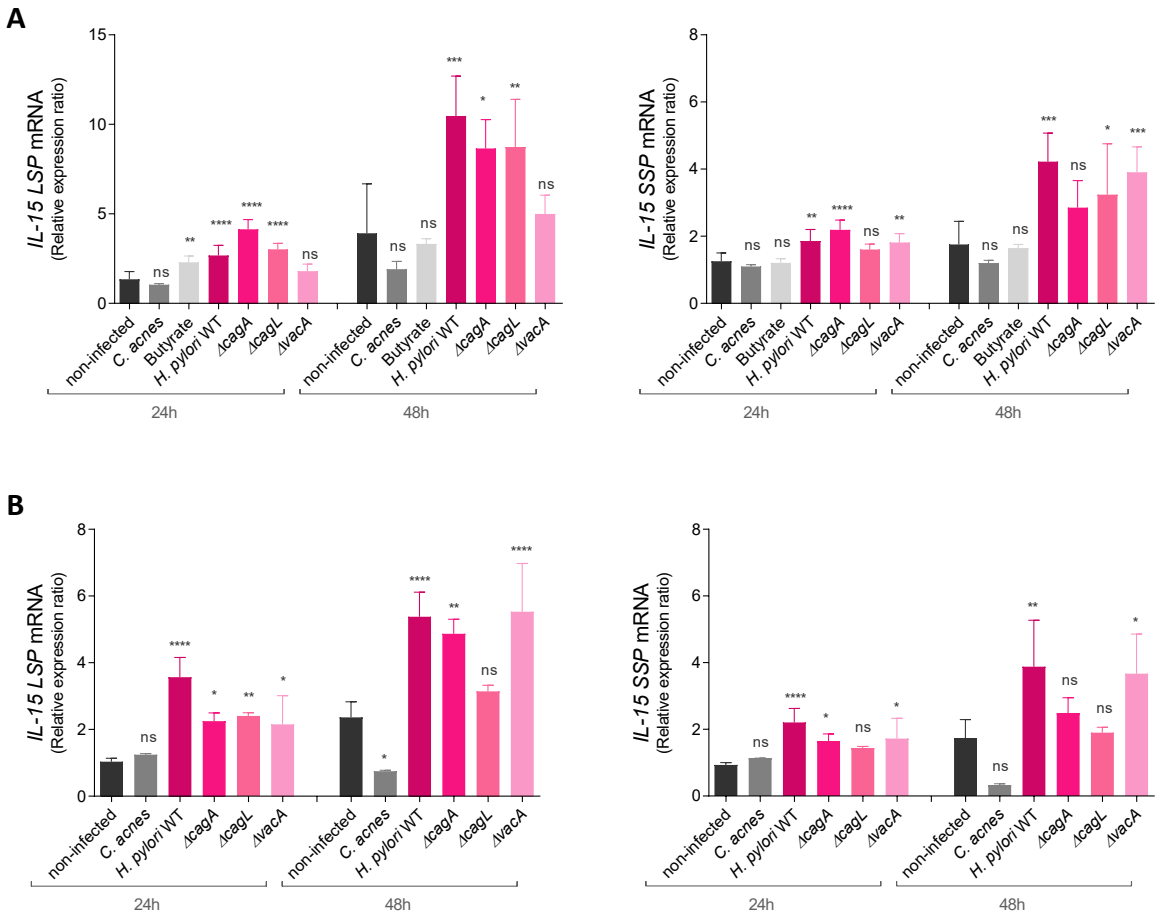

Figure 9. Gene expression analysis of *IL-15 LSP* and *IL-15 SSP*. Gastric epithelial cell lines MKN28 (A) and AGS (B) were infected with *H. pylori* wild-type (WT) or isogenic mutants *ΔcagA, ΔcagL, ΔvacA* for 24 h and 48 h. Gene expression was determined by qPCR analysis. The results are presented as the relative expression ratio of gene expression after treatment versus baseline gene expression (pre-treatment). Mean +/- SD. Asterisks indicate statistically significant differences of treated cells compared to control cells at the corresponding timepoint. One-way ANOVA and Dunnett's test. Reproduced with modifications from Anthofer et al., Front Immunol, 2024 with permission through the Creative Commons Attribution licence CC-BY, version 4.0.

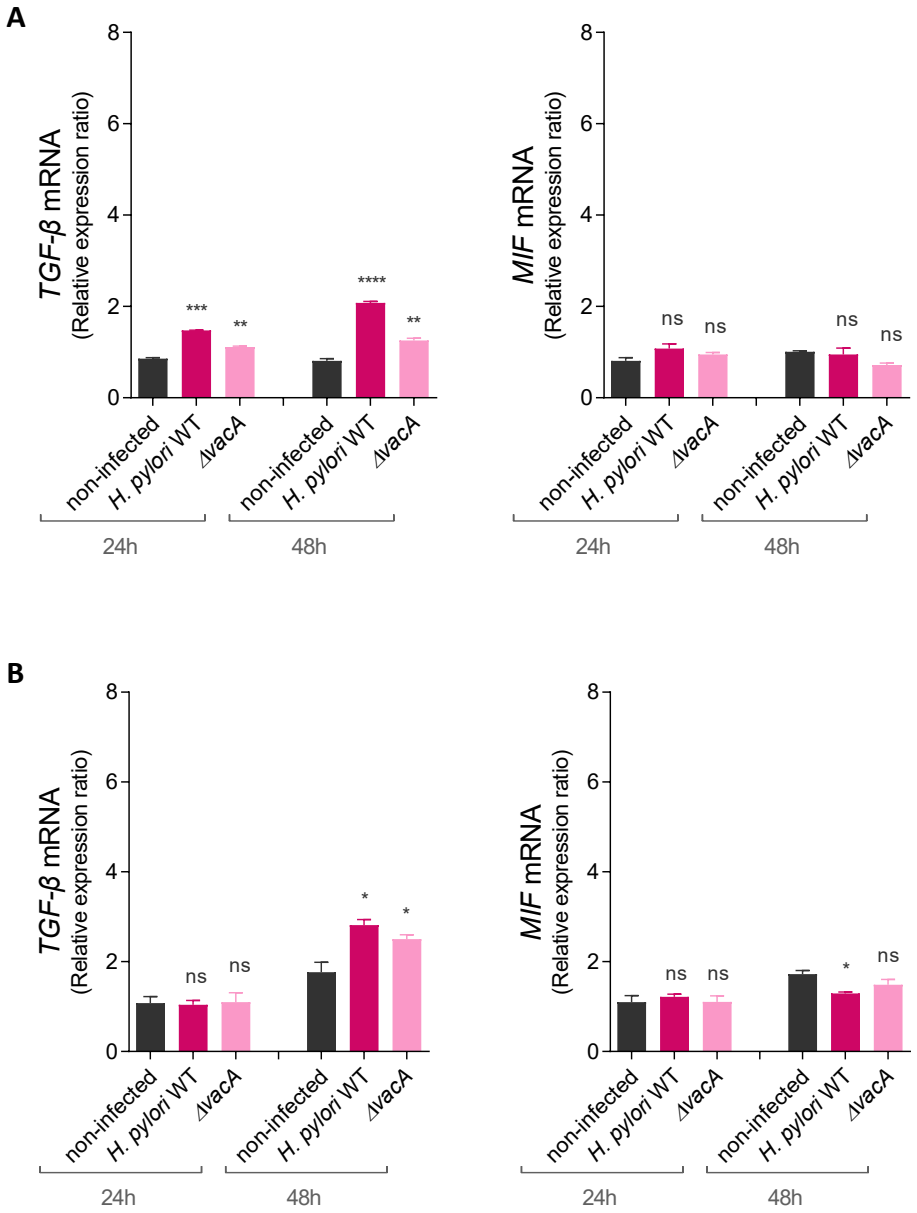

Figure 10. Gene expression analysis of *TGF*-β and *MIF*. Gastric epithelial cell lines MKN28 (A) and AGS (B) were infected with *H. pylori* wild-type (WT) or isogenic mutant *ΔvacA* for 24 h and 48 h. Gene expression was determined by qPCR analysis. The results are presented as the relative expression ratio of gene expression after treatment versus baseline gene expression (pre-treatment). Mean +/- SD. Asterisks indicate statistically significant differences of treated cells compared to control cells at the corresponding timepoint. One-way ANOVA and Dunnett's test. Reproduced with modifications from Anthofer et al., Front Immunol, 2024 with permission through the Creative Commons Attribution licence CC-BY, version 4.0.

A summary heat-map of the gene expression analysis of the mediators of the NKG2D axis is shown in Figure 11. It demonstrates great induction of several activators of NKG2D, and a minor or no induction of the repressors of NKG2D. Taken together, this gene expression analysis suggests an overall induction of the NKG2D axis in *H. pylori* infection. This status would typically lead to the killing of the infected epithelial cells by NKG2D-expressing cytotoxic cells. Under these circumstances, it is highly likely for *H. pylori* to have developed a strategy to evade the NKG2D-axis, being a master in immune evasion and persistence in its niche.

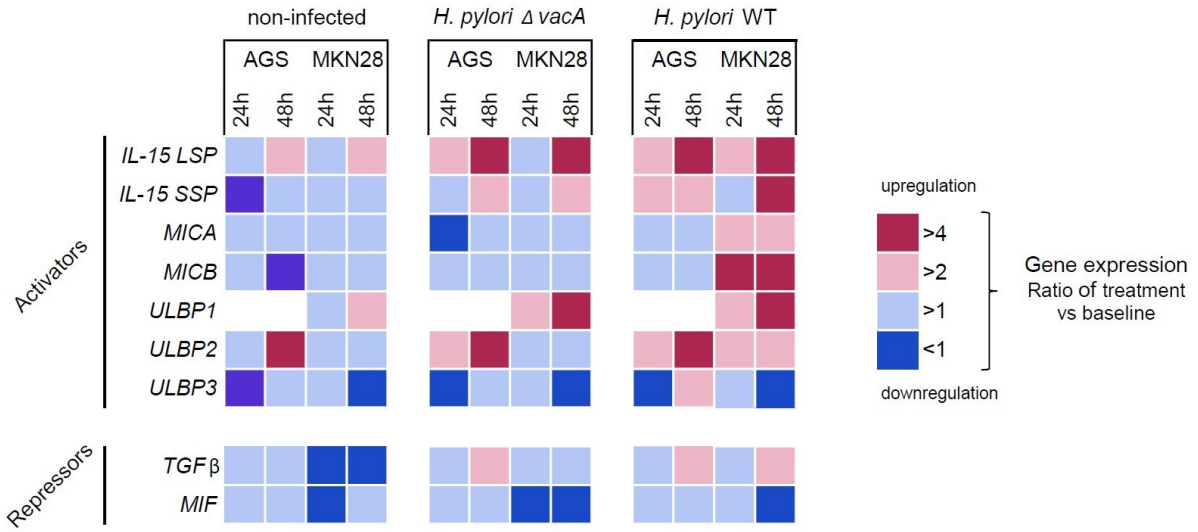

Figure 11. Summary heat-map of the gene expression analysis of the mediators of the NKG2D axis in *H. pylori*-infected gastric epithelial cell lines.

3.5. *H. pylori* induces soluble release of MICA and MICB proteins in gastric epithelial cells, independent of its effect on NKG2D-L gene expression

To identify a potential evasion strategy by release of soluble NKG2D-Ls we quantified MICA and MICB protein levels in cell culture supernatants by ELISA, after 24 h and 48 h of infection. In MKN28 cells, both, the treatment with butyrate and the infection with *H. pylori* WT resulted in significantly increased levels of soluble MICA and MICB in the cell culture supernatants (Figure 12A). The effect of *H. pylori* WT increased from 24 h to 48 h, while the

butyrate-induced induction of soluble MICB diminished over time. Infection with the isogenic mutants *ΔcagA*, *ΔcagL* and Δ*vacA* induced no increase of soluble MICA and a much less pronounced increase of soluble MICB, compared to infection with the WT. In the case of Δ*vacA* infection, the low levels of soluble MICA/B may be due to the lack of induced MICA/B gene expression, which we had observed earlier (see Figure 6A). In the case of *ΔcagA* and *ΔcagL* infection, however, *MICA/B* gene expression levels had been induced similarly as in infection with the WT. Therefore, the lower induction of soluble MICA/B suggests a potential role for the virulence factors CagA and CagL in the soluble release of MICA and MICB.

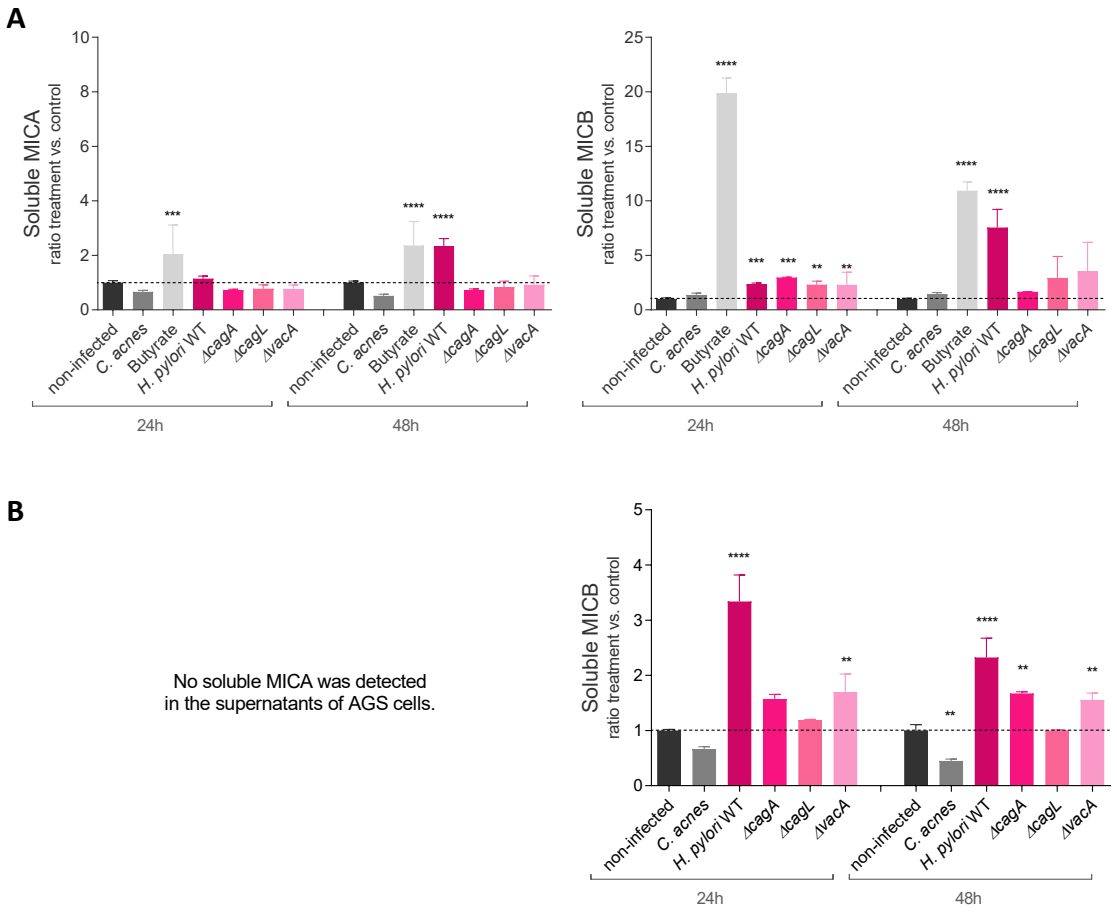

Figure 12. *H. pylori* induces soluble release of MICA and MICB proteins in gastric epithelial cells. Gastric epithelial cell lines MKN28 (A) and AGS (B) were infected with *C. acnes*, treated with 2 mM butyrate or infected with *H. pylori* wild-type (WT) or isogenic mutants *ΔcagA, ΔcagL, ΔvacA* for 24 h and 48 h. Soluble MICA and MICB proteins in cell culture supernatants were determined by ELISA analysis. The results are presented as the ratio of treated cells versus non-infected cells at the corresponding timepoint. Mean +/- SD. Asterisks indicate statistically significant differences of treated

cells compared to non-infected cells at the corresponding timepoint, One-way ANOVA and Dunnett's test. Reproduced with modifications from Anthofer et al., Front Immunol, 2024 with permission through the Creative Commons Attribution licence CC-BY, version 4.0.

In AGS cells, *H. pylori* WT had induced only a minor increase of *MICB* gene expression (see Figure 6B). Nevertheless, also in this cell line the levels of soluble MICB increased distinctively, after WT infection (Figure 12B). Similar as in MKN28, the isogenic mutants *ΔcagA*, *ΔcagL* and *ΔvacA* induced lower levels of soluble MICB, compared to the WT. No soluble MICA was detectable in culture supernatants from AGS cells, as others have reported before (157). Taken together, *H. pylori* WT infection significantly increased the levels of soluble MICA and MICB in cell culture supernatants of infected gastric epithelial cell lines and CagA/CagL might play a role in this induction.

To identify the overall effect of *H. pylori* on the release of soluble NKG2D-Ls, we measured the levels of soluble ULBP1, ULBP2, ULBP3 and ULBP4 in the cell culture supernatants of MKN28 and AGS cells, after 48 h of infection with *H. pylori* WT and the isogenic mutant Δ*vacA*. ULBP2 has high sequence similarity with ULBP5 and ULBP6, therefore a combined antibody was used for the detection of these three NKG2D-Ls. Ligands were detectable but no significant differences were identified between the different treatment groups (Figure 13A, B). Overall, levels of soluble ULBPs were lower in AGS cells, compared to MKN28 cells. Especially ULBP1 and ULBP2 were close to the limit of detection of the assay in supernatants from AGS cells. In conclusion, these data demonstrate that *H. pylori* does not affect soluble release of all NKG2D-Ls but specifically affects MICA and MICB.

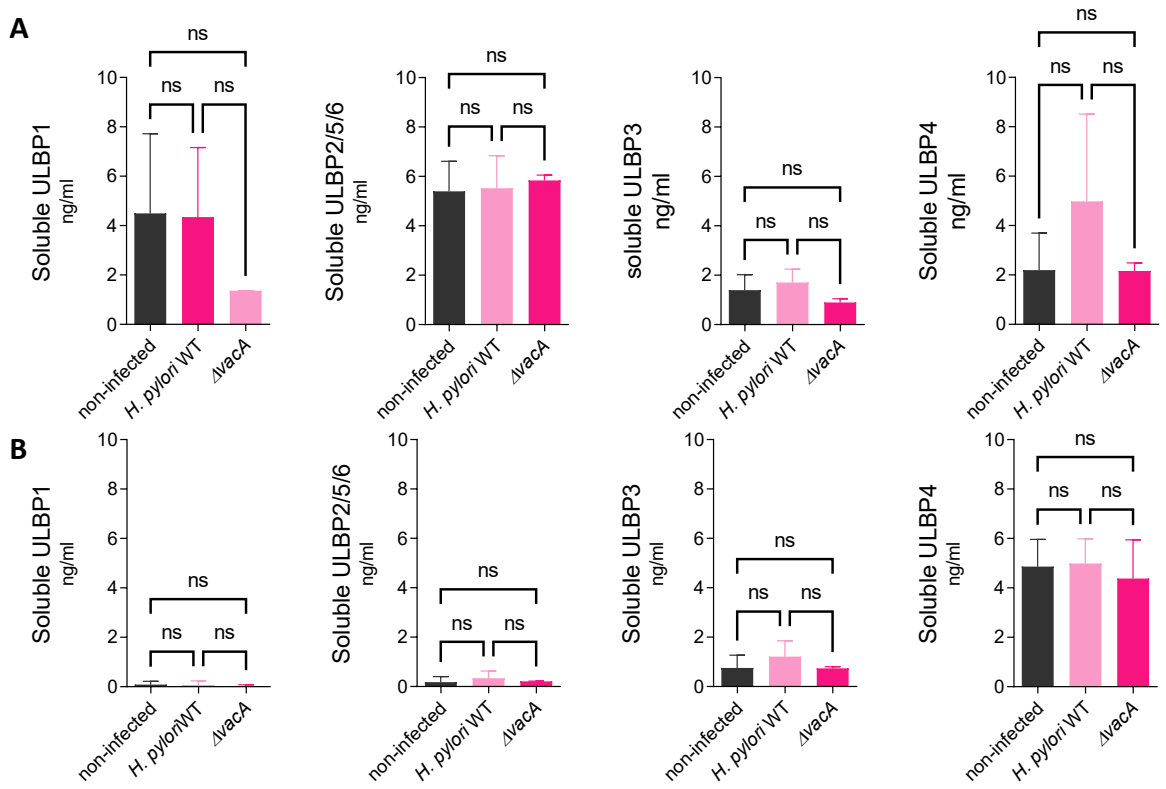

Figure 13. Analysis of soluble ULBPs in cell culture supernatants of gastric epithelial cells. Gastric epithelial cell lines MKN28 (A) and AGS (B) were infected with *H. pylori* wild-type (WT) or isogenic mutant *ΔvacA* for 48 h. Soluble ULBP1, ULBP2/5/6, ULBP3 and ULBP4 proteins in cell culture supernatants were determined by ELISA analysis. Mean +/- SD, one-way ANOVA and Tukey's test**.**

MICA and MICB are normally expressed intracellularly in healthy GI epithelia (108,109) and their expression is tightly regulated at multiple levels ranging from gene expression and mRNA stability to transfer to the cell surface and soluble release (104). Many tumor cells, including the cell lines used in this study, have overcome these regulatory mechanisms, and continuously release soluble NKG2D-Ls. Therefore, it was unclear to what extent the levels of soluble NKG2D-Ls we measured in the supernatants of *H. pylori*-infected cells, were influenced by changes in NKG2D-L gene expression upon *H. pylori* infection. To clarify whether *H. pylori* specifically activates the soluble release of MICA/B, independent of its effect on MICA/B gene expression, we aimed to use a different experimental model, that would allow us to study the soluble release of MICA/B, independent from changes in MICA/B gene expression. For this purpose, we used the stomach epithelial cell line AGS which is naturally MICA protein-deficient due to a single point mutation in the *MICA* gene that prevents

proper protein folding (238), and we did not detect any levels of soluble MICA in cell culture supernatants (see Figure 12B). We transfected AGS cells via lentivirus transfection to constitutively express *MICA* from an SFFV promoter (Figure 14A). Then we infected these AGS-MICA transfectants with *H. pylori* and measured *MICA* gene expression, total cellular MICA protein and soluble MICA protein in cell culture supernatants. As expected, *MICA* gene expression (Figure 14B) and total cellular MICA protein (Figure 14C,D) were not altered in AGS-MICA cells after infection with the WT or any of the mutants. However, soluble MICA levels in cell culture supernatants were significantly increased after infection with the WT (Figure 14E), indicating that *H. pylori* induces soluble release of MICA, independent of its effect on *MICA* gene expression. Cells infected with the isogenic mutant *ΔvacA* also showed an induction of soluble MICA, albeit smaller than cells infected with the WT. Thus, the virulence factor VacA likely plays no major role in the soluble release of MICA. However, cells infected with the isogenic mutants *ΔcagA* and Δ*cagL* showed no induction of soluble MICA indicating that the virulence factors CagA and CagL play a critical role in the soluble release of MICA. Since there was no difference between the two mutant strains, we assumed that CagA might be directly involved in the induction of soluble release while CagL's role in this process might be the transfer of CagA into host cells. No additional, independent effect of CagL seemed to be at play in the soluble release of MICA.

Taken all analyses of AGS and MKN28 cells together, the two cell lines reacted differently to *H. pylori* infection on the level of gene expression, however, they showed a similar trend concerning the release of soluble MICA and MICB protein. In both cell lines, *H. pylori* infection induced the accumulation of soluble MICA/B protein in the cell culture supernatants. The use of AGS-MICA cells allowed us to study the release of soluble MICA, independent from changes in *MICA* gene expression. This experiment confirmed that *H. pylori* induces the soluble release of MICA independent of *H. pylori's* effects on MICA gene expression, and the pathogenicity factor CagA appeared to be essential for this induction. In summary, we found that *H. pylori* manipulates expression of MICA and MICB on two different levels, by the action of its two main pathogenicity factors, with VacA increasing gene expression, and CagA initiating the soluble release of MICA/B. Consequently, *H. pylori* has the potential to induce the release of high quantities of soluble MICA/B proteins from infected epithelial cells, and thereby potently provoke NKG2D evasion.

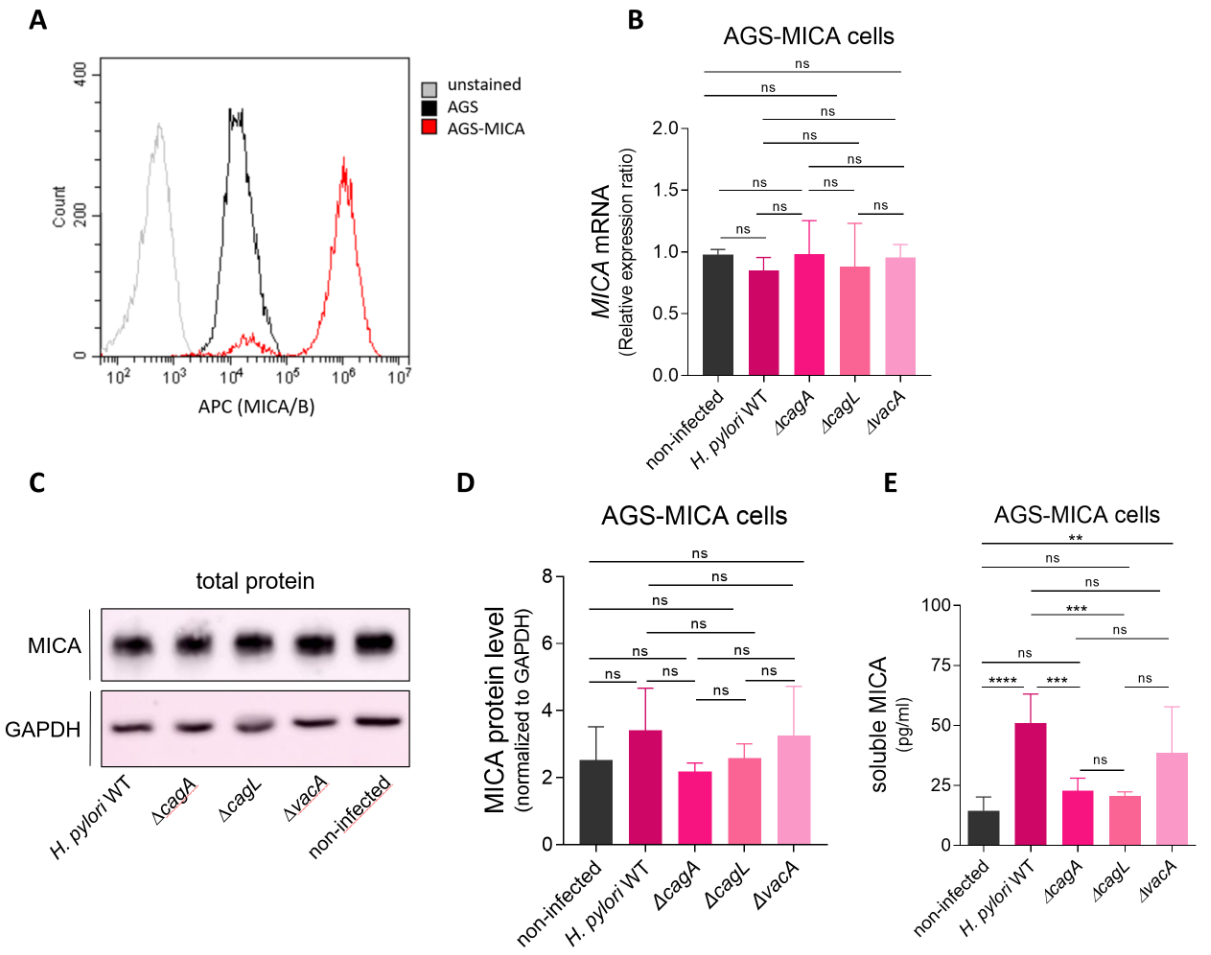

Figure 14. Release of soluble MICA is induced by *H. pylori*, independent of its effect on *MICA* gene expression. (A) Gastric epithelial cell line AGS was transfected to stably express *MICA*, thereby creating AGS-MICA transfectants. MICA/B cell surface expression of AGS cells (grey line) and AGS-MICA transfectants (red line) was determined by Flow cytometry. (B) AGS-MICA transfectants were infected with *H. pylori* wild-type (WT) or isogenic mutants *ΔcagA, ΔcagL, ΔvacA* for 24 h. *MICA* gene expression was determined by qPCR analysis. The results are presented as the relative expression ratio of gene expression after treatment versus baseline gene expression (pre-treatment). (C) MICA protein in cell lysates was determined by Western Blot. (D) Western Blot band intensities were quantified using Image Lab Software (Bio-Rad). (E) Soluble MICA protein in cell culture supernatants was determined by ELISA. Mean +/- SD. One-way ANOVA and Tukey's test. Reproduced with modifications from Anthofer et al., Front Immunol, 2024 with permission through the Creative Commons Attribution licence CC-BY, version 4.0.

3.6. *H. pylori* reduces cell surface MICA/B expression on gastric epithelial cells and induces the accumulation of MICA/B protein in the lamina propria

A major outcome of soluble release of NKG2D-Ls as an evasion strategy is the reduction of cell-associated MICA/B protein, which makes cells less susceptible to detection and eradication by NKG2D-expressing killer cells (173). We aimed to analyze the long-term effect of *H. pylori* infection on cell-associated MICA/B protein on stomach epithelial cells. To do this we infected AGS-MICA cells with the *H. pylori* WT for 24 h, 48 h and 72 h and subjected them to immunofluorescence staining of total cellular MICA/B protein and flow cytometry staining of cell surface MICA/B. MICA/B protein expression mainly localized to the cell membranes, as indicated by the honeycomb-like staining pattern (Figure 15A). After a longer infection period, MICA staining intensities increased at the cell borders of control cells, suggesting that these cells accumulated MICA/B protein at the cell membrane over time. In *H. pylori*-infected cells, however, staining intensities for MICA/B remained relatively stable over time, indicating that these cells did not accumulate MICA/B protein, likely because of continuous shedding. A quantification of staining intensities resulted in a statistically significant difference between *H. pylori*-infected and non-infected cells, after 72 h (Figure 15B). Flow cytometry analysis confirmed these observations with no differences in cell surface MICA/B staining after 24 h and 48 h and a significantly increased cell surface MICA/B staining in control cells, compared to *H. pylori*-infected cells, after 72 h of infection (Figure 15C).

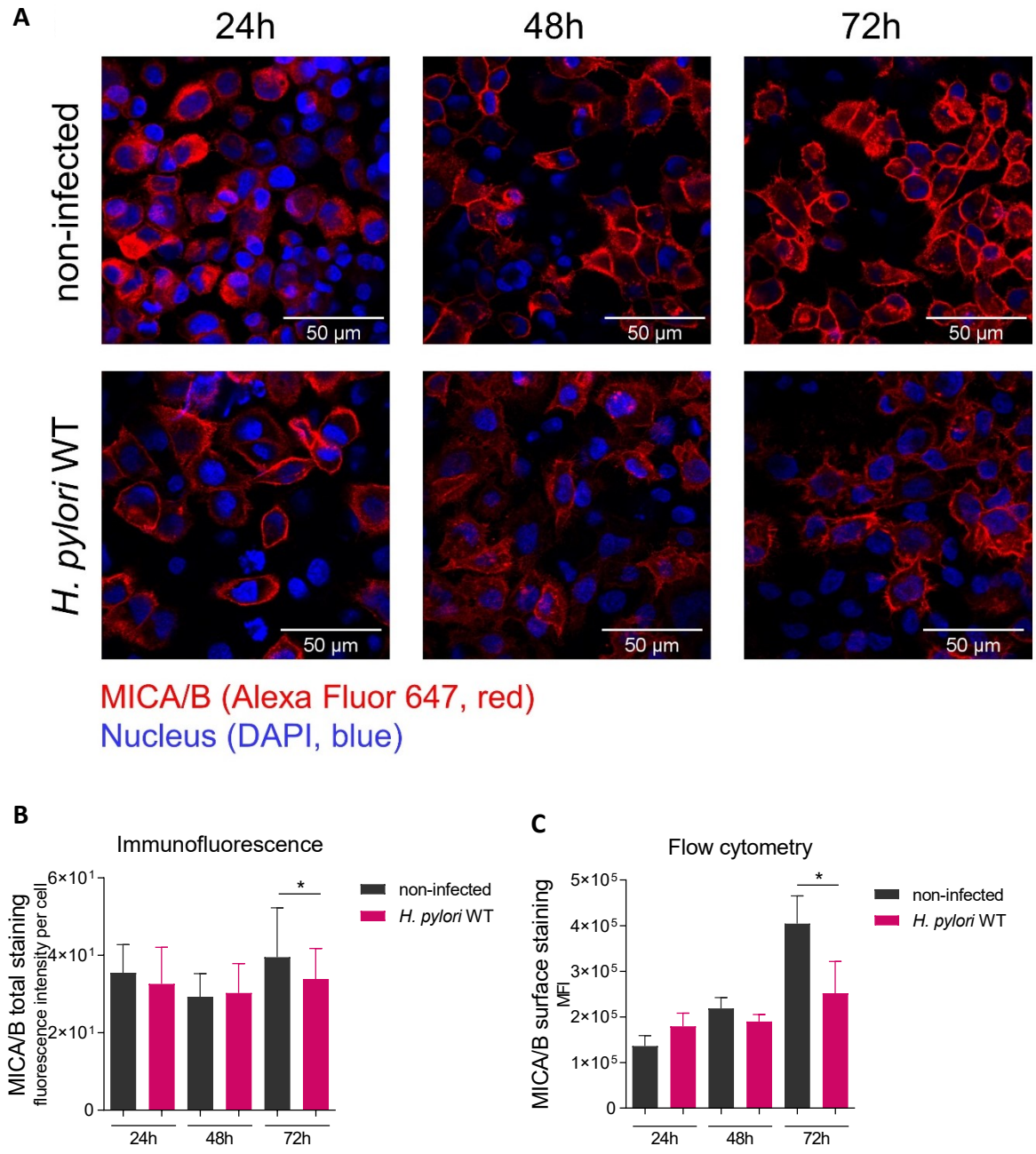

Figure 15. *H. pylori* reduces cell surface MICA/B expression on gastric epithelial cell lines. AGS-MICA cells were infected with *H. pylori* WT for 24 h, 48 h and 72 h. (A-B) Total cellular MICA/B protein was visualized by immunofluorescence staining with an α-MICA/B antibody (red) and DAPI (blue). Representative images are shown in A and quantification is shown in B (T test of infected cells compared to non-infected cells at each timepoint). (C) MICA/B cell surface expression was quantified by flow cytometry (T test of infected cells compared to non-infected cells at each timepoint. Reproduced with modifications from Anthofer et al., Front Immunol, 2024 with permission through the Creative Commons Attribution licence CC-BY, version 4.0.

Next, to analyze the distribution of MICA/B protein expression in *H. pylori* infection *in vivo*, we subjected fresh frozen HpG Biopsies to immunohistochemical staining of MICA/B (Figure 16). Great levels of MICA/B staining were observed in the lamina propria, and the staining appeared both as cell-associated (arrow) and as 'free' (arrowhead) (Figure 16). 'Free' MICA/B staining appeared as a staining-rim below the basal site of epithelial cells and possibly represents soluble MICA/B proteins that were released from infected epithelial cells and which can shield epithelia from NKG2D-expressing effector cells. Cell-associated MICA/B staining in the lamina propria might occur due to the binding of soluble MICA/B to NKG2D and might also be due to MICA/B expression of immune cells. In pathologies such as celiac disease and Crohn's disease, NKG2D ligand expression was reported in B cells, plasma cells, CD4+ T cells, macrophages and dendritic cells (241–243) and was associated with either immunostimulatory or immunosuppressive effects on NKG2D+ effector cells, depending on the distribution and level of NKG2D ligand expression (244,245)

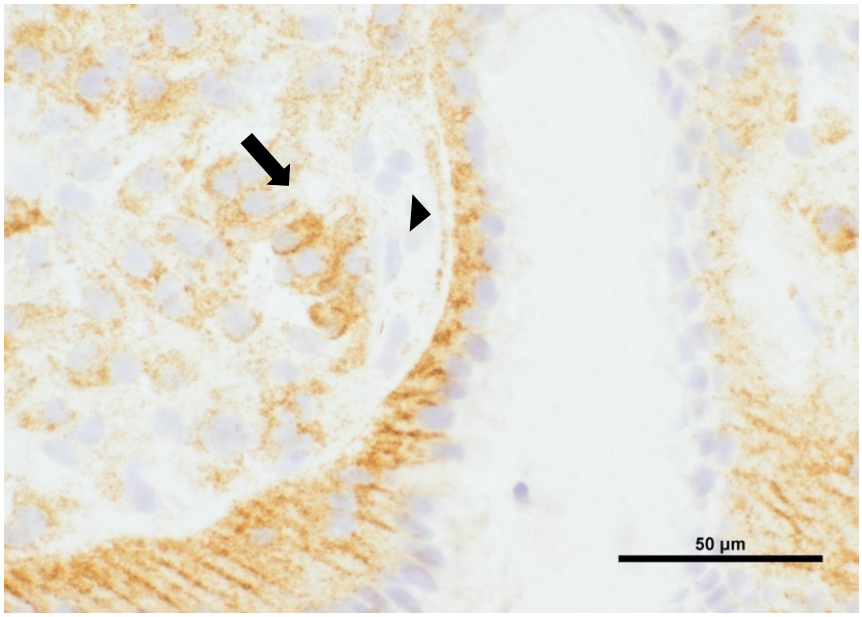

Figure 16. Visualization of MICA/B protein distribution in *H. pylori* gastritis. Representative image of IHC staining of MICA/B in frozen HpG biopsies, (arrow pointing out cell-associated MICA/B and arrowhead highlighting 'free' MICA/B); scale bar: 50µm. Reproduced with modifications from Anthofer et al., Front Immunol, 2024 with permission through the Creative Commons Attribution licence CC-BY, version 4.0.

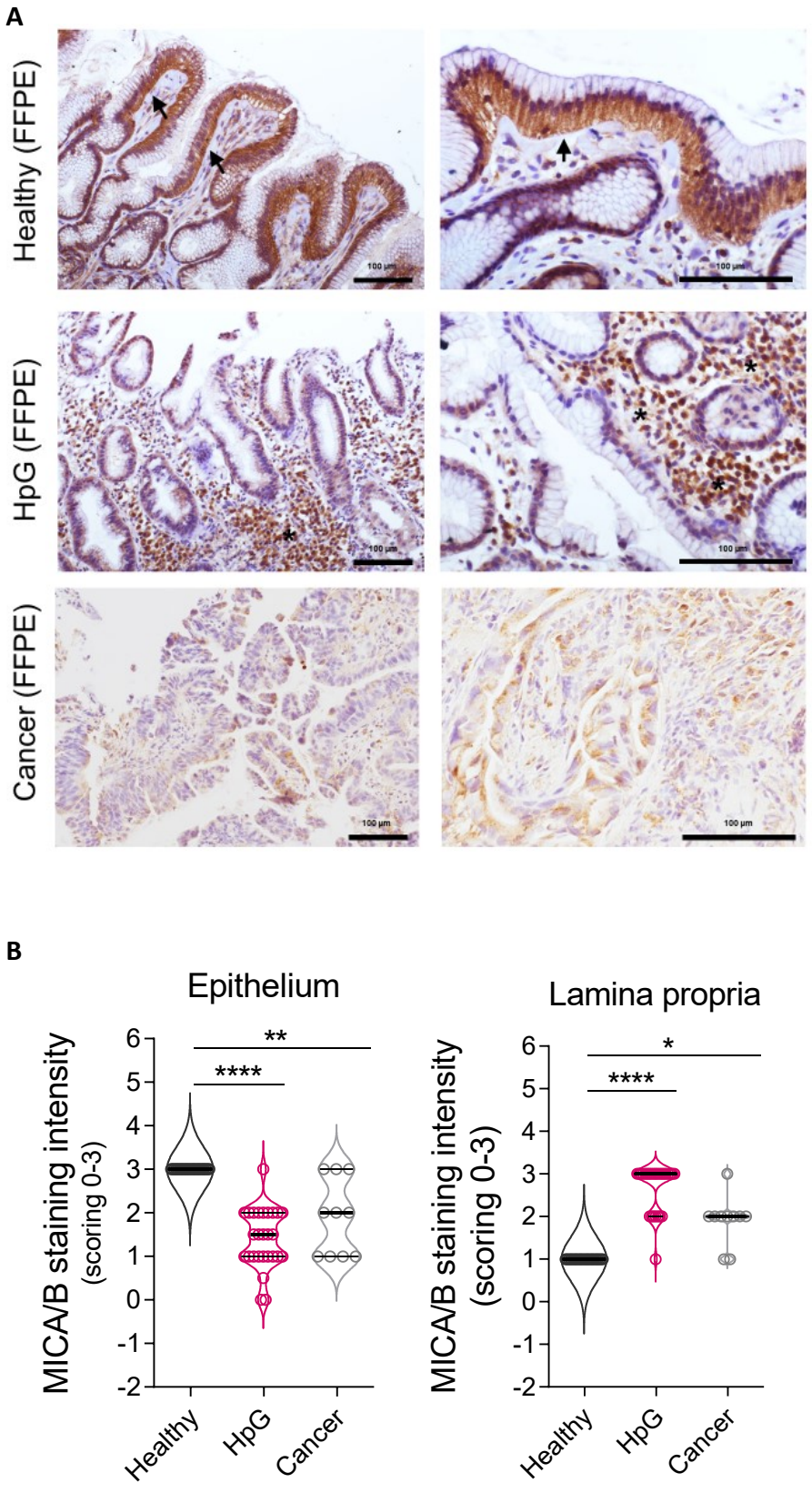

Figure 17. *H. pylori* reduces cell surface MICA/B expression on gastric epithelial cells, and induces the accumulation of MICA/B protein in the lamina propria, *in vivo*. (A) Stomach corpus and antrum biopsies (FFPE) of healthy controls (Healthy), *H. pylori* gastritis (HpG) and gastric adenocarcinoma (Cancer) were subjected to immunohistochemical staining of MICA/B. Representative images with

arrows indicating basolateral epithelial staining and stars indicating lamina propria staining; scale bars are 100µm. (B) Quantification of IHC staining by scoring of MICA/B staining intensity at the epithelia and in the lamina propria (values 0-3), n=10-27 per group, the data do not follow normal distribution, violin plots (median, quartiles and all points), Kruskal-Wallis test and Dunn's multiple comparisons test. Quantification was done by Gregor Gorkiewicz. Reproduced with modifications from Anthofer et al., Front Immunol, 2024 with permission through the Creative Commons Attribution licence CC-BY, version 4.0.

To quantify the effect of *H. pylori* infection on MICA/B protein expression *in vivo*, we then subjected a sample set of gastric FFPE tissue specimens from healthy controls, patients with HpG and patients with stomach cancer to immunohistochemical staining of MICA/B (Figure 17A, B). Control tissues showed strong epithelial expression (arrow), which was mainly at a baso-lateral location. This observation confirms previous reports of MICA/B expression in healthy gastric epithelial cells (108,109) and possibly demonstrates a constant readiness of epithelial cells, to respond to stress. In the lamina propria, positive signals were rare in healthy tissues. HpG cases demonstrated a significant reduction of epithelial expression and showed a significant increase in lamina propria staining (stars). Cancer cases showed similar changes compared to healthy controls, with reduced epithelial staining and increased lamina propria staining, albeit to a lesser extent than in HpG.

Since our earlier cell culture experiments had shown, that MICA/B modulation was associated with the main *H. pylori* virulence factors CagA and VacA, we next aimed to determine a potential CagA/VacA-association of MICA/B modulation in human tissues. For this purpose, we genotyped *H. pylori* genes in our sample set, concerning *vacA* allele types (s1/2, m1/2 and i1/2). The *cagA* status (positive/negative) had been previously characterized for this sample set. The *cagA* gene may be absent or present in *H. pylori* and strains encoding *cagA* are more virulent (29). All *H. pylori* strains carry the *vacA* gene, but genetic variations exist in the signal region (genotypes s1 and s2) and in the mid region (genotypes m1 and m2) and in the intermediate region (genotypes i1 and i2). The alleles s1, m1 and i1 are associated with an increased risk for gastric carcinoma (38–41). After completing the genotyping of our sample set, we observed interesting associations between the *H. pylori* virulence factor genotypes: The majority of *cagA* positive strains carried the more pathogenic *vacA* allele s1 (97%), while the *cagA* negative strains were more frequently of the *vacA* s2 genotype (70%, P<0,0001) (Table 2). The *vacA* m1 allele was more common in *cagA*-positive strains (61%),

and conversely the m2 allele was more frequently found in the *cagA*-negative strains (80%, P=0,0077). Furthermore, the *cagA* positive strains were also more frequently of the *vacA* i1 genotype (75%), while *cagA* negative strains were more commonly of the *vacA* i2 genotype (78%, P=0,0168). These results demonstrated a strong association between *cagA* and *vacA* s, m and i genotypes and confirmed earlier reports of these virulence factor associations (41).

Table 2. Relationship between *H. pylori cagA* status and the genotypes of the *vacA* s, m and i region.

	Frequency of allele by region (no. of strains [%])					
	vacA s region		*vacA* m region		*vacA* i region	
	s1	s2	m1	m2	i1	i2
cagA positive	28 [97 %]	1 [3 %]	17 [61 %]	11 [39 %]	12 [75 %]	4 [25 %]
cagA negative	6 [30 %]	14 [70 %]	4 [20 %]	16 [80%]	2 [22 %]	7 [78 %]
P value[a]		<0,0001		0,0077		0,0168

[a] Fisher's exact test. Only the single genotypes for the *vacA* s, m, and i regions were included in this analysis.

Next, we analyzed the results of the MICA/B immunohistochemistry scoring in consideration of the *cagA* and *vacA* genotypes (Figure 18). Patients infected with *cagA*-positive and *cagA*-negative *H. pylori* strains demonstrated significantly lower epithelial MICA/B staining and higher lamina propria MICA/B staining, compared to healthy controls (Figure 18A). There was no significant difference in MICA/B immunohistochemical staining between patients infected with *cagA*-positive and *cagA*-negative *H. pylori* strains. Yet, patients infected with *cagA*-positive *H. pylori* strains showed slightly higher epithelial MICA/B staining and a trend towards lower lamina propria staining, compared to patients infected with *cagA*-positive *H. pylori* strains, suggesting that *cagA* might contribute to the translocation of MICA/B proteins from the epithelia to the lamina propria *in vivo*. A larger sample set would be required to examine this phenomenon in more detail. Regarding *vacA* genotypes, no significant differences in MICA/B epithelial- and lamina propria staining were observed between s1 and s2, between m1 and m2 and between i1 and i2 genotypes (Figure 18B). These results indicate that *vacA* genotypes seem to play no relevant role in the translocation of MICA/B from epithelia to the lamina propria.

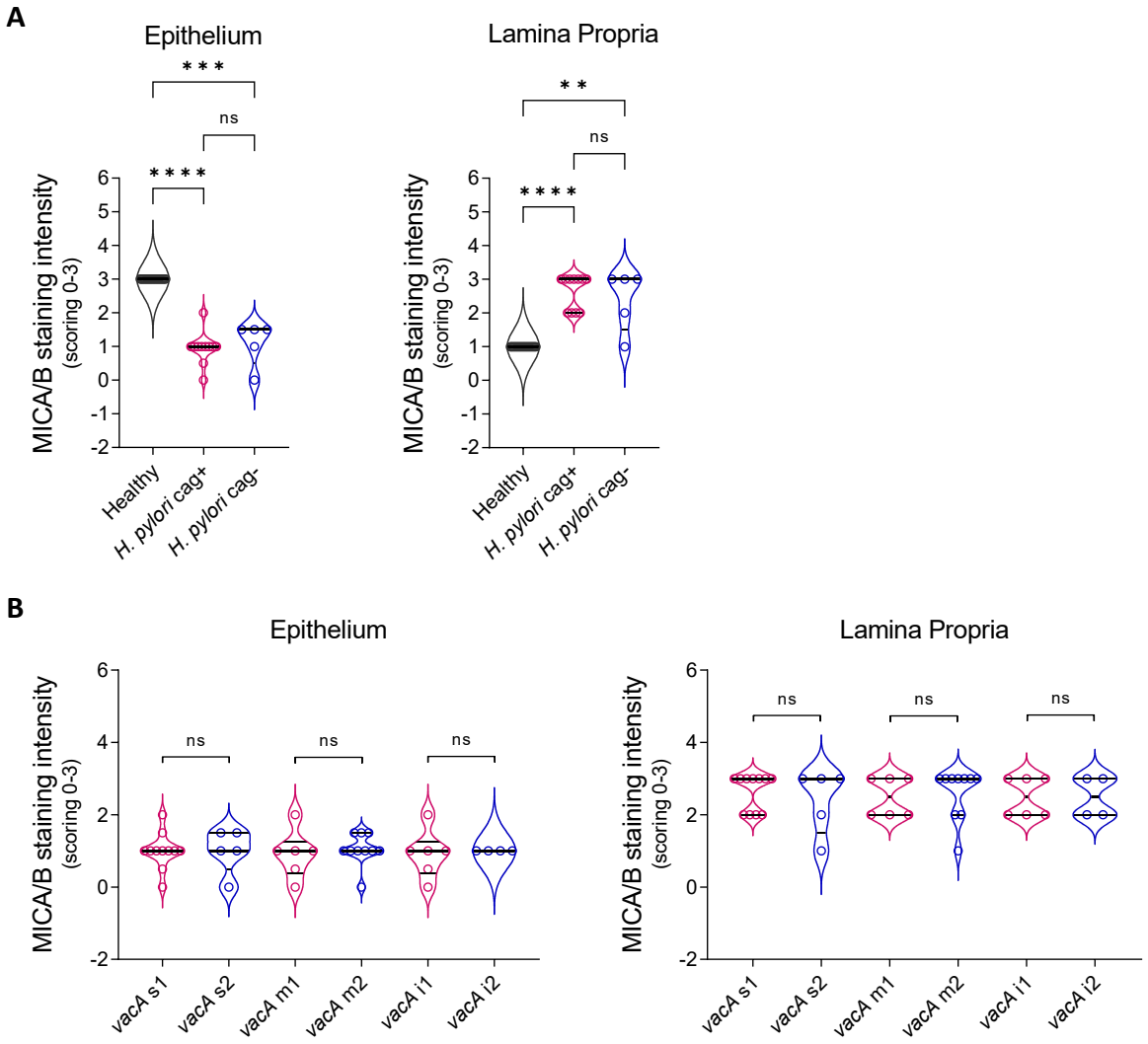

Figure 18. Association between *H. pylori cagA* and *vacA* genotypes and MICA/B distribution in *H. pylori* gastritis tissues. Stomach corpus and antrum biopsies (FFPE) of healthy controls (Healthy) and *H. pylori* gastritis (HpG) of defined *cagA* status (A) and *vacA* s, m and i genotypes (B) were subjected to Immunohistochemical staining of MICA/B. Quantification of IHC staining by scoring of MICA/B staining intensity at the epithelia and in the lamina propria (values 0-3), the data do not follow normal distribution, violin plots (median, quartiles and all points). Kruskal-Wallis test with Dunn's multiple comparisons test was used in A and Mann Whitney test was used in B.

Taken together, these data demonstrate that *H. pylori* infection leads to a reduction of cell-associated MICA/B protein at the infected epithelial cells, *in vitro* and *in vivo*. A reduction in surface expression of NKG2D-Ls has the potential to protect *H. pylori*-infected epithelial cells from eradication by NKG2D+ effector cells and could thereby contribute to keeping *H. pylori's*

living habitat intact. In addition, we found that MICA/B proteins accumulate in the lamina propria *in vivo,* where they could encounter with NKG2D+ lymphocytes and act as NKG2D-repressors.

3.7. Soluble MICA/B proteins in *H. pylori* infection reduce NKG2D surface expression and cytotoxic degranulation of NK cells

Soluble MICA/B molecules are known to act as repressors of NKG2D. They reduce the surface expression of NKG2D and, consequently, dampen NKG2D-associated cell functions, in NKG2D+ leucocytes. We aimed to analyze whether the soluble MICA/B proteins, that are released form *H. pylori* infected epithelial cells, influence NKG2D+ leucocytes. For this purpose, we aimed to challenge an NKG2D-expressing leucocyte cell line with cell culture supernatants from *H. pylori*-infected gastric epithelial cells (Figure 19).

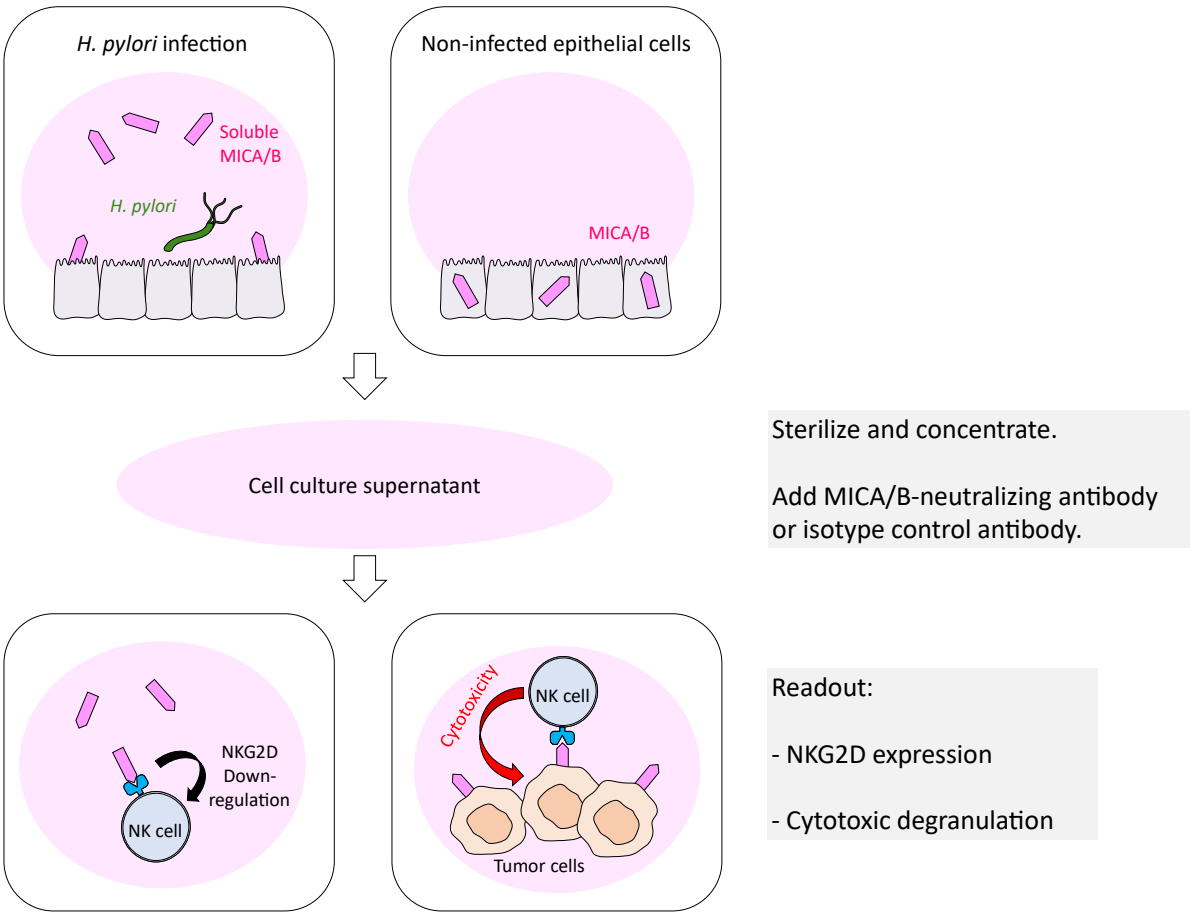

Figure 19. Experimental workflow for assessing the effect of soluble MICA/B in cell culture supernatants of *H. pylori*-infected stomach epithelial cells, on NKG2D-expression and cytotoxic degranulation of NKG2D-bearing cytotoxic leucocytes. Stomach epithelial cells were infected with *H. pylori* WT or left untreated. After 48 h, cell culture supernatants were filter-sterilized and concentrated and a neutralizing anti-MICA/B antibody (=α-MICA/B) or an Isotype control antibody were added. NK cells were challenged with these supernatants for 24 h and NKG2D expression was assessed by Flow cytometry. To determine cytotoxic degranulation, pre-treated NK cells were co-cultivated with tumor target cells and cytotoxic degranulation was assessed by flow cytometry. This image was created with Microsoft PowerPoint and contains elements from Servier Medical Art (https://smart.servier.com/), adapted with permission through the Creative Commons Attribution licence CC-BY, version 4.0 (https://creativecommons.org/licenses/by/4.0/).

As a model for NKG2D+ leucocytes, we used an NK cell line, since cytotoxicity of NK cells can be directly activated via NKG2D, while in CTLs, NKG2D acts only as a costimulatory signal for TCR activation (106). The cell line NKL expresses NKG2D and is frequently used in assays for the analysis of NKG2D regulation and stimulation (105,246–248). As treatment we used cell culture supernatants from AGS-MICA transfectants since these supernatants, contained greater levels of soluble MICA/B than those of MKN28 and non-transfected AGS cells, making them the most potent effectors for our experimental setup. In addition, AGS-MICA cells were expected to produce lower levels of other soluble NKG2D-mediators (ULBPs), compared to MKN28 (see Figure 13), which would be beneficial for specifically studying the effect of soluble MICA/B on NKG2D. We infected AGS-MICA cells with *H. pylori* P12 WT or left cells untreated for 48 h, then harvested the supernatants. We filter-sterilized the supernatants in order to study the effect of the soluble components in the supernatants, independent of potential effects of direct contact between *H. pylori* and NK cells. We also concentrated the cell culture supernatants with concentrating-filter-devices and used different concentrations, in order to determine whether the effect would be dose-dependent. Subsequently, we treated NKL cells with these supernatants for 24 h. During the NK cell treatment, we added a neutralizing anti-MICA/B antibody (=α-MICA/B) to block the effects of soluble MICA/B in the supernatants. Alternatively, we used an isotype control antibody (=Isotype). After 24 h of challenge, we analyzed cell surface expression of NK cell proteins by flow cytometry.

Expression of the NK cell surface marker CD94 was not affected by any treatment (Figure 20A) which assures that changes in surface proteins are specific and not due to general rearrangements of NK cell surface proteins. NKG2D surface expression was reduced by treatment with supernatant from non-infected AGS-MICA cells (+ Isotype), compared to untreated NK cells, and was reduced even further by treatment with supernatant from *H. pylori*-infected AGS-MICA cells (+ Isotype), in a dose-dependent manner (Figure 20B, C, D). Addition of the α-MICA/B antibody significantly elevated NKG2D expression in both treatment groups, indicating that soluble MICA/B in the cell culture supernatants was causative for the reduction of NKG2D expression. Interestingly, in NK cells treated with *H. pylori*-infected supernatant, the addition of the α-MICA/B antibody did not recover NKG2D expression up to the level of untreated NK cells. This suggests that additional factors in the supernatants of *H. pylori*-infected cells contribute to NKG2D reduction. This might be attributed to other NKG2D-mediators (e.g. TGF-β) that are potentially also induced in *H. pylori*-infected cells, as well as soluble factors secreted by *H. pylori*.

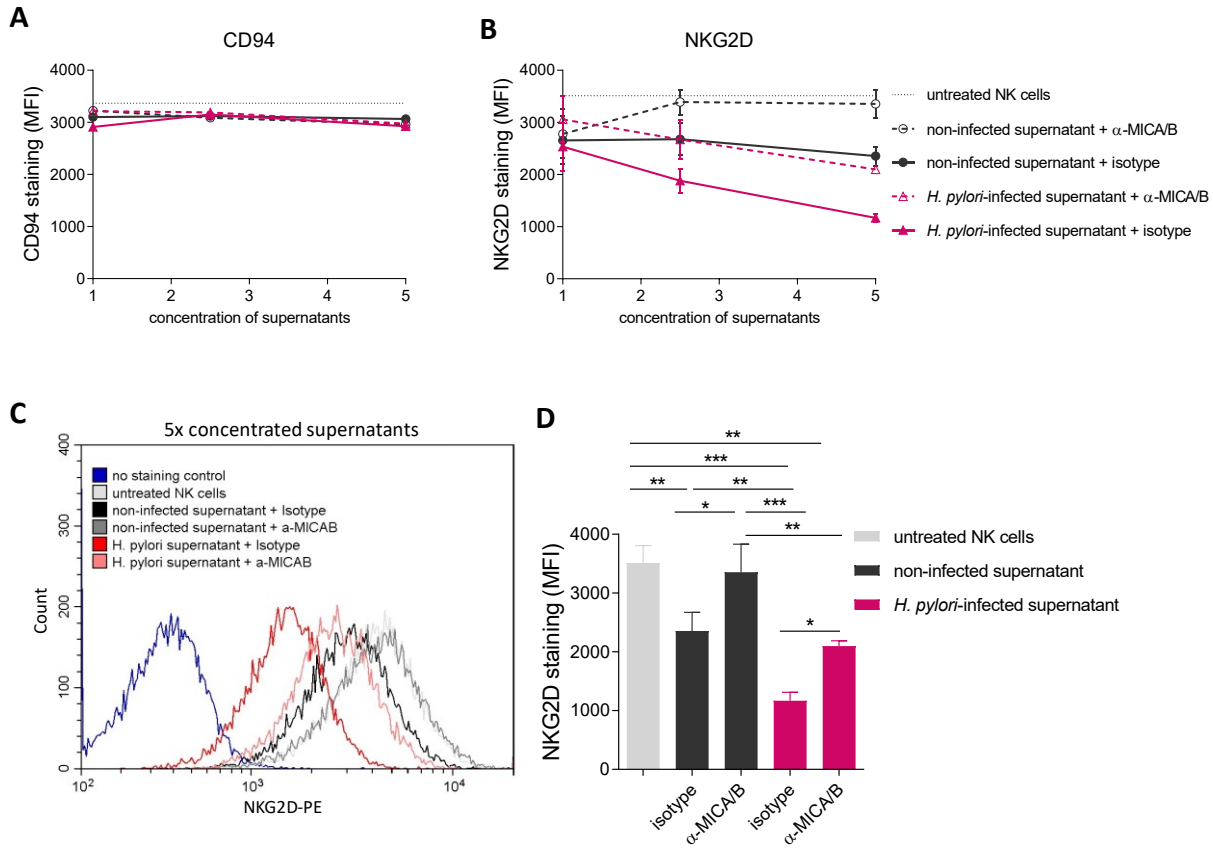

Figure 20. Soluble MICA/B proteins in *H. pylori* infection reduce NKG2D surface expression of NK cells. (A-B) The NK cell line NKL was challenged with filter-sterilized cell culture supernatants

from *H. pylori*-infected or non-infected AGS-MICA cells at three concentrations (1x/2,5x/5x). A neutralizing α-MICA/B antibody or an isotype control antibody were added to the cultures. After 24 h, surface expressions of CD94 (A) and NKG2D (B) were analyzed by Flow cytometry. (C-D) NKG2D expression after treatment with 5x concentrated supernatants is shown in C (raw data plots) and D (quantification). Mean +/- SD, One-way ANOVA and Tukey's test. Reproduced with modifications from Anthofer et al., Front Immunol, 2024 with permission through the Creative Commons Attribution licence CC-BY, version 4.0.

To analyze the functional consequence of the observed NKG2D-reduction we treated NKL cells as described above and subsequently co-cultivated them with K562 cells for 2 h. K562 is a tumor cell line that is typically used as target cell line in assays for the analysis of NK cell cytotoxicity (247,248). Cytotoxicity of NKL cells towards K562 cells is mostly mediated by NKG2D (249). We measured LAMP-1 expression on the cell surface of NKL cells as a marker of NK cell degranulation (163). When NK cells get activated, they release the contents of intracellular granules. These granules may contain cell-killing proteins such as perforin, granzymes and granulysin which kill target cells (99). Therefore, LAMP-1 as a marker for degranulation is often used as an indirect marker of NK cell cytotoxic activity (163). In addition, cytokines may also be released during degranulation (250). Untreated NK cells were induced to express LAMP-1 after co-cultivation with K562 cells, representing the activation of NK cells during contact with tumor cells. (Figure 21A, B). The percentage of LAMP-1+ NK cells was severely reduced by pre-treatment with non-infected supernatant (+ Isotype) and even further reduced by pre-treatment with *H. pylori*-infected supernatant (+Isotype), compared to untreated NK cells. Addition of the α-MICA/B antibody significantly elevated the percentage of LAMP-1+ NK cells in the *H. pylori* treatment group, indicating that soluble MICA/B proteins in the cell culture supernatant were responsible for the reduction of LAMP-1+ NK cells. Interestingly, addition of the α-MICA/B antibody did not elevate the percentage of LAMP-1+ NK cells up to the level of untreated NK cells, neither in the *H. pylori*-infected nor in the non-infected treatment group. This indicates that other factors in the cell culture supernatant of AGS-MICA cells additionally reduced NK cell activation, independent of the NKG2D axis and *H. pylori* infection.

Taken together, these data demonstrate that the cell culture supernatants of the cell line AGS-MICA caused a reduction of NKG2D surface expression and a reduction of cytotoxic activity of NK cells towards tumor cells. *H. pylori* infection of these epithelial cells significantly

intensified these effects of their supernatants on NK cells, by the action of soluble MICA/B. This shows that soluble MICA/B proteins, released from *H. pylori*-infected stomach epithelial cells, have a functional consequence on NKG2D expression and cytotoxic activity of NK cells.

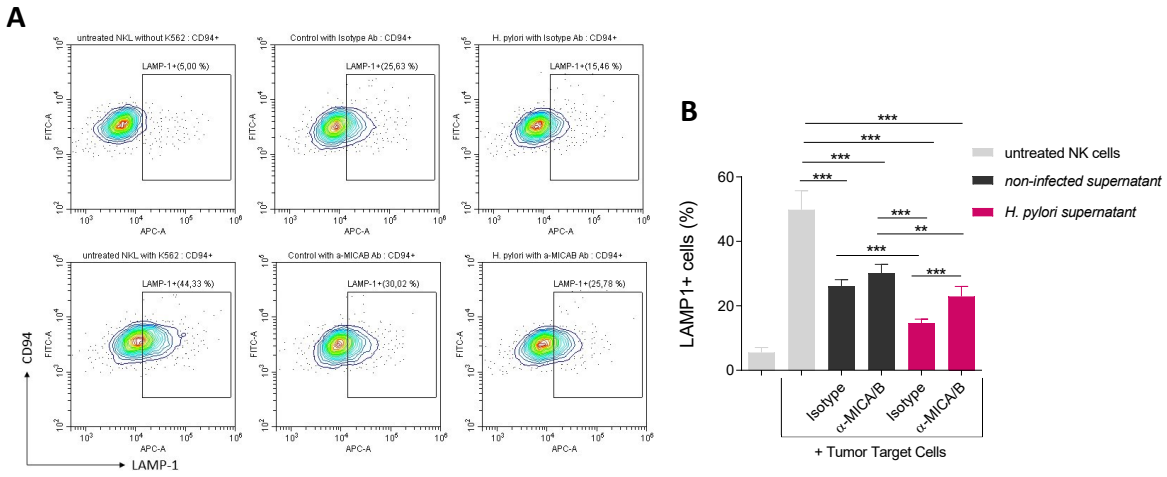

Figure 21. Soluble MICA/B proteins in *H. pylori* infection reduce cytotoxic degranulation of NK cells. NKL cells were treated with 5x concentrated supernatants as described above and then co-cultivated with target cell line K562 for 2 h. Percent of LAMP-1+ of CD94+ cells was determined by Flow cytometry. (A) Raw data plots and (B) quantification. Mean +/- SD. One-way ANOVA and Tukey's test. Reproduced with modifications from Anthofer et al., Front Immunol, 2024 with permission through the Creative Commons Attribution licence CC-BY, version 4.0.

3.8. Soluble MICA and MICB in *H. pylori* infection are released by proteolytic shedding

After having determined that *H. pylori*-induced soluble MICA/B proteins have a functional consequence on immune cell activity we aimed to better understand the molecular mechanisms underlying soluble release of MICA/B. Soluble MICA and MICB are typically released from the cell surface via ectodomain shedding that is mediated by proteases of the matrix metalloproteases (MMP) or proteases of the a disintegrin and metalloprotease (ADAM) family (251) (Figure 22). In contrast, the frequent MICA allele (MICA*008/A5.1), which occurs in about 42% of Caucasians (126,252), is not cleavable by proteases, but is released on extracellular vesicles (EVs) instead, specifically on exosomes (215). This is due to a single nucleotide insertion in the transmembrane domain and consequently a frame shift that leads to

an early stop codon. The truncated protein acquires a GPI (glycosylphosphatidylinositol) anchor that determines various distinct biological features of this MICA allele, including trafficking, localization and exosome release (215).

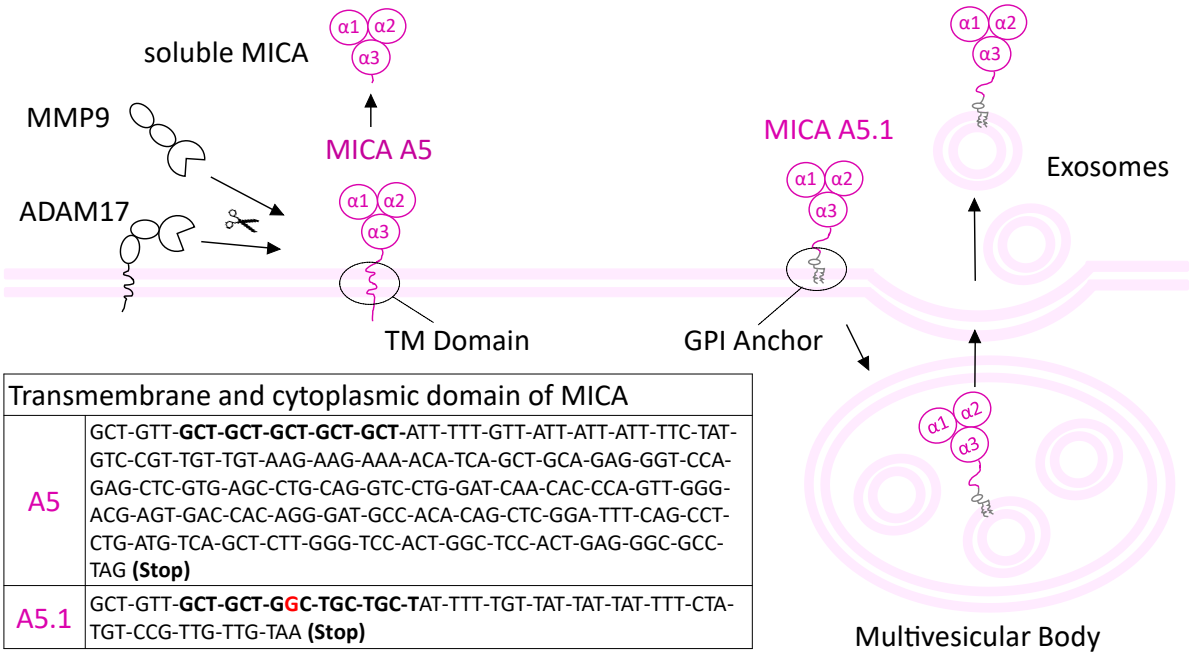

Transmembrane and cytoplasmic domain of MICA	
A5	GCT-GTT-**GCT-GCT-GCT-GCT-GCT**-ATT-TTT-GTT-ATT-ATT-ATT-TTC-TAT-GTC-CGT-TGT-TGT-AAG-AAG-AAA-ACA-TCA-GCT-GCA-GAG-GGT-CCA-GAG-CTC-GTG-AGC-CTG-CAG-GTC-CTG-GAT-CAA-CAC-CCA-GTT-GGG-ACG-AGT-GAC-CAC-AGG-GAT-GCC-ACA-CAG-CTC-GGA-TTT-CAG-CCT-CTG-ATG-TCA-GCT-CTT-GGG-TCC-ACT-GGC-TCC-ACT-GAG-GGC-GCC-TAG **(Stop)**
A5.1	GCT-GTT-**GCT-GCT-GGC-TGC-TGC-T**AT-TTT-TGT-TAT-TAT-TAT-TTT-CTA-TGT-CCG-TTG-TTG-TAA **(Stop)**

Figure 22. Graphical scheme demonstrating the mechanisms of soluble release of different MICA alleles. All full-length MICA alleles, such as MICA A5, are released as soluble proteins via metalloprotease-mediated shedding. The allele MICA A5.1 is truncated due to a single nucleotide insertion in the short tandem repeat in the transmembrane (TM) domain that leads to an early stop codon. This allelic variant is attached to the membrane with a GPI anchor and is not susceptible to shedding but can be released on extracellular vesicles (EVs), specifically on exosomes. (The passage of MICA A5.1 through MVBs, shown in this scheme, is hypothetical and has not been experimentally demonstrated to date.) This image was created with Microsoft PowerPoint. Reproduced with modifications from Anthofer et al., Front Immunol, 2024 with permission through the Creative Commons Attribution licence CC-BY, version 4.0.

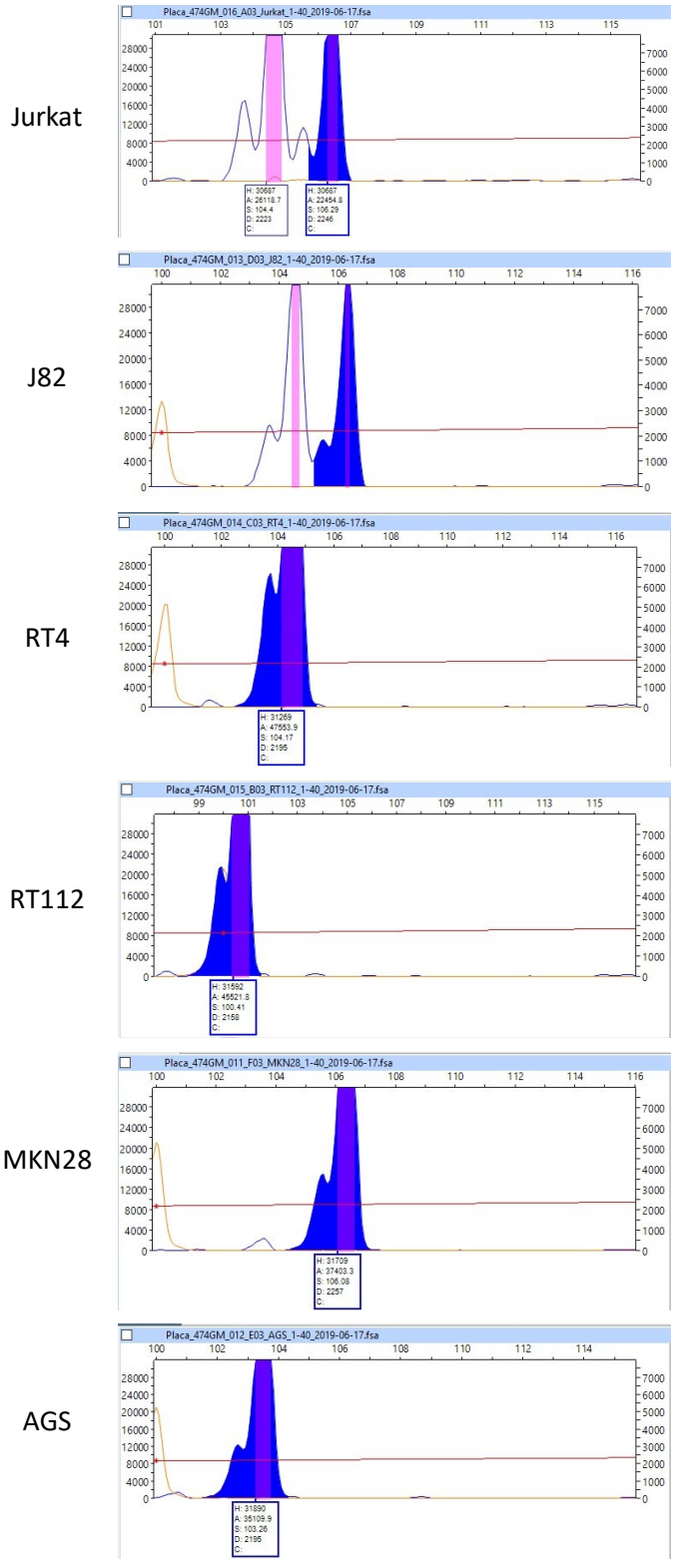

Figure 23. Genotyping of the microsatellite repeat polymorphism in the transmembrane region of the MICA gene. MKN28 and AGS cells were subjected to genotyping as described by Gonzalez et al. (234). As controls, the cell lines Jurkat, J82, RT4 and RT112, with known genotypes, were included in the analysis. Here the fragment sizes of the cell lines are shown as displayed by the Peak Scanner v1.0 software (Applied Biosystems).

To identify, by which mechanism *H. pylori* might induce the release of soluble MICA in the cell lines used in this study, we performed genotyping of the transmembrane domain of MICA in MKN28 and AGS cells. As control cell lines with known MICA alleles, DNA from the cell lines Jurkat (A5.1/A6), J82 (A5.1/A6), RT4 (A5.1) and RT112 (A4) was used. The observed fragment sizes of the amplified PCR products differed slightly from previous reports (234) but with the use of the control cell lines genotyping was possible (Figure 23 and Table 3). We identified MKN28 and AGS cell lines to be homozygous for the alleles A5 (AGS) and A6 (MKN28), both alleles with a full-length transmembrane region that are prone to release via proteolytic shedding. Also the AGS-MICA transfectants created in this study encode a full-length MICA allele (215). Concerning MICB, no EV-associated alleles are known so far.

Table 3. Genotyping of the microsatellite repeat polymorphism in the transmembrane region of the *MICA* gene. MKN28 and AGS cells and the control cell lines Jurkat, J82, RT4 and RT112 were subjected to genotyping. Shown are the expected fragment sizes according to Gonzalez et al. (234), the observed fragment sizes from the last study in this lab and from this study and the corresponding MICA alleles.

Cell line	**Expected size [bp]** (234)	**Observed size, last study in this lab [bp]**	**Observed size, this study [bp]**	**MICA Allele**
Jurkat	108/110	103/105	104/106	A5.1/A6
J82	108/110	103/105	104/106	A5.1/A6
RT4	108	103	104	A5.1
RT112	104	99	100	A4
MKN28			106	A6
AGS			103	A5

To determine experimentally, whether MICA and MICB are released as soluble proteins or via exosomes in *H. pylori* infection, we harvested cell culture supernatants from *H. pylori*-infected and non-infected MKN28 and AGS cells and performed a sequential centrifugation protocol to obtain exosome-enriched preparations (Figure 24). This protocol uses sequential centrifugation steps to separate small extracellular vesicles (especially exosomes with a size of

30-150 nm) from other components in the cell culture supernatant such as cell debris, larger particles, larger EVs and apoptotic bodies. Of note, the yield of this method is quite low and the protocol only enables an enrichment of exosomes (214). However, contrary to other isolation methods, such as commercial kits, the exosomes are assumed to be pure after isolation with ultracentrifugation (253). Therefore sequential centrifugation remains the gold standard among the available techniques for exosome isolation (214).

To confirm successful exosome enrichment, we subjected exosome-enriched preparations to electron microscopy (Figure 25). We observed intact vesicles with visible lipid bilayers. Their sizes were between 25 and 75 nm, which is within the typical size range of exosomes (214).

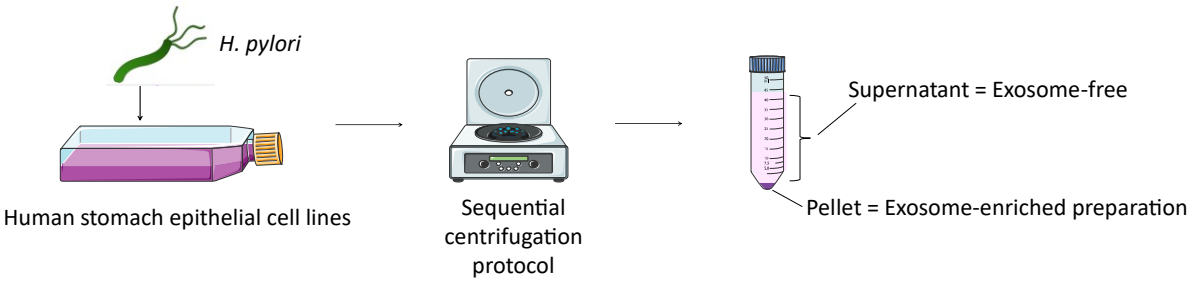

Figure 24. Experimental workflow for producing exosome-enriched preparations and exosome-free supernatants from cell culture media of *H. pylori*-infected human stomach epithelial cell lines (simplified). Cells were cultured with or without *H. pylori* WT for 48 h, then cell culture supernatants were subjected to a sequential centrifugation protocol to obtain exosome-enriched preparations (= pellet after final centrifugation step at 100.000 g) and exosome-free supernatants (= supernatant after final centrifugation step at 100.000 g). This image was created with Microsoft PowerPoint and contains elements from Servier Medical Art (https://smart.servier.com/), adapted with permission through the Creative Commons Attribution licence CC-BY, version 4.0 (https://creativecommons.org/licenses/by/4.0/).

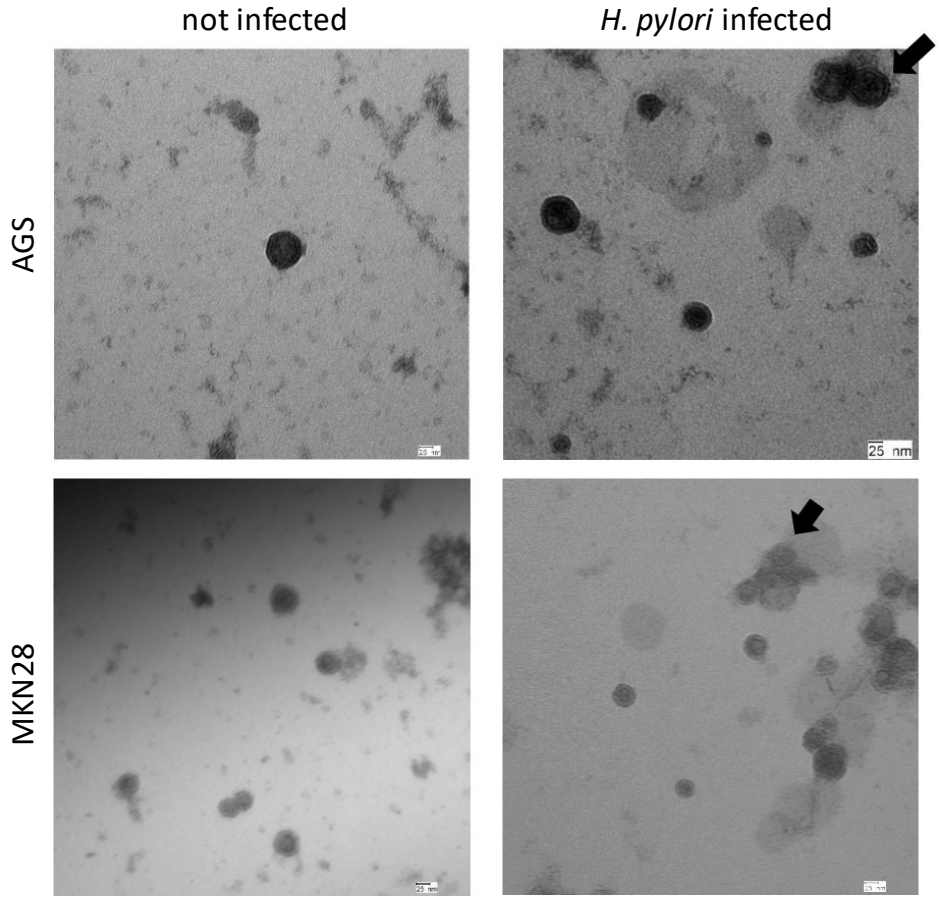

Figure 25. Electron microscopy of exosome-enriched preparations from not infected and infected AGS and MKN28 cells. Scale bars are 25nm. Arrows indicating visible lipid bilayers. (Iris Kufferath from the Institute of Pathology performed visualization of exosomes by electron microscopy.) Reproduced with modifications from Anthofer et al., Front Immunol, 2024 with permission through the Creative Commons Attribution licence CC-BY, version 4.0.

Next, we determined particle counts using NanoSight technology. For both cell lines, the particle count was greater in exosome-enriched preparations from *H. pylori*-infected cells (Table 4), suggesting that *H. pylori* infection could potentially increase exosome production. More in-depth analyses would be required to confirm this hypothesis. Next, to assess MICA and MICB protein amounts in these exosome-enriched preparations as well as in the exosome-free supernatants and in total cell lysates, we performed western blot analysis (Figure 26 and Figure 27). All samples were PNGase digested in order to deglycosylize MICA and MICB proteins, which is necessary to determine the exact sizes of these proteins by Western Blot (206,215). For cell lysates and exosome-free supernatants we loaded 20 µg of total protein per slot. For exosome-enriched preparations, a defined number of particles per slot was loaded on

the gel in order to determine whether *H. pylori* infection increases the amount of MICA/B protein per exosome – see calculation in Table 4.

Table 4. Particle counts in exosome-preparations of not-infected and *H. pylori*-infected AGS and MKN28 cells, determined by Nanosight technology and calculations for western blot.

Cell line	Treatment group	Particles/ml, detected by Nanosight	Particles per slot for western blot	Volume per slot for western blot	% of the whole preparation (lysed in 45 µl)
AGS	not-infected	5,91*10^10	5,319*10^8	9 µl	20 %
AGS	*H. pylori*-infected	3,65*10^11	5,319*10^8	1,46 µl	3,24 %
MKN28	not-infected	9,10*10^10	8,19*10^8	9 µl	20 %
MKN28	*H. pylori*-infected	3,38*10^11	8,19*10^8	2,42 µl	5,38 %

In AGS cell lysates, we detected bands for MICB at approximately 42 kDa, which corresponds to full-length MICA and MICB protein (130,206,215) (Figure 26B). GAPDH as a loading control was detected in cell lysates but was not expected to be detected in supernatants and exosome-preparations (254). In exosome-free supernatants from AGS cells, we detected bands for MICB at ~32 kDa, which is the expected size of metalloprotease-cleaved MICA and MICB protein (130,206,215) (Figure 26B). *H. pylori* infection resulted in stronger signals for MICB in cell lysates and in exosome-free supernatants, compared to non-infected cells, which complemented our earlier measurements by ELISA and qPCR (see Figures 6B and 12B). Surprisingly, we also detected these bands in a western blot for MICA (Figure 26A), although the cell line AGS was reported to be MICA protein-deficient due to a single amino acid substitution that prevents successful protein folding (238). Possibly, the polyclonal anti-MICA antibody used here for western blot also detected MICB, although the company claims less than 0,2 % cross reactivity with recombinant human MICB. Curiously, we detected additional bands at unexpected sizes with staining for MICA and MICB. In the cell lysates, bands appeared at ~32 kDa, which might correspond to an alternative isoform, produced via alternative splicing that was already reported (https://www.uniprot.org/uniprotkb/Q29983/entry, as of august 2023). Another unexpected band for MICA appeared in cell lysates from *H. pylori*-infected cells at ~25 kDa. This band was particularly interesting as it seemed to be induced by the

infection and appeared only for MICA but not for MICB, thus seemed to be a specific MICA signal. Moreover, no 25 kDa band appeared in the cell culture supernatants or exosome-preparations, suggesting that this protein is not released from cells but is contained intracellularly. This band might indicate a novel alternative splice isoform of MICA. This is likely, since numerous alternative splice isoforms of MICA have been identified, with varying combinations of the three extracellular domains, the TM domain and the cytoplasmic domain of MICA, including variants that lack the TM domain and remain intracellular (255). *H. pylori* was shown to be able to induce alternative splicing (256), thus the bacterium might induce the synthesis of this alternative MICA isoform whose biological impact remains to be elucidated.

The exosome-enriched preparations from both, not-infected and *H. pylori*-infected cells, showed weak bands for MICA and MICB at ~32 kDa. This might correspond to an alternative isoform or a cleavage product. The signal for MICB appeared stronger for exosome-enriched preparations from *H. pylori*-infected cells, compared to those from not-infected cells, especially when considering that the percentage of the whole exosome-enriched preparation loaded on the gel was 20 % for not-infected cells and 3,24 % for *H. pylori*-infected cells. When comparing exosome-free supernatants and exosome-enriched preparations, we observed stronger signals for MICA and MICB in exosome-free supernatants, especially when considering that the percentage of the whole preparation loaded on the gel was only 0,3-0,6% for exosome-free supernatants and 3,24-20% for exosome-enriched preparations. We therefore concluded that most of the MICA and MICB protein released by *H. pylori*-infected AGS cells appeared to be released as soluble protein. Exosome-associated MICA/B was detectable but seemed to play a minor role in this cell line.

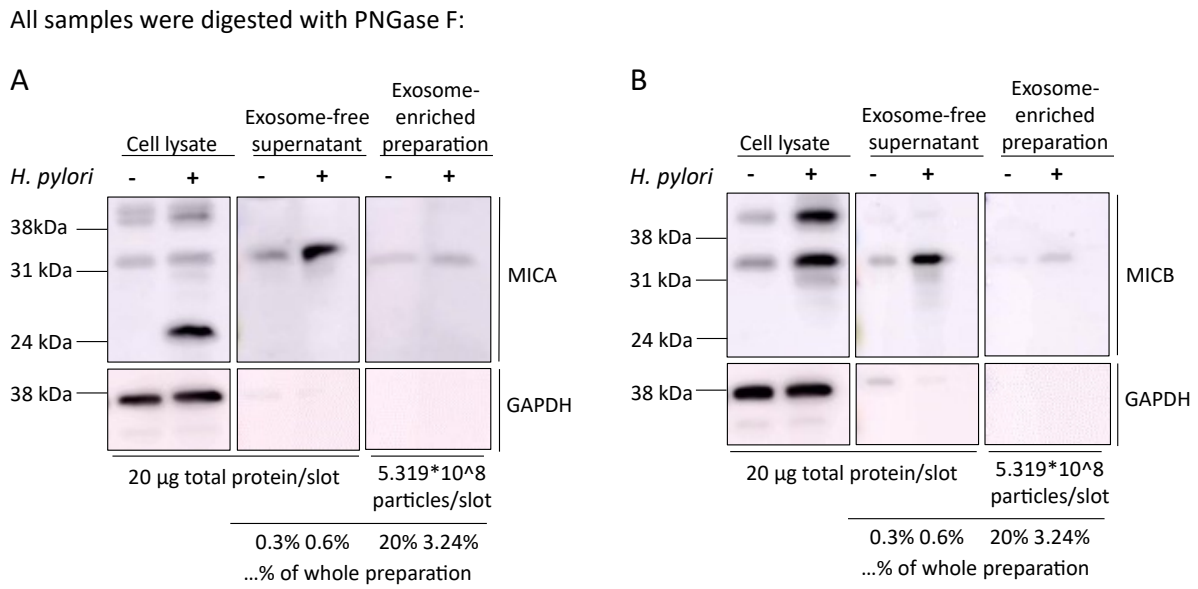

Figure 26. Analysis of cell-associated, exosome-associated, and soluble MICA and MICB in supernatants of *H. pylori* infected AGS cells. Protein preparations from whole cell lysates, exosome-preparations and exosome-free supernatants were digested with PNGase F for deglycosylation and then analyzed by Western Blot. (A) Results for MICA. (B) Results for MICB. Reproduced with modifications from Anthofer et al., Front Immunol, 2024 with permission through the Creative Commons Attribution licence CC-BY, version 4.0.

MKN28 cells also showed the expected bands for MICA and MICB at 42 kDa in cell lysates, corresponding to full-length MICA and MICB, and bands at 32 kDa in exosome-free supernatants, corresponding to metalloprotease-cleaved MICA/B (130,206,215) (Figure 27A, B). In addition, we observed MICA and MICB signals at 42 kDa in exosome-free supernatants and a band at 25 kDa, only for MICA, only in *H. pylori*-infected cells. Regarding exosome-enriched preparations, we observed comparatively strong signals for MICB at 42 kDa and 32 kDa, suggesting that there is a considerable amount of exosome-associated MICB released by MKN28 cells. Of note, there are hardly any reports in the literature about exosome-associated MICB. Nevertheless, also in MKN28 cells, the comparison of exosome-free supernatants and exosome-enriched preparations showed stronger signals for MICA and MICB in exosome-free supernatants, especially when considering that the percentage of the whole preparation loaded on the gel was 0,9-1,3 % for exosome-free supernatants and 5,38-20 % for exosome-enriched preparations. Taken together, this western blot analyses of MICA and MICB in different fractions of AGS and MKN28 cells illustrated several unexpected band sizes that open new topics of investigation. A more in-depth analysis would be required to understand these new

findings. For now, this analyses allowed the crude conclusion that most of the MICA and MICB protein released by *H. pylori*-infected AGS and MKN28 cells appears to be released as soluble protein. Exosome-associated MICA/B was detectable but seemed to play a minor role in these cell lines.

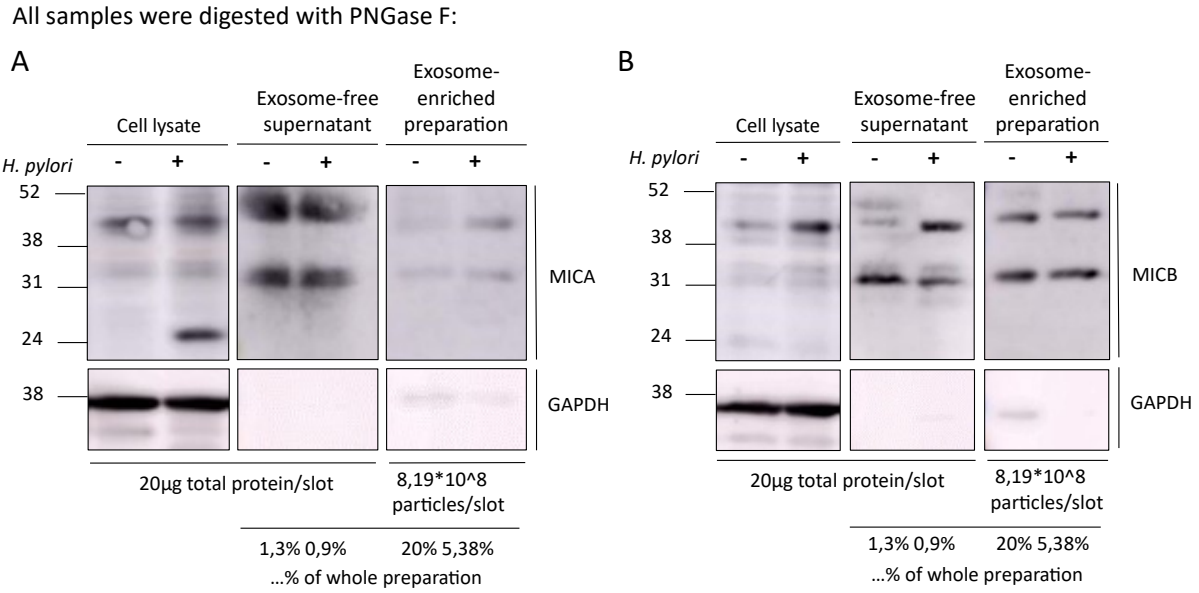

Figure 27. Analysis of cell-associated, exosome-associated, and soluble MICA and MICB in supernatants of *H. pylori* infected MKN28 cells. Protein preparations from whole cell lysates, exosome-preparations and exosome-free supernatants were digested with PNGase F for deglycosylation and then analyzed by western blot. (A) Results for MICA. (B) Results for MICB.

Next, to clarify whether metalloproteases are involved in the soluble release of MICA and MICB in *H. pylori* infection, we challenged MKN28 and AGS cells with *H. pylori* P12 WT or butyrate and added the broad spectrum metalloprotease inhibitor batimastat (175). After 48 h of challenge, we determined levels of soluble MICA and MICB by ELISA. Batimastat strongly reduced the levels of soluble MICA and MICB in control cells as well as in cells treated with *H. pylori* or butyrate, in MKN28 (Figure 28A) and AGS (Figure 28B). This result indicated that these cell lines generally release soluble MICA/B by the action of metalloproteases and that butyrate and *H. pylori* further stimulate this proteolytic shedding.

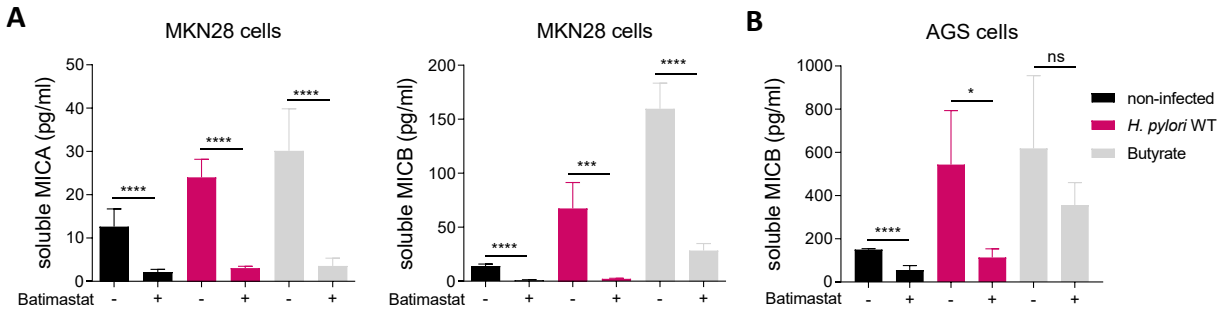

Figure 28. Proteases mediate the soluble release of MICA and MICB in *H. pylori* infection. MKN28 (A) and AGS cells (B) were infected with *H. pylori* WT or challenged with 2 mM butyrate. Additionally, cells were treated with either 10 µM batimastat or DMSO only (=mock) for 48 h. Soluble MICA and MICB in cell culture supernatants were determined by ELISA. (T test of batimastat vs. mock, for each treatment group. ** P <0.01; *** P <0.001; **** P <0.0001). Reproduced with modifications from Anthofer et al., Front Immunol, 2024 with permission through the Creative Commons Attribution licence CC-BY, version 4.0.

To identify the metalloprotease that is responsible for MICA/B shedding in stomach epithelial cells in *H. pylori* infection, we screened the literature for metalloproteases that were previously shown to be involved in MICA/B shedding (Table 5). We found that the proteases ADAM9 (198), ADAM10 (176,200,201), ADAM17 (175,176,200), MMP9 (195,196) and MMP14 (197) were shown to perform MICA and/or MICB shedding in different cell types and under different treatment conditions. Sometimes one specific protease was responsible (197), other times different proteases were involved and had additive effects (176).

Table 5. Overview of studies investigating the involvement of MMPs and ADAMs in MICA/B shedding

NKG2D-L studied	Cell line	This reduced MIC-shedding…	This did not reduce MIC-shedding…	Ref
MICA	B-cell line C1R-MICA	• GW280264X (inhibits ADAM10/17) • GI254023X (inhibits ADAM10)	• TIMP-2 (inhibitor of some MMPs and ADAM12)	(176)
MICA	embryonic fibroblast 293T	• ADAM10 & ADAM17 double silencing		(176)
MICA	cervix carcinoma HeLa	• ADAM10 & ADAM17 silencing		(176)
MICA	brain U373-MICA (CMV infected)	• TIMP-2 (MMP14, ADAM 12) • TIMP-3 (ADAMs 10, 12, 17, MMP14)	• TIMP-1 (ADAM10)	(163)
MICA	liver epithelial cells PLC/PRF/5 & HepG2	• ADAM10 silencing	• ADAM17 silencing	(201)
MICA	liver epithelial cells PLC/PRF/5 & HepG2	• ADAM 9 silencing		(198)
MICA	murine prostate tumor (TRAMP-C2 and MyC-CaP)-MICA	• MMP-14 silencing (shRNA) • ADAM10 silencing • ADAM17 silencing	• MMP 2,3,8, 9, 10, 11, 12, 13, 15, 16, 24 (shRNA) • ADAM 8 (shRNA)	(197)
MICA	prostate cancer M12	• MMP-14 silencing (shRNA)		(197)
MICA	gastric adenocarcinoma NUGC-3	• MMP-9 inhibition		(196)
MICA	gastric adenocarcinoma MKN45, MKN74, St-4		• MMP-9 inhibition	(196)
MICA	osteosarcoma	• MMP-9 inhibition		(257)
MICB	kidney fibroblast CV1-MICB	• TIMP-3 (inhibits ADAMs 10, 12, 17, MMP14) • ADAM17 silencing	• TIMP-1 (ADAM 10) • TIMP-2 (MMP14, ADAM 12)	(175)
MICA and MICB	pancreatic ductal adenocarcinoma Panc89	• MICA: double silencing of ADAM10 & 17 • MICB: ADAM17 silencing	• MICA: single silencing of either ADAM10 or 17 • MICB: ADAM10 silencing (minor role)	(200)
MICA and MICB	pancreatic ductal adenocarcinoma PancTu-I	• MICA: ADAM17 silencing • MICB: ADAM10 & ADAM17 silencing	• MICA: ADAM10 silencing	(200)
MICA and MICB	mammary carcinoma MDA-MB-231	• MICA: ADAM17 silencing • MICB: ADAM17 silencing	• MICA: ADAM10 silencing • MICB: ADAM10 silencing	(200)
MICA and MICB	prostate carcinoma PC-3	• MICB: ADAM17 silencing	• MICB: ADAM10 silencing (minor role)	(200)

To clarify which of these proteases might be eligible for MICA/B shedding in *H. pylori* infection, we analyzed gene expression of all potential candidate metalloproteases in stomach biopsies of *H. pylori* gastritis and in infected stomach epithelial cell lines. Gene expression of all tested metalloproteases was detectable in stomach biopsies and stomach cell lines (Figure 29A-C), making all of these metalloproteases potential candidates for MICA/B shedding in the stomach. In biopsies, ADAM9, ADAM10 and MMP14 were significantly reduced in HpG, ADAM17 gene expression was unchanged and MMP9 gene expression was greatly induced in HpG, with a wide variation among patients (Figure 29A). In the cell lines MKN28 (Figure 29B) and AGS (Figure 29C), most metalloproteases were upregulated by approximately 1,5-fold, after 24 h of *H. pylori* infection. MMP9, however, was greatly induced by 45-fold in MKN28 and almost 200-fold in AGS cells. Infection with the isogenic mutants *ΔcagA* and Δ*cagL* lacked induction of MMP9, whereas deletion of *vacA* only slightly reduced MMP9 induction (Figure 29D). The CagA/L-dependency of *MMP9* induction suggested that MMP9 might be important for MICA/B shedding, since we had seen earlier, that induction of MICA/B shedding in *H. pylori* infection was CagA/L-dependent (see Figure 14). In addition, we also considered ADAM17 as a promising candidate since it was not downregulated in HpG biopsies and it was frequently identified to be responsible for MICA/B shedding in the literature (Table 5 and Table 6). In the context of *H. pylori* infection, ADAM17 also was shown to be activated by CagL on the level of protease activity rather than gene expression (64). Based on our experiments and literature research, we concluded, that MMP9 and ADAM17 were the most promising candidate proteases to be responsible for MICA/B shedding in *H. pylori* infection (Table 6).

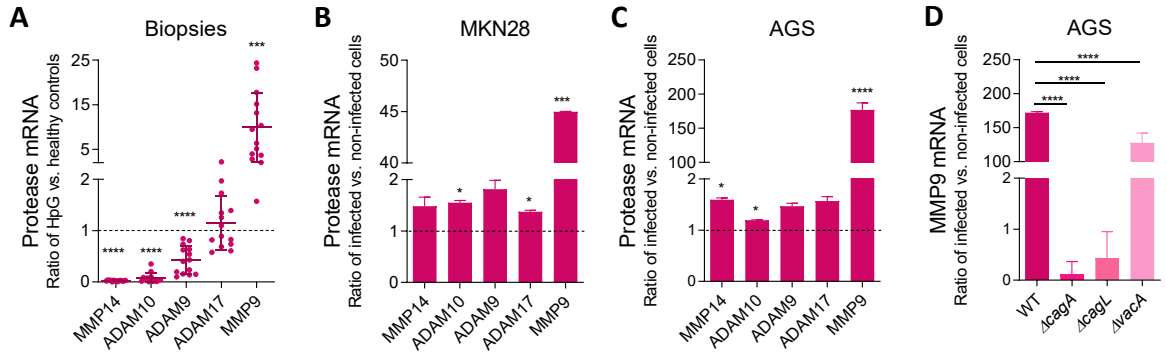

Figure 29. Gene expression analysis of proteases *MMP14, MMP9, ADAM9 ADAM10* and *ADAM17* in stomach biopsies and stomach epithelial cell lines. mRNA expression of *ADAM9, ADAM10, ADAM17, MMP9* and *MMP14* in stomach biopsies of healthy controls and HpG (n= 6-14) (A) and in

MKN28 cells (B) and AGS cells (C), after *H. pylori* infection for 24 h, was determined by qPCR. The results are presented as the ratio of infection vs. no infection, with GAPDH as reference gene. Mean ± SD, one sample t-test vs. a theoretical mean of 1. (D) AGS cells were infected with *H. pylori* WT and isogenic mutants *ΔcagA* and *ΔcagL* for 24 h. MMP9 gene expression was determined by qPCR analysis. The results are presented as the ratio of infected cells vs. non-infected cells, with GAPDH as reference gene Mean ± SD, One-way ANOVA and Dunnett's test. Reproduced with modifications from Anthofer et al., Front Immunol, 2024 with permission through the Creative Commons Attribution licence CC-BY, version 4.0.

Table 6. Summary of literature research and our experiments to identify the most promising protease candidates to be responsible for MICA/B shedding.

	Literature		**Our experiments**	
	Shedding of MICA/B	Activated by *H. pylori*	Expressed in *H. pylori*-infected cells	Direction of regulation in HpG vs. healthy controls
MMP14	✓ (197)	N/A*	✓	down
ADAM9	✓ (198)	N/A*	✓	down
ADAM10	✓ (197,201)	✓ (258)	✓	down
ADAM17	✓ (175,197,200)	✓ (64,259)	✓	no change
MMP9	✓ (196,257)	✓ (260,261)	✓	up

*N/A: No research available to date.

To test the involvement of MMP9 and ADAM17 in NKG2D-L shedding in *H. pylori* infection, we aimed to perform siRNA-mediated knockdown of these two metalloproteases. For the knockdown of ADAM17, we tested four different ADAM17-targeting siRNAs in order to identify the siRNA with the best knockdown efficiency in AGS cells, as it is recommended by the manufacturer (Figure 30A). In addition, we also tested two different non-targeting siRNAs as controls. We also applied different amounts of the transfection reagent Dharmafect 1 (1, 4, 7 and 10µl per well) to establish the ideal treatment conditions for ADAM17 knockdown. To assessed the effect of siRNA-mediated knockdown on ADAM17 protein expression, we

performed western blot analyses (Figure 30). Difficulties with protein quantification in this experiment resulted in varying amounts of total protein loaded on the gel, as apparent from the varying band intensities of the control protein GAPDH (Figure 30A). Still, we carefully evaluated band intensities for ADAM17 and GAPDH in the different samples and were able to conclude, that siRNAs #2 and #3 appeared to have greater knockdown efficiencies, compared to siRNAs #1 and #4 (Figure 30A). Moreover, knockdown efficiency appeared to depend on the amount of Dharmafect 1. The use of 1µl of Dharmafect 1 per well was remarkably less effective than all other conditions (4µ, 7µl and 10µl per well) (Figure 30A). In parallel, we also observed microscopically that increasing amounts of Dharmafect 1 were associated a greater degree of vacuolization of the treated cells, suggesting increased cell stress. Thus, we decided to use 4µl of Dharmafect 1 per well for our experimental setup, as this amount seemed to provide satisfying knockdown efficiency while causing minimal cellular stress.

Next, we repeated the testing of siRNAs #2 and #3 and to further optimize the experimental conditions, we tested two different concentrations of siRNA (50 nmol/L and 100 nmol/L) and two sampling timepoints after transfection, namely 48 h and 72 h (Figure 30B). siRNA #3 did not completely eliminate the ADAM17 band signals, but greatly reduced them, at both siRNA concentrations and at both timepoints (Figure 30B). Regarding siRNA#2, knockdown efficiency was not as strong and diminished over time with no knockdown effect visible after 72 h, when using 50 nm of siRNA (Figure 30B). Thus, we decided to use siRNA#3 in further experiments. Since there was no difference in knockdown efficiency between 50 nmol/L and 100 nmol/L of siRNA#3, we decided to use the lower concentration for our experiments, with the intention to minimize cellular stress and unwanted off-target effects.

We then aimed to test these established knockdown conditions in combination with *H. pylori* infection (Figure 30C). ADAM17 knockdown efficiency was satisfactory in both, non-infected and *H. pylori*-infected cells (Figure 30C). Curiously, *H. pylori* infection seemed to affect ADAM17 protein expression. ADAM17 protein exists in two forms, the precursor form with a size of 120 kDa and the mature form with a size of 100 kDa (262). The precursor form is larger due to a prodomain that keeps ADAM17 inactive on its way from the ER to the Golgi apparatus. In the Golgi apparatus, the pro-domain is cleaved off prior to transfer to the cell surface (263). We detected mostly the precursor form in cell lysates from non-infected AGS cells (Figure 30A-C). *H. pylori* infection increased the intensity of the band at 100 kDa which corresponds to mature ADAM17 protein (Figure 30C) (262), suggesting that *H. pylori* infection increases the amount of active ADAM17 protein in the infected cells.

In order to exclude off-target effects of the siRNA-mediated knockdown on the cognate metalloprotease ADAM10, we also analyzed protein expression of ADAM10 (Figure 30C). Western blot showed that treatment with ADAM17-targeting siRNA had no effect on ADAM10 protein expression (Figure 30C). However, *H. pylori* infection seemed to affect ADAM10 protein. ADAM10 is expected to be detected in its precursor form with a size of 90 kDa and in its mature form with a size of 68 kDa (264). Both bands were detectable in non-infected cells, with a greater intensity of the precursor form (Figure 30C). In *H. pylori* infected cells, a third band appeared below the mature form, suggesting an additional cleavage of ADAM10 protein in *H. pylori* infection.

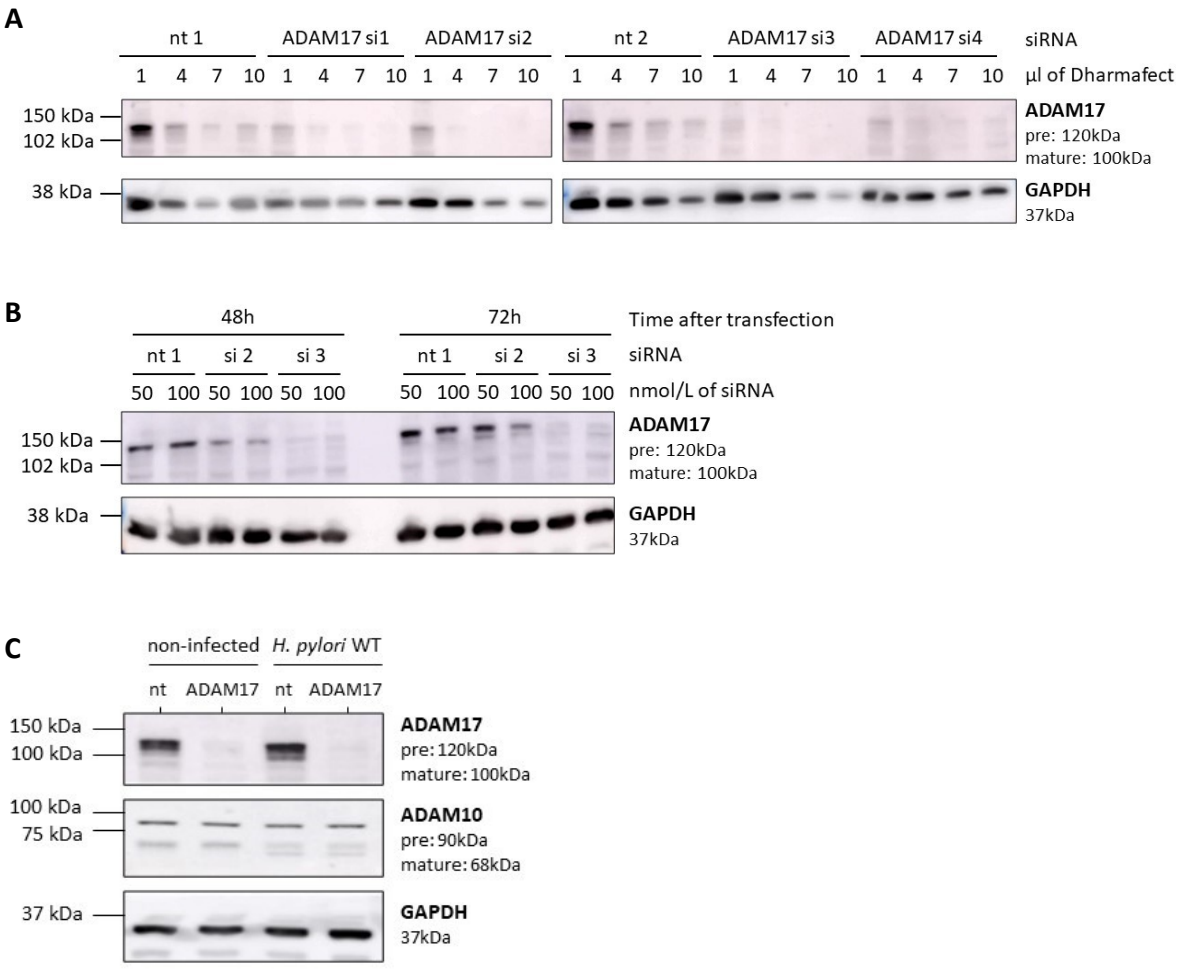

Figure 30. Testing different conditions for the knockdown of *ADAM17* in AGS cells. For the knockdown of *ADAM17* in AGS cells, knockdown efficacy was determined by western blot. (A) We tested two non-targeting (nt) siRNAs and four *ADAM17*-targeting siRNAs in combination with different volumes of Dharmafect (1, 4, 7 and 10µl). (B) We tested different siRNA concentrations (50 nmol/L

and 100 nmol/L) and different sampling timepoints after transfection (48 h and 72 h). (C) We tested ADAM17 knockdown with versus without *H. pylori* WT infection. Reproduced with modifications from Anthofer et al., Front Immunol, 2024 with permission through the Creative Commons Attribution licence CC-BY, version 4.0.

For the knockdown of MMP9, we used the same experimental conditions that we had established for the knockdown of ADAM17 in AGS cells. We then tested four different MMP9-targeting siRNAs in order to identify the siRNA with the best knockdown efficiency in AGS cells, as it is recommended by the manufacturer. Since MMP9 is barely expressed in non-infected cells, we infected AGS cells with *H. pylori* to induce MMP9 expression. To assess MMP9 knockdown we performed qPCR, since MMP9 is a secreted protein and western blotting of cell lysates might not be adequate to determine total MMP9 protein produced by these cells. The four siRNAs resulted in varying knockdown efficiencies with siRNA #4 reducing *MMP9* gene expression most strongly (Figure 31). Thus, we chose to use this siRNA for our next experiments.

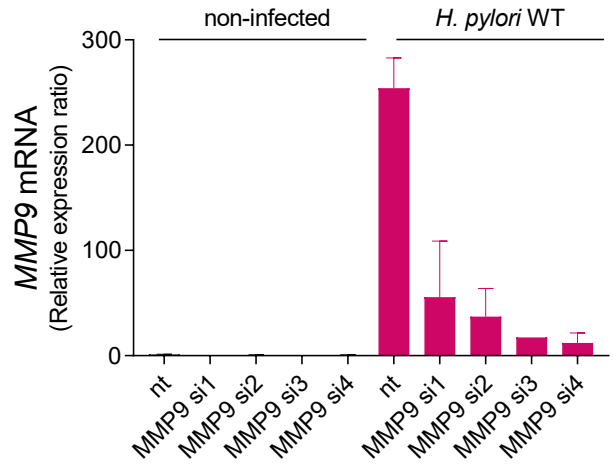

Figure 31. Testing different conditions for the knockdown of *MMP9* in AGS cells. For the knockdown of *MMP9* in AGS cells, knockdown efficacy was determined by qPCR, since MMP9 is a secreted protein. We tested one non-targeting (nt) and four *MMP9*-targeting siRNAs, with and without *H. pylori* WT infection. Reproduced with modifications from Anthofer et al., Front Immunol, 2024 with permission through the Creative Commons Attribution licence CC-BY, version 4.0.

Finally, AGS cells were transfected with the respective siRNA knock-down constructs or a non-targeting (nt) siRNA and after 48 h cells were infected with *H. pylori* WT and cultured for further 24 h. After 24 h of infection we confirmed metalloprotease knockdown by qPCR. *MMP9*-targeting siRNA almost abolished *MMP9* gene expression while *ADAM17* gene expression was not affected (Figure 32A, B). *ADAM17*-targeting siRNA reduced *ADAM17* mRNA approximately by half and did not affect *MMP9* gene expression (Figure 32A, B). Next, we measured levels of soluble MICB by ELISA (Figure 32C). Neither the knockdown of MMP9 nor that of ADAM17 affected the induction of soluble MICB in *H. pylori* infected cells, suggesting that individual activities of these two proteases are not essential for MICB shedding in AGS cells. Thus, the identity of the protease triggering the release of soluble MICA/B in *H. pylori* infection, remains to be elucidated.

In conclusion, our data show that *H. pylori* induces proteolytic shedding of MICA and MICB. Of the tested proteases, MMP9 was most strikingly induced in *H. pylori* infection and this induction required CagA. Nevertheless, knockdown of MMP9 did not prevent MICB shedding in *H. pylori* infection. ADAM17 was also not responsible for the shedding of MICB. The responsible protease or combination of proteases and the way by which CagA might stimulate MIC shedding remain to be clarified.

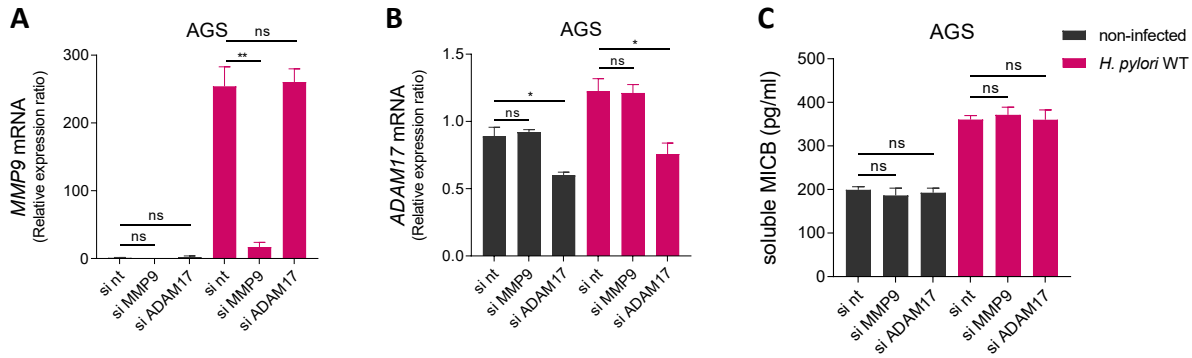

Figure 32. siRNA-mediated knockdown of ADAM17 and MMP9. AGS cells were transfected with a non-targeting (nt) siRNA and siRNAs targeting *MMP9* and *ADAM17*. 48 h after transfection, cells were infected with *H. pylori* for 24 h. qPCR was used to determine *MMP9* (A) and *ADAM17* (B) gene expression. (C) ELISA was performed to quantify sMICB in cell culture supernatants. Mean+/- SD, One-way ANOVA and Dunnett's test. Reproduced with modifications from Anthofer et al., Front Immunol, 2024 with permission through the Creative Commons Attribution licence CC-BY, version 4.0.

4. Discussion

4.1. Modulation of the NKG2D axis in *H. pylori* infection

Helicobacter pylori is specifically adapted to life in the human stomach. It uses an arsenal of mechanisms to cope with this hostile environment, to subvert the immune system and successfully persist. The interactions between *H. pylori* and host cells are complex and multifaceted and despite decades of research, novel mechanisms of bacterial-host interactions and modifications are still being identified. Rather understudied is the effect of *H. pylori* on cytotoxic leucocytes, namely NK cells and CTLs. However, these cell types are of great interest in this context since they are key to detect and actively eradicate cancer cells. A modulation of these cells by *H. pylori* could reduce the efficacy of anti-tumor immunosurveillance.

The NKG2D/NKG2D-L axis is important for the activation of CTLs and NK cells in response to cellular stress, infections and oncogenic transformation and is best studied for its contribution to anti-tumor immune surveillance (104). NKG2D-Ls are typically absent on healthy cell surfaces (109) and are co-regulated by the gut microbiota (137). Expression and cell surface display of NKG2D-Ls is induced during conditions of cellular stress, infection or neoplastic transformation (106,110–112). However, viruses and tumors often counteract this expression of NKG2D-Ls by downregulating the expression of NKG2D-Ls or by inducing the release of soluble NKG2D-Ls from the cell surface (151,161,265). These strategies result in reduced cell surface expression of NKG2D-Ls and therefore reduced immunological visibility of the tumor cells or the infected cells. In addition, soluble NKG2D-Ls reduce the strength of the immune response by acting as repressors of NKG2D-expressing cells. When soluble NKG2D-Ls bind to the NKG2D receptor, this leads to downregulation of NKG2D expression and consequently reduced NKG2D-mediated immunity, as well as an overall impairment of immune cell function (172,179,266,267).

We previously detected a potential dysregulation of the NKG2D/NKG2D-L axis in *H. pylori* infection (223). Thereupon we hypothesized, that *H. pylori* might employ an evasion strategy to subvert NKG2D-mediated immunity. In this study we aimed to determine whether *H. pylori* modulates the NKG2D/NKG2D-L axis and how such a process might work. Analyzing human stomach biopsies, we found no heightened NK cell and CTL numbers, despite great overall immune infiltration in *H. pylori* gastritis. In addition, we observed reduced *NKG2D* expression and increased *MICB* expression in *H. pylori*-gastritis, which were

suggestive for NKG2D evasion. *In vitro* infection experiments of stomach epithelial cell lines revealed that *H. pylori* induced NKG2D-L expression and soluble release and showed the contribution of the major pathogenicity factors VacA and CagA in these processes. MICA/B protein did not accumulate at the cell surface of infected epithelial cells but instead accumulated in the lamina propria, in *H. pylori*-infected patients. With an NK cell culture model, we showed that soluble NKG2D-Ls, released from *H. pylori*-infected stomach epithelial cells, reduced NKG2D expression and cytotoxic degranulation of NK cells, confirming NKG2D evasion in *H. pylori* infection (Figure 33). Evasion of NKG2D-mediated immunity is common in virus infections and cancers. Our findings are the first report of NKG2D evasion induced by *H. pylori*.

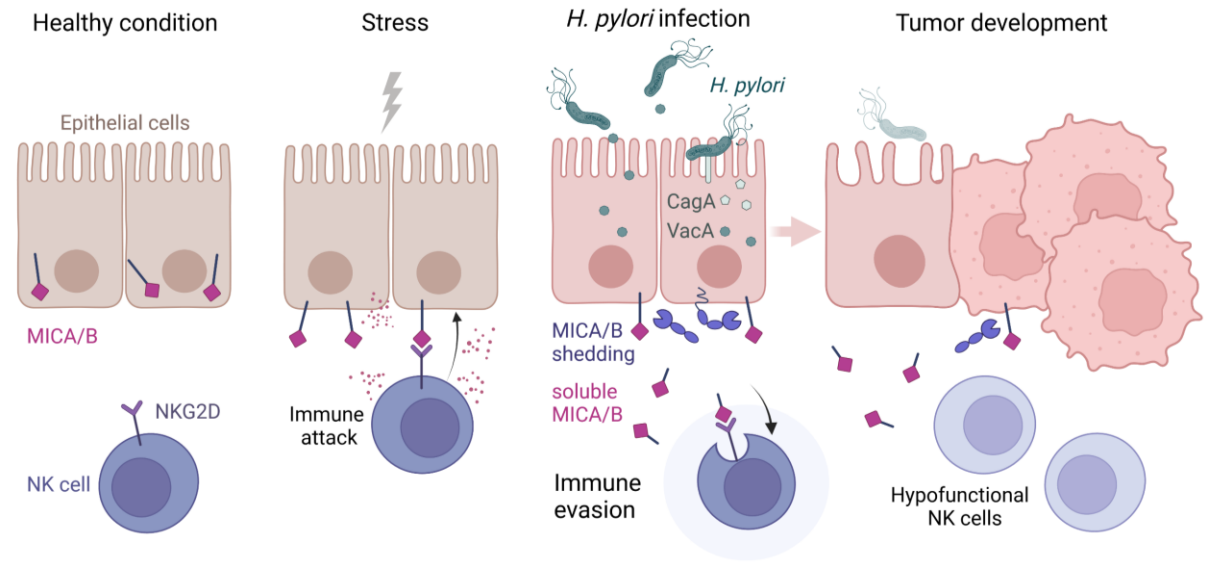

Figure 33. Scheme of NKG2D system modulation in *H. pylori* infection. In healthy epithelial cells, MICA/B proteins are stored intracellularly. During stress, MICA and MICB are exposed at the cell surface where they can interact with NKG2D on the surface of NK cells and CTLs. This interaction activates immune attack and eradication of the stressed cell. The *H. pylori* virulence factors CagA and VacA induce expression and soluble release of MICA/B. Soluble MICA/B bind NKG2D, which leads to the internalization of NKG2D, resulting in immune evasion. The resulting hypofunctional NK cells and CTLs are less effective in detecting cancer cells which could facilitate cancer development. This scheme was created with Biorender (https://biorender.com). Reproduced from Anthofer et al., Front Immunol, 2024 with permission through the Creative Commons Attribution licence CC-BY, version 4.0.

4.2. Previous research

To date, only one other group investigated the effect of *H. pylori* on the NKG2D axis. The group of M. Molina used heat-killed *H. pylori* and showed that this stimulus induced an approximately 2-fold MICA expression in gastric epithelial cell lines via TLR4, and this effect was driven by *H. pylori* LPS. They also showed that cells, treated with heat-killed *H. pylori,* activated the cytotoxicity of peripheral blood lymphocytes (PBLs) (222). The differences between these findings and ours may be attributed to the fact that this group used heat-killed *H. pylori* while we infected cells with live *H. pylori*. Intact *H. pylori* was shown to stimulate a different TLR response, compared to *H. pylori* LPS, which stimulates TLR 4 (268). In addition, heat-killed *H. pylori* does not exert the actions of the pathogenicity factors VacA and CagA, which we identified as the major players of NKG2D-L dysregulation.

4.3. Role of *H. pylori* virulence factors CagA and VacA

Cancer risk in *H. pylori* infection is associated with the presence and allele type of the virulence factors CagA and VacA (29). CagA and VacA are both proteins that enter host cells and exert a multitude of effects, manipulating the host cells in various aspects (2,32–36,42–56). All *H. pylori* strains express VacA but might be positive or negative for CagA. In addition, different allelic variants exist for VacA and CagA, which are associated with varying levels of pathogenicity (28,29,38–41,57). We observed that VacA seemed to induce MIC expression, which would normally activate an immune response and possibly an eradication of the infection. CagA, however, appeared to induce shedding which leads to immune evasion. Opposing effects of VacA and CagA have been reported for several aspects such as the hummingbird phenotype, vacuolization and apoptosis (269). Interestingly, most *H. pylori* strains that harbor the *cagA* gene, carry the more pathogenic allelic variants of *vacA* (Table 2) (41). A possible explanation for this genetic linkage might be that the antagonism of CagA and VacA allows *H. pylori* to colonize without gross cellular damage to the infected epithelium (269). This notion fits with our observation where the action of VacA (increased NKG2D-L expression) would probably induce tissue damage, which is prevented by the action of CagA (increased NKG2D-L shedding). Apart from the antagonism of CagA and VacA, there are also reports where the combined actions of these pathogenicity factors lead to a beneficial effect for *H. pylori*. For instance, iron acquisition, which is essential for colonization, is dependent on the

combined actions of CagA and VacA – CagA promotes increased basolateral uptake and transcytosis of transferrin, and VacA drives mislocalization of the transferrin receptor to sites of bacterial attachment (2). Concerning the NKG2D/NKG2D-L axis, the combined actions of CagA and VacA could potentiate the amount of soluble NKG2D-Ls released into the lamina propria, leading to a strong suppression of NKG2D-mediated immunity. In summary, our findings complement existing knowledge about the importance of CagA and VacA and their combined actions, for *H. pylori* pathogenicity.

We found that the *vacA* gene was essential for the induction of *MICA* and *MICB* gene expression. Further research should aim at unravelling the detailed molecular mechanisms by which VacA might induce NKG2D-L gene expression. MIC expression was shown to be induced by cellular response mechanisms to oxidative stress (143,270), heat shock (133) and DNA damage (144,145) as well as by increased cellular proliferation (143) and the intracellular detection of viral RNA (146). These mechanisms affect either MIC transcription (133,143) via binding sites for the transcription factors HSF1, Sp1 (133,143), E2F1 (145) and NFkB (147) in the MIC promoter. VacA might affect MIC transcription by influencing transcription factors. VacA was reported to induce the transcription factor E2F1 (271) and was shown to reduce STAT3 (272) which activates the transcription factors NFκB and E1F1, targets ER and Golgi and interferes with late endosomal pathways. STAT3 inhibition was shown to increase MICB expression in gastric adenocarcinoma cells (157). Alternatively, MICA and MICB mRNA levels may be regulated on the level of MIC mRNA stability (148) via modulation of RNA-binding proteins (148,149) and micro-RNAs (150).

In the current study we used the *H. pylori* strain P12, that harbors the highly pathogenic s1/m1 variant, and observed a VacA-dependent induction of NKG2D-L gene expression. In contrast, in our previous study we did not observe an induction of NKG2D-L mRNA expression after infection with the *H. pylori* strain PMSS1, that contains the less pathogenic s2/m2 VacA allelic variant (223). It would be interesting to investigate whether induction of NKG2D-L gene expression is associated with the s/m allelic variants of VacA by using isogenic mutants and complementation strains, containing the different allelic variants. In addition, a cohort of patients could be screened for the VacA allele and the induction of NKG2D-L gene expression. A VacA allelic variant-dependency of NKG2D-L gene expression may contribute to the differential disease outcomes seen in individuals infected with different *H. pylori* strains.

4.4. Efforts to elucidate the molecular mechanisms underlying the proteolytic shedding of MICA/B

We found that *H. pylori* induced the soluble release of NKG2D-Ls. Initially, we hypothesized that the underlying mechanism might be an induction of the human metalloprotease ADAM17 by *H. pylori* CagL. ADAM17 is one of the most frequently identified and best studied metalloproteases in the context of MICA/B shedding. It is embedded in the cell membrane and is inactive when bound to α5β1 integrin (263). CagL is the protein at the tip of *H. pylori's* T4SS. It binds to the host transmembrane receptor α5β1 integrin (61) and thereby activates the metalloprotease ADAM17 (273), and also induces aberrant signaling within host cells (62) and IL-8 secretion (63). In addition, CagL is part of the T4SS that is essential for the translocation of CagA into host cells. CagA, CagL and the other proteins of the T4SS are encoded in the *cag* PAI which is a 40-kilobase genomic island within *H. pylori*. The cag PAI might be absent or present in *H. pylori* strains and *cag* PAI positive strains are more virulent (2). Many pathogenic actions of *H. pylori* are attributable to the *cag* PAI. When a certain effect is associated with the *cag* PAI, it remains unclear whether this effect is attributable to the toxin CagA or to individual proteins of the T4SS. In our study, we observed that genetic deletion of either CagA or CagL abrogated *H. pylori* induced MICA shedding to the same extent. Since there was no difference between the two mutant strains, we speculated that CagA might be the key driver while CagL's role might be the transfer of CagA into host cells. Additional individual effects of CagL did not appear to play a significant role in the soluble release of MICA.

Soluble release of NKG2D-Ls is achieved either by proteolytic cleavage of the extracellular domain of MICA (199,274) and MICB (175) by metalloproteases, or by the release on exosomes (130). With the use of a broad-spectrum metalloprotease inhibitor and through the enrichment and analysis of exosomes from the cell culture supernatants, we found that *H. pylori* induced the metalloprotease-mediated shedding of NKG2D-Ls. Next, we attempted to identify the protease that mediates NKG2D-L shedding in *H. pylori* infection. The metalloproteases reported in the literature to be involved in MIC shedding are MMP9 (195,196), MMP14 (197), ADAM9 (198), ADAM10 (199–201) and ADAM17 (175,199,200). We detected all of these proteases to be expressed in stomach biopsies and in MKN28 and AGS cells. Therefore, all tested proteases were potential candidates for the shedding of NKG2D-Ls in *H. pylori* infection. Of these proteases, MMP9 appeared most promising since *H. pylori* infection highly induced MMP9 expression in stomach biopsies and cell lines, induction was CagA-dependent, and a *cag* PAI-dependence of MMP9 induction was reported earlier (260). Nevertheless, knockdown

of MMP9 did not affect *H. pylori*-induced MICB shedding in AGS cells. We also tested the involvement of ADAM17 in MICB shedding, to no avail. Possibly not a single but a combination of proteases are responsible for MICA/B shedding and compensate each other's function in *H. pylori* infection, as it has been reported in other settings (199,200). In our study we focused only on a small set of proteases, that were already known to mediate MICA/B shedding. However, *H. pylori* activates many other metalloproteases (275) which may be potential candidates. In addition, we only investigated the shedding of MICB, since AGS cells are MICA-deficient (238). It might be possible that MMP9 or ADAM17 knockdown would affect MICA shedding, since some studies reported differential shedding susceptibilities of MICA and MICB (200). In general, the proteases involved in NKG2D-L shedding vary depending on the cell type, the ligand and the stimulus and proteases are regulated on several levels such as gene expression, membrane localization and activation (263). Therefore, a more extensive analysis would be required to identify the proteases that are responsible for NKG2D-L shedding in *H. pylori* infection.

Potentially, bacterial proteases might be involved in NKG2D-L shedding. *H. pylori* expresses multiple proteases that are important virulence factors and modulate host cells in various ways (275). The best studied *H. pylori* protease HtrA, however, is likely not involved in NKG2D-L shedding since it is a serine-protease and not sensitive to batimastat inhibition (276). The protease(s) responsible for *H. pylori*-induced NKG2D-L shedding still need to be identified.

In this study we focused on unravelling a potential activation of metalloprotease activity by *H. pylori* as the cause of induced NKG2D-L shedding. Alternatively, *H. pylori* might affect shedding by modulating the trafficking and localization of NKG2D-Ls. In healthy tissues NKG2D-Ls are mainly expressed intracellularly (109,136), which we also observed in our analyses (Figure 17A). For NKG2D-Ls to serve as stress signals, a translocation to the cell surface is required. While considerable knowledge exists about the regulation of NKG2D-Ls at the transcriptional level, very little is known about the mechanisms by which NKG2D-L proteins are retained in the cytoplasm during homeostasis and are translocated to the cell surface upon stress. *H. pylori* might induce NKG2D-L shedding by promoting NKG2D-L translocation to the surface. At the cell surface, full-length MICA localizes to the basolateral side of polarized cells due to a sorting motif in the cytoplasmic tail (129). *H. pylori* prominently disrupts cell polarity (48), which might affect distribution of NKG2D-Ls at the cell membrane, making this a potential mechanism of intervention. Another important aspect for shedding of NKG2D-Ls is

the lipid environment of the plasma membrane. NKG2D-Ls have a limited stability at the cell surface until they are internalized, which varies between individual ligands (219). MICB has a particularly short half-life at the plasma membrane and the lipid environment of the membrane plays a crucial role in the internalization of MICB (277). In addition, for shedding it is required that MICA/B localize to lipid rafts (175,278) which are specific regions of the cell membrane that are rich in cholesterol and sphingolipids (279). Active ADAM17 and other proteases are restricted to lipid rafts (280,281) and disruption of lipid rafts by cholesterol depletion allows movement of active ADAM17 into the non-raft region of the membrane and increases ADAM17-dependent shedding, which demonstrates the importance of lipid rafts to keep shedding under control (175,280,282). In order to transfer to lipid rafts, MICA needs to be palmitoylated (278), which is the addition of a fatty acid by thioester linkage to cysteine residues. Palmitoylation of MICA is reversible and can be regulated by extracellular stimuli (283). Potentially, *H. pylori* affects NKG2D-L shedding by modulating the localization of MICA/B and metalloproteases to lipid rafts, for instance by affecting MICA/B palmitoylation or by modifying lipid composition of the plasma membrane. In fact, *H. pylori* was reported to deplete cholesterol and thereby disrupts lipid rafts in the plasma membrane of infected stomach epithelial cells, by the action of cholesterol-α-glucosyltransferase (284). Interestingly, cholesterol depletion in *H. pylori* was a requirement for successful CagA translocation into host cells and CagA-induced responses in stomach epithelial cells (285). In summary, multiple factors seem to be involved in NKG2D-L shedding, which may be modulated by *H. pylori*.

4.5. Potential effect on tumor development

We hypothesize that evasion of the NKG2D axis in *H. pylori* infection could facilitate tumor development (Figure 33). NKG2D is expressed by NK cells and CTLs, both essential cell types for the detection and eradication of cancer cells (78). NK cells are particularly important for the early detection of neoplastically transformed cells (78). As a first line of defense, NK cells do not require antigen-presentation but get activated by a loss of MHC-I expression, which frequently occurs in tumors, in addition to an induction of stress ligands (79). Thus, a suppression of NK cells in the stomach mucosa of *H. pylori*-infected individuals could facilitate the persistence of spontaneously transformed cells and allow their outgrowth to overt cancer.

4.6. Potential effect on chronic persistence

We also speculate that evasion of the NKG2D axis is one of the strategies, that help to ensure chronic *H. pylori* persistence in the stomach. Beside their anti-tumor activity NK cells are important in the fight against bacterial infections (81,82,84,286). NK cells detect bacterial infection and contribute to inflammation by secreting IFN-γ, by activating monocytes and macrophages and by killing bacteria-infected host-cells and bacteria directly (287,288). A suppression of NK cells by *H. pylori* could reduce their anti-bacterial immunity and thereby facilitate chronic *H. pylori* persistence. Another cell type that expresses the NKG2D receptor is the γδ T cell lineage (105). This T cell lineage has an alternative type of the T cell receptor, compared to αβ CD8+ and CD4+ T cells. They are highly abundant in the gut mucosa as intraepithelial lymphocytes (IELs) where they are important for immune surveillance, counteracting infections and are important for tissue homeostasis (289). *H. pylori*-induced soluble NKG2D-Ls in the stomach mucosa could affect γδ T cell-mediated immune surveillance and thus promote chronic bacterial persistence.

4.7.Potential therapeutic applications

Our data indicate a dysregulation of the NKG2D axis in premalignant stomach disease and gastric cancer which opens novel opportunities for diagnostic and therapeutic applications. For instance, *H. pylori* gastritis patients might show detectable levels of soluble NKG2D-Ls in the serum which could serve as diagnostic markers for assessing cancer risk. High serum levels of soluble NKG2D ligands are common in advanced cancers and correlate with a systemic reduction of NKG2D expression and functionality of NK and CTLs, as well as with a high cancer stage, metastasis and poor prognosis (172,185,187,290). Serum levels of MICA were for instance also evaluated in hepatitis C virus infection and might serve as a prognostic factor (291). Furthermore, therapeutic applications that target and re-activate the NKG2D axis in cancer are considered a promising tool in addition to existing forms of tumor immunotherapy and are currently under exploration (151). Based on such therapeutic applications, high-risk *H. pylori* infection could be treated with novel host-directed therapies that target the NKG2D-axis. Host-directed therapies for infectious diseases aim to activate host innate immune activities to fight bacterial infections (292). This is of particular interest in the context of infectious diseases

where antibiotic therapy is not sufficiently effective, which is the case for *H. pylori* infection (293).

4.8. Potential impact on immunological diseases

Another interesting aspect, that our findings may shed light on is the potential protective effect of *H. pylori* against a range of diseases. For instance, *H. pylori* infection was shown to protect from celiac disease as well as and the 2 major forms of inflammatory bowel disease Crohn's disease and ulcerative colitis, among others. However, no functional mechanism for this protective effect was identified to date. Notably, the NKG2D/NKG2D-L axis was shown to be dysregulated and contribute to a number of inflammatory disorders, including celiac disease and Crohn's disease (242,243,294), where intestinal cells are attacked by NKG2D-expressing effector cells. A suppression of NKG2D-mediated immunity by *H. pylori* could protect from disorders that are associated with an overreactive NKG2D axis.

4.9. Potential role of NKG2D-L polymorphism

The two genes *MICA* and *MICB* originate from a gene duplication event and are located in the highly polymorphic major histocompatibility complex (MHC)-class I locus (122,124). *MICA* and *MICB* are highly homologous, but some genetic differences exist and currently 531 *MICA* alleles and 244 *MICB* alleles are known (http://hla.alleles.org/alleles/classo.html, March 2023) (126). Several of the genetic differences between *MICA* and *MICB* are associated with differential gene expression and regulation (143,149,151,152,154,156,159,196,237). Studies have observed differential levels of expression for MICA and MICB and we also found differences in expression levels for *MICA* and *MICB – MICB* was expressed at lower levels compared to *MICA* in stomach biopsies and in the cell lines AGS and MKN28 and inducibility in response to *H. pylori* infection was greater for *MICB* compared to *MICA* in these cell lines. The regulatory differences of the different NKG2D-Ls are proposed to be a result of evolutionary selective pressure, in reaction to the evasion strategies of pathogens. Moreover, the variations in NKG2D-L regulation might enable a diversified reaction of the system to differential stressors (104).

H. pylori infection has variable clinical outcomes. While most infected persons are asymptomatic, some progress to symptomatic gastritis, duodenal ulceration, or gastric cancer. This variability in disease outcome was associated with several parameters such as environmental factors, bacterial genetics and host genetics (15). Considering host genetics, the polymorphism of MICA and MICB might contribute to this variability. MICA/B polymorphism was shown to affect transcriptional regulation (237), NKG2D-binding affinity (128) as well as protein trafficking and secretion (129,130) and was associated with genetic predisposition for multiple diseases such as the already mentioned diseases including coeliac disease and ulcerative colitis (221), as well as several types of cancer (122). Gastric adenocarcinoma was associated with the MICA alleles A9 and *009/049 (122,295). In the allele MICA A9, the microsatellite repeat polymorphism in the transmembrane domain is relatively long, compared to other MICA variants (296). Proteolytic cleavage takes place in the stalk region close to this microsatellite polymorphism region, and the process is sensitive to shortenings of the sequence (199). Thus, it is possible that the MICA allele A9 is particularly susceptible to proteolytic shedding due to its long microsatellite sequence, which likely suggests the association of this variant with gastric cancer (295). In contrast, the frequent allele MICA*008 (A5.1), is not susceptible to proteolytic-shedding. It has a truncated transmembrane domain and is anchored to the membrane by a GPI anchor instead (215). Consequently, it is not shed by metalloproteases and it is also not susceptible to certain immune evasion strategies of viruses that suppress MICA expression (166,297). It would be interesting to investigate whether persons with a MICA*008 allele are less susceptible to *H. pylori*-induced NKG2D evasion and consequently have a reduced risk of developing *H. pylori*-induced gastric cancer. Intriguingly, the frequency of MICA*008 is around 42% in Caucasians (126,252) but only around 25% in east Asians (217,218), the latter have the highest incidence rates of stomach cancer worldwide (298). Since *H. pylori* has co-evolved with humans for at least 100.000 years (3), it may be possible that *H. pylori* has put selective pressure on NKG2D-Ls and thereby has driven MICA/B polymorphism, especially considering that *H. pylori* has other known HLA allele associations (299). Further research may focus on understanding the role of NKG2D-L allelic variants in *H. pylori*-induced NKG2D evasion. In the future it may be possible to assess cancer risk of *H. pylori* infected persons based on their NKG2D-L genotypes.

4.10. Future work

A next step in evaluating the relevance of the identified mechanism in anti-tumor immunity would be to determine whether soluble NKG2D-Ls released by *H. pylori*-infected cells have the capacity to reduce tumor cell killing by NK cells, in addition to their reductive effects on NKG2D-expression and NK cell degranulation. This may be tested by a fluorometric assay using a substance such as resazurin that indicates cell viability (300). A more state-of-the-art approach might be a flow-cytometry-based cytotoxicity assay (301,302). In the course of such experiments, it would be interesting to include additional cytotoxic cell types such as CD8+ T cells and γδT cells, both cell lines and primary cells, as they also play important roles in anti-tumor immunity, mucosal homeostasis and infections. One might also include additional measures of effector cell activation such as determining cytokine expression and secretion. In addition, one might add other target cells, especially stomach cancer cells. To better understand the role of NKG2D-L polymorphism and variability, different stomach cancer cell lines as well as isolates from patients could be genotyped for their NKG2D-L alleles and characterized for their NKG2D-L expression profile and response pattern to *H. pylori* infection and how those translate to amounts of secreted soluble NKG2D-Ls and strength of effector cell inhibition. Potentially, different NKG2D-L alleles would prove to be less or more susceptible to *H. pylori*-induced shedding. For conformational studies in this direction, transfectants of specific NKG2D-L alleles could be created and comparatively assessed for their response to *H. pylori* infection. To determine the involvement of the genetic variability of *H. pylori* pathogenicity factors in NKG2D-evasion, different *H. pylori* strains with different *VacA* and *CagA* alleles could be applied and tested for their capacity to induce NKG2D-evasion.

To address whether the results from these *in vitro* experiments translate to the *in vivo* situation, one could assess soluble NKG2D-Ls present in the sera via ELISA and use flow cytometry to assess NKG2D-expression and activity of circulating and stomach resident NK cells, CTLs and γδT cells in patients of *H. pylori* gastritis, peptic ulcer disease and stomach cancer.

In addition to these experimental approaches, meta-analysis of available datasets of human genetics, bacterial genetics and/or transcriptional data in combination with clinical metadata from patients of *H. pylori*-gastritis and gastric cancer might help to and predict susceptibility and risk of disease development in infected individuals in association with the NKG2D system.

5. Conclusion

In conclusion, our study identifies NKG2D evasion in *H. pylori* infection. This mechanism has the potential to facilitate tumor development by reducing anti-tumor immunity of NK cells and CTLs, to support chronic bacterial persistence by diminishing anti-bacterial immunity, to contribute to *H. pylori's* protective effect against inflammatory disorders that are associated with an overreactive NKG2D axis and to contribute to the variability in disease outcome based on the polymorphism of *H. pylori* virulence factors and NKG2D-Ls. Future research should aim to elucidate the detailed molecular mechanisms and identify the cell types and processes affected by NKG2D evasion in order to promote the development of novel tools for the diagnosis and therapy of *H. pylori* associated pathologies.

6. References

1. Marshall BJ, Warren JR. Unidentified Curved Bacilli in the Stomach of Patients With Gastritis and Peptic Ulceration. Lancet. 1984;323(8390):1311–5.

2. Salama NR, Hartung ML, Müller A. Life in the human stomach: Persistence strategies of the bacterial pathogen Helicobacter pylori. Nat Rev Microbiol. 2013;11(6):385–99.

3. Moodley Y, Linz B, Bond RP, Nieuwoudt M, Soodyall H, Schlebusch CM, et al. Age of the association between Helicobacter pylori and man. PLoS Pathog. 2012;8(5).

4. Peleteiro B, Bastos A, Ferro A, Lunet N. Prevalence of Helicobacter pylori infection worldwide: A systematic review of studies with national coverage. Dig Dis Sci. 2014;59(8):1698–709.

5. Pérez-Pérez GI, Sack RB, Reid R, Santosham M, Croll J, Blaser MJ. Transient and persistent Helicobacter pylori colonization in native American children. J Clin Microbiol. 2003;41(6):2401–7.

6. Miyaji H, Azuma T, Ito S, Abe Y, Gejyo F, Hashimoto N, et al. Helicobacter pylori infection occurs via close contact infected individuals in early childhood. J Gastroenterol Hepatol. 2000;15(3):257–62.

7. Mamishi S, Eshaghi H, Mahmoudi S, Bahador A, Hosseinpour Sadeghi R, Najafi M, et

al. Intrafamilial transmission of Helicobacter pylori: Genotyping of faecal samples. Br J Biomed Sci. 2016;73(1):38–43.

8. Blaser MJ, Atherton JC. Helicobacter pylori persistence: Biology and disease. J Clin Invest. 2004;113(3):321–33.

9. Blaser MJ. Helicobacters are indigenous to the human stomach: duodenal ulceration is due to changes in gastric microecology in the modern era. Gut. 1998;43:721–727.

10. Robinson K, Atherton JC. The Spectrum of Helicobacter-Mediated Diseases. Annu Rev Pathol Mech Dis. 2021;16:123–44.

11. Bray F, Ferlay J, Soerjomataram I, Siegel RL, Torre LA, Jemal A. Global cancer statistics 2018: GLOBOCAN estimates of incidence and mortality worldwide for 36 cancers in 185 countries. CA Cancer J Clin. 2018;68(6):394–424.

12. Doorakkers E, Lagergren J, Engstrand L, Brusselaers N. Helicobacter pylori eradication treatment and the risk of gastric adenocarcinoma in a Western population. Gut. 2018;1–5.

13. Savoldi A, Carrara E, Graham D, Conti M, Tacconelli E. Prevalence of Antibiotic Resistance in Helicobacter pylori: A Systematic Review and Meta-analysis in World Health Organization Regions. Gastroenterology. 2018;155(5):1372–82.

14. Xie Y, Song C, Cheng H, Xu C, Zhang Z, Wang J, et al. Long-term follow-up of Helicobacter pylori reinfection and its risk factors after initial eradication: a large-scale multicentre, prospective open cohort, observational study. Emerg Microbes Infect. 2020;9(1):548–57.

15. Amieva MR, El-Omar EM. Host-Bacterial Interactions in Helicobacter pylori Infection. Gastroenterology. 2008;134(1):306–23.

16. Arnold IC, Dehzad N, Reuter S, Martin H, Becher B, Taube C, et al. Helicobacter pylori infection prevents allergic asthma in mouse models through the induction of regulatory T cells. J Clin Invest. 2011;121(8):3088–93.

17. Kienesberger S, Cox LM, Livanos A, Zhang XS, Chung J, Perez-Perez GI, et al. Gastric Helicobacter pylori Infection Affects Local and Distant Microbial Populations

and Host Responses. Cell Rep. 2016;14(6):1395–407.

18. Labenz J, Blum AL, Bayerdörffer E, Meining A, Stolte M, Börsch G. Curing Helicobacter pylori Infection in Patients With Duodenal Ulcer May Provoke Reflux Esophagitis. Gastroenterology. 1997;112(5):1442–7.

19. Corley DA, Kubo A, Levin TR, Block G, Habel L, Zhao W, et al. Helicobacter pylori infection and the risk of Barrett's oesophagus: a community-based study. Gut. 2008;57(6):727–33.

20. Cohen D, Shoham O, Orr N, Muhsen K. An inverse and independent association between Helicobacter pylori infection and the incidence of shigellosis and other diarrheal diseases. Clin Infect Dis. 2012;54(4):35–42.

21. Borbet TC, Zhang X, Müller A, Blaser MJ. The role of the changing human microbiome in the asthma pandemic. J Allergy Clin Immunol. 2019;144(6):1457–66.

22. Konturek PC, Rienecker H, Hahn EG, Raithel M. Helicobacter pylori as a protective factor against food allergy. Med Sci Monit. 2008;14(9):453–8.

23. Lebwohl B, Blaser MJ, Ludvigsson JF, Green PHR, Rundle A, Sonnenberg A, et al. Decreased risk of celiac disease in patients with helicobacter pylori colonization. Am J Epidemiol. 2013;178(12):1721–30.

24. Engler DB, Leonardi I, Hartung ML, Kyburz A, Spath S, Becher B, et al. Helicobacter pylori -specific protection against inflammatory bowel disease requires the NLRP3 inflammasome and IL-18. Inflamm Bowel Dis. 2015;21(4):854–61.

25. Altobelli A, Bauer M, Velez K, Cover TL, Müller A. Helicobacter pylori VacA targets myeloid cells in the gastric lamina propria to promote peripherally induced regulatory T-cell differentiation and persistent infection. MBio. 2019;10(2):1–13.

26. Leying H, Suerbaum S, Geis G, Haas R. Cloning and genetic characterization of a Hellcobacter pylori flagellin gene. Mol Microbiol. 1992;6(19):2863–74.

27. Perez-Perez GI, Olivares AZ, Cover TL, Blaser MJ. Characteristics of Helicobacter pylori variants selected for urease deficiency. Infect Immun. 1992;60(9):3658–63.

28. Noto JM, Peek RM. The Helicobacter pylori cag Pathogenicity Island. Methods Mol

Biol. 2012;921(22):41–50.

29. Cover TL. Helicobacter pylori diversity and gastric cancer risk. MBio. 2016;7(1):1–19.

30. Gauthier NC, Monzo P, Kadda V, Doye A, Ricci V, Boquet P. Helicobacter pylori VacA Cytotoxin: A Probe for a Clathrin-independent and Cdc42-dependent Pinocytic Pathway Routed to Late Endosomes. Mol Biol Cell. 2005;16(October):4852–4866.

31. Tombola F, Carlesso C, Szabò I, De Bernard M, Reyrat JM, Telford JL, et al. Helicobacter pylori vacuolating toxin forms anion-selective channels in planar lipid bilayers: Possible implications for the mechanism of cellular vacuolation. Biophys J. 1999;76(3):1401–9.

32. Backert S, Tegtmeyer N. The versatility of the Helicobacter pylori vacuolating cytotoxin VacA in signal transduction and molecular crosstalk. Toxins (Basel). 2010;2(1):69–92.

33. Cover TL, Blanke SR. Helicobacter pylori VacA, a paradigm for toxin multifunctionality. Nat Rev Microbiol. 2005;3(4):320–32.

34. Papini E, Satin B, Norais N, De Bernard M, Telford JL, Rappuoli R, et al. Selective increase of the permeability of polarized epithelial cell monolayers by Helicobacter pylori vacuolating toxin. J Clin Invest. 1998;102(4):813–20.

35. Gebert B, Fischer W, Weiss E, Hoffmann R, Haas R. Helicobacter pylori vacuolating cytotoxin inhibits T lymphocyte activation. Science. 2003;301(5636):1099–102.

36. Torres VJ, VanCompernolle SE, Sundrud MS, Unutmaz D, Cover TL. Helicobacter pylori Vacuolating Cytotoxin Inhibits Activation-Induced Proliferation of Human T and B Lymphocyte Subsets . J Immunol. 2007;179(8):5433–40.

37. Malfertheiner P, Link A, Selgrad M. Helicobacter pylori: perspectives and time trends. Nat Rev Gastroenterol Hepatol. 2014;11(10):628–38.

38. Figueiredo C, Machado JC, Pharoah P, Seruca R, Sousa S, Carvalho R, et al. Helicobacter pylori and interleukin 1 genotyping: an opportunity to identify high-risk individuals for gastric carcinoma. J Natl Cancer Inst. 2002;94(22):1680–7.

39. Nogueira C, Figueiredo C, Carneiro F, Gomes AT, Barreira R, Figueira P, et al.

Helicobacter pylori genotypes may determine gastric histopathology. Am J Pathol. 2001;158(2):647–54.

40. Rhead JL, Letley DP, Mohammadi M, Hussein N, Mohagheghi MA, Eshagh Hosseini M, et al. A New Helicobacter pylori Vacuolating Cytotoxin Determinant, the Intermediate Region, Is Associated With Gastric Cancer. Gastroenterology. 2007;133(3):926–36.

41. Ferreira RM, Machado JC, Letley D, Atherton JC, Pardo ML, Gonzalez CA, et al. A novel method for genotyping the Helicobacter pylori vacA intermediate region directly in gastric biopsy specimens. J Clin Microbiol. 2012;50(12):3983–9.

42. Segal ED, Cha J, Lo J, Falkow S, Tompkins LS. Altered states: Involvement of phosphorylated CagA in the induction of host cellular growth changes by Helicobacter pylori. Proc Natl Acad Sci U S A. 1999;96(25):14559–64.

43. Jones KR, Whitmire JM, Merrell DS. A tale of two toxins: Helicobacter pylori CagA and VacA modulate host pathways that impact disease. Front Microbiol. 2010;1(Nov):1–17.

44. Brandt S, Kwok T, Hartig R, König W, Backert S. NF-κB activation and potentiation of proinflammatory responses by the Helicobacter pylori CagA protein. Proc Natl Acad Sci U S A. 2005;102(26):9300–5.

45. Saadat I, Higashi H, Obuse C, Umeda M, Murata-Kamiya N, Saito Y, et al. Helicobacter pylori CagA targets PAR1/MARK kinase to disrupt epithelial cell polarity. Nature. 2007;447(7142):330–3.

46. Umeda M, Murata-Kamiya N, Saito Y, Ohba Y, Takahashi M, Hatakeyama M. Helicobacter pylori CagA causes mitotic impairment and induces chromosomal instability. J Biol Chem. 2009;284(33):22166–72.

47. Amieva MR, Vogelmann R, Covacci A, Tompkins LS, Nelson WJ, Falkow S. Disruption of the epithelial apical-junctional complex by Helicobacter pylori CagA. Science. 2003;300(5624):1430–4.

48. Bagnoli F, Buti L, Tompkins L, Covacci A, Amieva MR. Helicobacter pylori CagA induces a transition from polarized to invasive phenotypes in MDCK cells. Proc Natl

Acad Sci U S A. 2005;102(45):16339–44.

49. Murata-Kamiya N, Kurashima Y, Teishikata Y, Yamahashi Y, Saito Y, Higashi H, et al. Helicobacter pylori CagA interacts with E-cadherin and deregulates the β-catenin signal that promotes intestinal transdifferentiation in gastric epithelial cells. Oncogene. 2007;26(32):4617–26.

50. Oliveira MJ, Costa AM, Costa AC, Ferreira RM, Sampaio P, Machado JC, et al. CagA associates with c-met, E-cadherin, and p120catenin in a multiproteic complex that suppresses helicobacter pylori-induced cell-invasive phenotype. J Infect Dis. 2009;200(5):745–55.

51. Zeaiter Z, Huynh HQ, Kanyo R, Stein M. CagA of Helicobacter pylori alters the expression and cellular distribution of host proteins involved in cell signaling. FEMS Microbiol Lett. 2008;288(2):227–34.

52. Mimuro H, Suzuki T, Tanaka J, Asahi M, Haas R, Sasakawa C. Grb2 is a key mediator of Helicobacter pylori CagA protein activities. Mol Cell. 2002;10(4):745–55.

53. Chang YJ, Wu MS, Lin JT, Pestell RG, Blaser MJ, Chen CC. Mechanisms for Helicobacter pylori CagA-induced cyclin D1 expression that affect cell cycle. Cell Microbiol. 2006;8(11):1740–52.

54. Lee O, Kim JH, Choi YJ, Pillinger MH, Kim SY, Blaser MJ, et al. Helicobacter pylori CagA phosphorylation status determines the gp130-activated SHP2/ERK and JAK/STAT signal transduction pathways in gastric epithelial cells. J Biol Chem. 2010;285(21):16042–50.

55. Mimuro H, Suzuki T, Nagai S, Rieder G, Suzuki M, Nagai T, et al. Helicobacter pylori Dampens Gut Epithelial Self-Renewal by Inhibiting Apoptosis, a Bacterial Strategy to Enhance Colonization of the Stomach. Cell Host Microbe. 2007;2(4):250–63.

56. Ohnishi N, Yuasa H, Tanaka S. Transgenic expression of Helicobacter pylori CagA induces gastrointestinal and hematopoietic neoplasms in mouse. Chemtracts. 2008;21(3):121–3.

57. Yamaoka Y. Mechanisms of disease: Helicobacter pylori virulence factors. Nat Rev Gastroenterol Hepatol. 2010;7(11):629–41.

58. Chen Y, Blaser MJ. Inverse associations of Helicobacter pylori with asthma and allergy. Arch Intern Med [Internet]. 2007 Apr 23 [cited 2024 Apr 24];167(8):821–7. Available from: https://pubmed.ncbi.nlm.nih.gov/17452546/

59. Reibman J, Marmor M, Filner J, Fernandez-Beros M-E, Rogers L, Perez-Perez GI, et al. Asthma is inversely associated with Helicobacter pylori status in an urban population. PLoS One. 2008;3(12):e4060.

60. Backert S, Blaser MJ. Cancer Research 75th Annivsersary Commentary: The role of CagA in the gastric biology of Helicobacter pylori. Cancer Res. 2016;76(14):4028–31.

61. Kwok T, Zabler D, Urman S, Rohde M, Hartig R, Wessler S, et al. Helicobacter exploits integrin for type IV secretion and kinase activation. Nature. 2007;449(7164):862–6.

62. Tegtmeyer N, Hartig R, Delahay RM, Rohde M, Brandt S, Conradi J, et al. A small fibronectin-mimicking protein from bacteria induces cell spreading and focal adhesion formation. J Biol Chem. 2010;285(30):23515–26.

63. Gorrell RJ, Guan J, Xin Y, Tafreshi MA, Hutton ML, Mcguckin MA, et al. A novel NOD1- and CagA-independent pathway of interleukin-8 induction mediated by the Helicobacter pylori type IV secretion system. Cell Microbiol. 2013 Apr;15(4):554–70.

64. Saha A, Backert S, Hammond CE, Gooz M, Smolka AJ. Helicobacter pylori CagL activates ADAM17 to induce repression of the gastric H, K-ATPase alpha subunit. Gastroenterology. 2010;139(1):239–48.

65. White JR, Winter JA, Robinson K. Differential inflammatory response to Helicobacter pylori infection: Etiology and clinical outcomes. J Inflamm Res. 2015;8:137–47.

66. Sundquist M, Quiding-Järbrink M. Helicobacter pylori and its effect on innate and adaptive immunity: New insights and vaccination strategies. Expert Rev Gastroenterol Hepatol. 2010;4(6):733–44.

67. Robinson K, Kenefeck R, Pidgeon EL, Shakib S, Patel S, Poison RJ, et al. Helicobacter pylori-induced peptic ulcer disease is associated with inadequate regulatory T cell responses. Gut [Internet]. 2008 Oct [cited 2024 Apr 24];57(10):1375–85. Available from: https://pubmed.ncbi.nlm.nih.gov/18467372/

68. Harris PR, Wright SW, Serrano C, Riera F, Duarte I, Torres J, et al. Helicobacter pylori gastritis in children is associated with a regulatory T-cell response. Gastroenterology [Internet]. 2008 [cited 2024 Apr 24];134(2):491–9. Available from: https://pubmed.ncbi.nlm.nih.gov/18242215/

69. Arnold IC, Lee JY, Amieva MR, Roers A, Flavell RA, Sparwasser T, et al. Tolerance rather than immunity protects from Helicobacter pylori-induced gastric preneoplasia. Gastroenterology [Internet]. 2011 [cited 2024 Apr 24];140(1):199-209.e8. Available from: https://pubmed.ncbi.nlm.nih.gov/20600031/

70. Cullen TW, Giles DK, Wolf LN, Ecobichon C, Boneca IG, Trent MS. Helicobacter pylori versus the host: remodeling of the bacterial outer membrane is required for survival in the gastric mucosa. PLoS Pathog [Internet]. 2011 Dec [cited 2024 Apr 24];7(12). Available from: https://pubmed.ncbi.nlm.nih.gov/22216004/

71. Andersen-Nissen E, Smith KD, Strobe KL, Rassoulian Barrett SL, Cookson BT, Logan SM, et al. Evasion of Toll-like receptor 5 by flagellated bacteria. Proc Natl Acad Sci U S A [Internet]. 2005 Jun 28 [cited 2024 Apr 24];102(26):9247–52. Available from: https://pubmed.ncbi.nlm.nih.gov/15956202/

72. Otani K, Tanigawa T, Watanabe T, Nadatani Y, Sogawa M, Yamagami H, et al. Toll-like receptor 9 signaling has anti-inflammatory effects on the early phase of Helicobacter pylori-induced gastritis. Biochem Biophys Res Commun [Internet]. 2012;426(3):342–9. Available from: http://dx.doi.org/10.1016/j.bbrc.2012.08.080

73. Luther J, Owyang SY, Takeuchi T, Cole TS, Zhang M, Liu M, et al. Helicobacter pylori DNA decreases pro-inflammatory cytokine production by dendritic cells and attenuates dextran sodium sulphate-induced colitis. Gut [Internet]. 2011 Nov [cited 2024 Apr 24];60(11):1479–86. Available from: https://pubmed.ncbi.nlm.nih.gov/21471567/

74. Owyang SY, Luther J, Owyang CC, Zhang M, Kao JY. Helicobacter pylori DNA's anti-inflammatory effect on experimental colitis. Gut Microbes. 2012;3(2):168–71.

75. Reyes VE, Peniche AG. Helicobacter pylori deregulates T and B cell signaling to trigger immune evasion. Curr Top Microbiol Immunol. 2019;421:229–65.

76. Lina TT, Alzahrani S, Gonzalez J, Pinchuk I V., Beswick EJ, Reyes VE. Immune evasion strategies used by Helicobacter pylori. World J Gastroenterol. 2014;20(36):12753–66.

77. Abel AM, Yang C, Thakar MS, Malarkannan S. Natural killer cells: Development, maturation, and clinical utilization. Front Immunol. 2018;9(Aug):1–23.

78. Huntington ND, Cursons J, Rautela J. The cancer–natural killer cell immunity cycle. Nat Rev Cancer. 2020;20(8):437–54.

79. Sivori S, Vacca P, Del Zotto G, Munari E, Mingari MC, Moretta L. Human NK cells: surface receptors, inhibitory checkpoints, and translational applications. Cell Mol Immunol. 2019;16(5):430–41.

80. Prager I, Watzl C. Mechanisms of natural killer cell-mediated cellular cytotoxicity. J Leukoc Biol. 2019;105(6):1319–29.

81. Souza-Fonseca-Guimaraes F, Adib-Conquy M, Cavaillon JM. Natural killer (NK) cells in antibacterial innate immunity: angels or devils? Mol Med. 2012;18(1):270–85.

82. Adib-Conquy M, Scott-Algara D, Cavaillon JM, Souza-Fonseca-Guimaraes F. TLR-mediated activation of NK cells and their role in bacterial/viral immune responses in mammals. Vol. 92, Immunology and Cell Biology. 2014. p. 256–62.

83. Schmidt S, Ullrich E, Bochennek K, Zimmermann S-Y, Lehrnbecher T. Role of natural killer cells in antibacterial immunity. Expert Rev Hematol. 2016;9(12):1119–27.

84. Theresine M, Patil ND, Zimmer J. Airway Natural Killer Cells and Bacteria in Health and Disease. Front Immunol. 2020;11(Sep):1–14.

85. Kupz A, Scott TA, Belz GT, Andrews DM, Greyer M, Lew AM, et al. Contribution of Thy1+ NK cells to protective IFN-γ production during Salmonella typhimurium infections. Proc Natl Acad Sci U S A [Internet]. 2013 Feb 5 [cited 2024 Apr 24];110(6):2252–7. Available from: https://pubmed.ncbi.nlm.nih.gov/23345426/

86. Small C-L, McCormick S, Gill N, Kugathasan K, Santosuosso M, Donaldson N, et al. NK cells play a critical protective role in host defense against acute extracellular Staphylococcus aureus bacterial infection in the lung. J Immunol [Internet]. 2008 Apr

15 [cited 2024 Apr 24];180(8):5558–68. Available from: https://pubmed.ncbi.nlm.nih.gov/18390740/

87. Vankayalapati R, Wizel B, Weis SE, Safi H, Lakey DL, Mandelboim O, et al. The NKp46 receptor contributes to NK cell lysis of mononuclear phagocytes infected with an intracellular bacterium. J Immunol [Internet]. 2002 Apr 1 [cited 2024 Apr 24];168(7):3451–7. Available from: https://pubmed.ncbi.nlm.nih.gov/11907104/

88. Lu C-C, Wu T-S, Hsu Y-J, Chang C-J, Lin C-S, Chia J-H, et al. NK cells kill mycobacteria directly by releasing perforin and granulysin. J Leukoc Biol. 2014;96(6):1119–29.

89. Sim MJW, Rajagopalan S, Altmann DM, Boyton RJ, Sun PD, Long EO. Human NK cell receptor KIR2DS4 detects a conserved bacterial epitope presented by HLA-C. Proc Natl Acad Sci U S A. 2019;116(26):12964–73.

90. Backert S. Molecular Mechanisms of Inflammation: Induction, Resolution and Escape by Helicobacter pylori. 1st ed. Backert S, editor. Cham, Switzerland: Springer Nature Switzerland AG; 2019. 359 p.

91. Yun CH, Lundgren A, Azem J, Sjöling Å, Holmgren J, Svennerholm AM, et al. Natural killer cells and Helicobacter pylori infection: Bacterial antigens and interleukin-12 act synergistically to induce gamma interferon production. Infect Immun. 2005;73(3):1482–90.

92. Tarkkanen J, Kosunen TU, Saksela E. Contact of lymphocytes with Helicobacter pylori augments natural killer cell activity and induces production of gamma interferon. Infect Immun. 1993;61(7):3012–6.

93. Rudnicka K, Miszczyk E, Matusiak A, Walencka M, Moran AP, Rudnicka W, et al. Helicobacter pylori-driven modulation of NK cell expansion, intracellular cytokine expression and cytotoxic activity. Innate Immun. 2015;21(2):127–39.

94. Chochi K, Ichikura T, Kinoshita M, Majima T, Shinomiya N, HironoriTsujimoto, et al. Helicobacter pylori augments growth of gastric cancers via the lipopolysaccharide-toll-like receptor 4 pathway whereas Its lipopolysaccharide attenuates antitumor activities of human mononuclear cells. Clin Cancer Res. 2008 May 15;14(10):2909–17.

95. Rudnicka K, Włodarczyk M, Moran AP, Rechciński T, Miszczyk E, Matusiak A, et al. Helicobacter pylori antigens as potential modulators of lymphocytes' cytotoxic activity. Microbiol Immunol. 2012;56(1):62–75.

96. Hafsi N, Voland P, Schwendy S, Rad R, Reindl W, Gerhard M, et al. Human Dendritic Cells Respond to Helicobacter pylori , Promoting NK Cell and Th1-Effector Responses In Vitro . J Immunol. 2004;173(2):1249–57.

97. Betten Å, Bylund J, Cristophe T, Boulay F, Romero A, Hellstrand K, et al. A proinflammatory peptide from Helicobacter pylori activates monocytes to induce lymphocyte dysfunction and apoptosis. J Clin Invest. 2001;108(8):1221–8.

98. Agnihotri N, Bhasin DK, Vohra H, Ray P, Singh K, Ganguly NK. Characterization of lymphocytic subsets and cytokine production in gastric biopsy samples from Helicobacter pylori patients. Scand J Gastroenterol. 1998;33(7):704–9.

99. Long EO, Sik Kim H, Liu D, Peterson ME, Rajagopalan S. Controlling natural killer cell responses: Integration of signals for activation and inhibition. Annu Rev Immunol. 2013;31:227–58.

100. Okumura G, Iguchi-Manaka A, Murata R, Yamashita-Kanemaru Y, Shibuya A, Shibuya K. Tumor-derived soluble CD155 inhibits DNAM-1-mediated antitumor activity of natural killer cells. J Exp Med. 2020;217(4):1–11.

101. Reiners KS, Topolar D, Henke A, Simhadri VR, Kessler J, Sauer M, et al. Soluble ligands for NK cell receptors promote evasion of chronic lymphocytic leukemia cells from NK cell anti-tumor activity. Blood. 2013 May 2;121(18):3658–65.

102. Schlecker E, Fiegler N, Arnold A, Altevogt P, Rose-John S, Moldenhauer G, et al. Metalloprotease-mediated tumor cell shedding of B7-H6, the ligand of the natural killer cell-activating receptor NKp30. Cancer Res. 2014;74(13):3429–40.

103. Pesce S, Tabellini G, Cantoni C, Patrizi O, Coltrini D, Rampinelli F, et al. B7-H6-mediated downregulation of NKp30 in NK cells contributes to ovarian carcinoma immune escape. Oncoimmunology. 2015;4(4).

104. Raulet DH, Gasser S, Gowen BG, Deng W, Jung H. Regulation of ligands for the NKG2D activating receptor. Annu Rev Immunol. 2013;31(1):413–41.

105. Bauer S, Groh V, Wu J, Steinle A, Phillips JH, Lanier LL, et al. Activation of NK cells and T cells by NKG2D, a receptor for stress- inducible MICA. Science. 1999;285(5428):727–9.

106. Groh V, Rhinehart R, Randolph-Habecker J, Topp MS, Riddell SR, Spies T. Costimulation of CD8αβ T cell by NKG2D via engagement by MIC induced on virus-infected cells. Nat Immunol. 2001 Mar;2(3):255–60.

107. Lanier LL. NKG2D receptor and its ligands in host defense. Cancer Immunol Res. 2015;3(6):575–582.

108. Groh V, Bahram S, Bauer S, Herman A, Beauchamp M, Spies T. Cell stress-regulated human major histocompatibility complex class I gene expressed in gastrointestinal epithelium. Proc Natl Acad Sci U S A. 1996;93(22):12445–50.

109. Ghadially H, Brown L, Lloyd C, Lewis L, Lewis A, Dillon J, et al. MHC class i chain-related protein A and B (MICA and MICB) are predominantly expressed intracellularly in tumour and normal tissue. Br J Cancer. 2017;116(9):1208–17.

110. Das H, Groh V, Kuijl C, Sugita M, Morita CT, Spies T, et al. MICA engagement by human Vγ2Vδ2 T cells enhances their antigen-dependent effector function. Immunity. 2001;15(1):83–93.

111. Tieng V, Le Bouguénec C, Du Merle L, Bertheau P, Desreumaux P, Janin A, et al. Binding of Escherichia coli adhesin AfaE to CD55 triggers cell-surface expression of the MHC class I-related molecule MICA. Proc Natl Acad Sci U S A. 2002;99(5):2977–82.

112. Groh V, Rhinehart R, Secrist H, Bauer S, Grabstein KH, Spies T. Broad tumor-associated expression and recognition by tumor-derived γδ T cells of MICA and MICB. Proc Natl Acad Sci U S A. 1999;96(12):6879–84.

113. Roberts AI, Lee L, Schwarz E, Groh V, Spies T, Ebert EC, et al. Cutting Edge: NKG2D Receptors Induced by IL-15 Costimulate CD28-Negative Effector CTL in the Tissue Microenvironment. J Immunol. 2001;167(10):5527–30.

114. Guerra N, Tan YX, Joncker NT, Choy A, Gallardo F, Xiong N, et al. NKG2D-Deficient Mice Are Defective in Tumor Surveillance in Models of Spontaneous

Malignancy. Immunity. 2008;28(5):723.

115. Watson NFS, Spendlove I, Madjd Z, McGilvray R, Green AR, Ellis IO, et al. Expression of the stress-related MHC class I chain-related protein MICA is an indicator of good prognosis in colorectal cancer patients. Int J Cancer. 2006;118(6):1445–52.

116. Steel JC, Waldmann TA, Morris JC. Interleukin-15 biology and its therapeutic implications in cancer. Trends Pharmacol Sci. 2012;33(1):35–41.

117. Park YP, Choi SC, Kiesler P, Gil-Krzewska A, Borrego F, Weck J, et al. Complex regulation of human NKG2D-DAP10 cell surface expression: Opposing roles of the γc cytokines and TGF-β1. Blood. 2011;118(11):3019–27.

118. Molfetta R, Quatrini L, Zitti B, Capuano C, Galandrini R, Santoni A, et al. Regulation of NKG2D Expression and Signaling by Endocytosis. Trends Immunol. 2016;37(11):790–802.

119. Raulet DH, Gasser S, Gowen BG, Deng W, Jung H. Regulation of ligands for the NKG2D activating receptor. Annu Rev Immunol. 2013;31:413–41.

120. Bahram S, Bresnahan M, Geraghty DE, Spies T. A second lineage of mammalian major histocompatibility complex class I genes. Proc Natl Acad Sci U S A. 1994 Jul 5;91(14):6259–63.

121. Complete sequence and gene map of a human major histocompatibility complex. The MHC sequencing consortium. Nature. 1999;401(6756):921–3.

122. Chen D, Gyllensten U. MICA polymorphism: biology and importance in cancer. Carcinogenesis. 2014;35(12):2633–42.

123. Shiina T, Tamiya G, Oka A, Takishima N, Yamagata T, Kikkawa E, et al. Molecular dynamics of MHC genesis unraveled by sequence analysis of the 1,796,938-bp HLA class I region. Proc Natl Acad Sci U S A. 1999;96(23):13282–7.

124. Fukami-Kobayashi K, Shiina T, Anzai T, Sano K, Yamazaki M, Inoko H, et al. Genomic evolution of MHC class I region in primates. Proc Natl Acad Sci U S A. 2005 Jun 28;102(26):9230–4.

125. Ohno S. Evolution by Gene Duplication. 1st ed. New York, USA: Springer Science+Business Media; 1970. 160 p.

126. Klussmeier A, Massalski C, Putke K, Schäfer G, Sauter J, Schefzyk D, et al. High-Throughput MICA/B Genotyping of Over Two Million Samples: Workflow and Allele Frequencies. Front Immunol. 2020;11(Feb):1–9.

127. Rodríguez-Rodero S, González S, Rodrigo L, Fernández-Morera JL, Martínez-Borra J, López-Vázquez A, et al. Transcriptional regulation of MICA and MICB: A novel polymorphism in MICB promoter alters transcriptional regulation by Sp1. Eur J Immunol. 2007;37(7):1938–53.

128. Steinle A, Li P, Morris DL, Groh V, Lanier LL, Strong RK, et al. Interactions of human NKG2D with its ligands MICA, MICB, and homologs of the mouse RAE-1 protein family. Immunogenetics. 2001;53(4):279–87.

129. Suemizu H, Radosavljevic M, Kimura M, Sadahiro S, Yoshimura S, Bahram S, et al. A basolateral sorting motif in the MICA cytoplasmic tail. Proc Natl Acad Sci U S A. 2002;99(5):2971–6.

130. Ashiru O, Boutet P, Fernández-Messina L, Agüera-González S, Skepper JN, Valés-Gómez M, et al. Natural killer cell cytotoxicity is suppressed by exposure to the human NKG2D ligand MICA*008 that is shed by tumor cells in exosomes. Cancer Res. 2010;70(2):481–9.

131. Lopez-Vazquez A, Rodrigo L, Fuentes D, Riestra S, Bousoño C, Garcia-Fernandez S, et al. MHC class I chain related gene A (MICA) modulates the development of coeliac disease in patients with the high risk heterodimer DQA1 *0501/DQB1 *0201. Gut. 2002;50(3):336–40.

132. Fdez-Morera JL, Rodrigo L, López-Vázquez A, Rodero SR, Martínez-Borra J, Niño P, et al. MHC class I chain-related gene a transmembrane polymorphism modulates the extension of ulcerative colitis. Hum Immunol. 2003;64(8):816–22.

133. Groh V, Steinle A, Bauer S, Spies T. Recognition of stress-induced MHC molecules by intestinal epithelial γδ T cells. Science. 1998;279(5357):1737–40.

134. Li P, Willie ST, Bauer S, Morris DL, Spies T, Strong RK. Crystal structure of the

MHC class I homolog MIC-A, a γδ T cell ligand. Immunity. 1999;10(5):577–84.

135. Li P, Morris DL, Willcox BE, Steinle A, Spies T, Strong RK. Complex structure of the activating immunoreceptor NKG2D and its MHC class I-like ligand MICA. Nat Immunol. 2001;2(5):443–51.

136. Borchers MT, Harris NL, Wesselkamper SC, Vitucci M, Cosman D. NKG2D ligands are expressed on stressed human airway epithelial cells. Am J Physiol - Lung Cell Mol Physiol. 2006;291(2).

137. Hansen CHF, Holm TL, Krych L, Andresen L, Nielsen DS, Rune I, et al. Gut microbiota regulates NKG2D ligand expression on intestinal epithelial cells. Eur J Immunol. 2013;43(2):447–57.

138. Camini FC, da Silva Caetano CC, Almeida LT, de Brito Magalhães CL. Implications of oxidative stress on viral pathogenesis. Arch Virol. 2017;162(4):907–17.

139. Filone CM, Caballero IS, Dower K, Mendillo ML, Cowley GS, Santagata S, et al. The Master Regulator of the Cellular Stress Response (HSF1) Is Critical for Orthopoxvirus Infection. PLoS Pathog. 2014;10(2).

140. Sinclair A, Yarranton S, Schelcher C. DNA-damage response pathways triggered by viral replication. Expert Rev Mol Med. 2006;8(5):1–11.

141. Bartkova J, Hořejší Z, Koed K, Krämer A, Tort F, Zleger K, et al. DNA damage response as a candidate anti-cancer barrier in early human tumorigenesis. Nature. 2005;434(7035):864–70.

142. Yamamoto K, Fujiyama Y, Andoh A, Bamba T, Okabe H. Oxidative stress increases MICA and MICB gene expression in the human colon carcinoma cell line (CaCo-2). Biochim Biophys Acta. 2001;1526(1):10–2.

143. Venkataraman GM, Suciu D, Groh V, Boss JM, Spies T. Promoter Region Architecture and Transcriptional Regulation of the Genes for the MHC Class I-Related Chain A and B Ligands of NKG2D. J Immunol. 2007;178(2):961–9.

144. Gasser S, Orsulic S, Brown EJ, Raulet DH. The DNA damage pathway regulates innate immune system ligands of the NKG2D receptor. Nature. 2005;436(7054):1186–90.

145. Soriani A, Iannitto ML, Ricci B, Fionda C, Malgarini G, Morrone S, et al. Reactive Oxygen Species– and DNA Damage Response–Dependent NK Cell Activating Ligand Upregulation Occurs at Transcriptional Levels and Requires the Transcriptional Factor E2F1. J Immunol. 2014;193(2):950–60.

146. Esteso G, Guerra S, Valés-Gómez M, Reyburn HT. Innate immune recognition of double-stranded RNA triggers increased expression of NKG2D ligands after virus infection. J Biol Chem. 2017;292(50):20472–80.

147. Lin D, Lavender H, Soilleux EJ, O'Callaghan CA. NF-κB regulates MICA gene transcription in endothelial cell through a genetically inhibitable control site. J Biol Chem. 2012;287(6):4299–310.

148. Vantourout P, Willcox C, Turner A, Swanson CM, Haque Y, Sobolev O, et al. Immunological visibility: Posttranscriptional regulation of human NKG2D ligands by the EGF receptor pathway. Sci Transl Med. 2014;6(231).

149. Nachmani D, Gutschner T, Reches A, Diederichs S, Mandelboim O. RNA-binding proteins regulate the expression of the immune activating ligand MICB. Nat Commun. 2014;5(May):1–13.

150. Stern-Ginossar N, Gur C, Biton M, Horwitz E, Elboim M, Stanietsky N, et al. Human microRNAs regulate stress-induced immune responses mediated by the receptor NKG2D. Nat Immunol. 2008;9(9):1065–73.

151. Schmiedel D, Mandelboim O. NKG2D ligands-critical targets for cancer immune escape and therapy. Front Immunol. 2018;9(Sep):1–10.

152. Tsukerman P, Stern-Ginossar N, Gur C, Glasner A, Nachmani D, Bauman Y, et al. MiR-10b downregulates the stress-induced cell surface molecule MICB, a critical ligand for cancer cell recognition by natural killer cells. Cancer Res. 2012;72(21):5463–72.

153. Nachmani D, Lankry D, Wolf DG, Mandelboim O. The human cytomegalovirus microRNA miR-UL112 acts synergistically with a cellular microRNA to escape immune elimination. Nat Immunol. 2010;11(9):806–13.

154. Stern-Ginossar N, Elefant N, Zimmermann A, Wolf DG, Saleh N, Biton M, et al. Host

immune system gene targeting by a viral miRNA. Science. 2007;317(5836):376–81.

155. Nachmani D, Stern-Ginossar N, Sarid R, Mandelboim O. Diverse Herpesvirus MicroRNAs Target the Stress-Induced Immune Ligand MICB to Escape Recognition by Natural Killer Cells. Cell Host Microbe. 2009;5(4):376–85.

156. Toledano T, Vitenshtein A, Stern-Ginossar N, Seidel E, Mandelboim O. Decay of the Stress-Induced Ligand MICA Is Controlled by the Expression of an Alternative 3′ Untranslated Region. J Immunol. 2018;200(8):2819–25.

157. Garrido-Tapia M, Hernández CJ, Ascui G, Kramm K, Morales M, Gárate V, et al. STAT3 inhibition by STA21 increases cell surface expression of MICB and the release of soluble MICB by gastric adenocarcinoma cells. Immunobiology. 2017;222(11):1043–51.

158. Agüera-González S, Boutet P, Reyburn HT, Valés-Gómez M. Brief Residence at the Plasma Membrane of the MHC Class I-Related Chain B Is Due to Clathrin-Mediated Cholesterol-Dependent Endocytosis and Shedding. J Immunol. 2009;182(8):4800–8.

159. del Toro-Arreola S, Arreygue-Garcia N, Aguilar-Lemarroy A, Cid-Arregui A, Jimenez-Perez M, Haramati J, et al. MHC class I-related chain A and B ligands are differentially expressed in human cervical cancer cell lines. Cancer Cell Int. 2011;11(15).

160. Dunn GP, Bruce AT, Ikeda H, Old LJ, Schreiber RD. Cancer immunoediting: From immunosurveillance to tumor escape. Nat Immunol. 2002;3(11):991–8.

161. Baugh R, Khalique H, Seymour LW. Convergent evolution by cancer and viruses in evading the nkg2d immune response. Cancers (Basel). 2020;12(12):1–27.

162. McGilvray RW, Eagle RA, Watson NFS, Al-Attar A, Ball G, Jafferji I, et al. NKG2D ligand expression in human colorectal cancer reveals associations with prognosis and evidence for immunoediting. Clin Cancer Res. 2009;15(22):6993–7002.

163. Esteso G, Luzón E, Sarmiento E, Gómez-Caro R, Steinle A, Murphy G, et al. Altered MicroRNA Expression after Infection with Human Cytomegalovirus Leads to TIMP3 Downregulation and Increased Shedding of Metalloprotease Substrates, Including MICA. J Immunol. 2014;193(3):1344–52.

164. Wu J, Chalupny NJ, Manley TJ, Riddell SR, Cosman D, Spies T. Intracellular retention of the MHC class I-related chain B ligand of NKG2D. J Immunol. 2003;170(8):4196–200.

165. Chalupny NJ, Rein-Weston A, Dosch S, Cosman D. Down-regulation of the NKG2D ligand MICA by the human cytomegalovirus glycoprotein UL142. Biochem Biophys Res Commun. 2006;346(1):175–81.

166. Thomas M, Boname JM, Field S, Nejentsev S, Salio M, Cerundolo V, et al. Down-regulation of NKG2D and NKp80 ligands by Kaposi's sarcoma-associated herpesvirus K5 protects against NK cell cytotoxicity. Proc Natl Acad Sci U S A. 2008;105(5):1656–61.

167. Wu J, Zhang X-J, Shi K-Q, Chen Y-P, Ren Y-F, Song Y-J, et al. Hepatitis B surface antigen inhibits MICA and MICB expression via induction of cellular miRNAs in hepatocellular carcinoma cells. Carcinogenesis. 2014;35(1):155–63.

168. Wen C, He X, Ma H, Hou N, Wei C, Song T, et al. Hepatitis C virus infection downregulates the ligands of the activating receptor NKG2D. Cell Mol Immunol. 2008;5(6):475–8.

169. Matusali G, Tchidjou HK, Pontrelli G, Bernardi S, D'Ettorre G, Vullo V, et al. Soluble ligands for the NKG2D receptor are released during HIV-1 infection and impair NKG2D expression and cytotoxicity of NK cells. FASEB J. 2013;27(6):2440–50.

170. Lee MJ, Leong MW, Rustagi A, Beck A, Zeng L, Holmes S, et al. SARS-CoV-2 escapes direct NK cell killing through Nsp1-mediated downregulation of ligands for NKG2D. Cell Rep [Internet]. 2022;41(13):111892. Available from: https://doi.org/10.1016/j.celrep.2022.111892

171. Fuertes MB, Girart M V, Molinero LL, Domaica CI, Rossi LE, Barrio MM, et al. Intracellular retention of the NKG2D ligand MHC class I chain-related gene A in human melanomas confers immune privilege and prevents NK cell-mediated cytotoxicity. J Immunol. 2008;180(7):4606–14.

172. Groh V, Wu J, Yee C, Spies T. Tumour-derived soluble MIC ligands impair expression of NKG2D and T-cell activation. Nature. 2002;419(6908):734–8.

173. Salih HR, Rammensee H-G, Steinle A. Cutting Edge: Down-Regulation of MICA on Human Tumors by Proteolytic Shedding. J Immunol. 2002;169(8):4098–102.

174. Salih HR, Goehlsdorf D, Steinle A. Release of MICB Molecules by Tumor Cells: Mechanism and Soluble MICB in Sera of Cancer Patients. Hum Immunol. 2006;67(3):188–95.

175. Boutet P, Agüera-González S, Atkinson S, Pennington CJ, Edwards DR, Murphy G, et al. Cutting Edge: The Metalloproteinase ADAM17/TNF-α-Converting Enzyme Regulates Proteolytic Shedding of the MHC Class I-Related Chain B Protein. J Immunol. 2009;182(1):49–53.

176. Waldhauer I, Goehlsdorf D, Gieseke F, Weinschenk T, Wittenbrink M, Ludwig A, et al. Tumor-associated MICA is shed by ADAM proteases. Cancer Res. 2008;68(15):6368–76.

177. Andrade LF De, Tay RE, Pan D, Luoma AM, Ito Y, Badrinath S, et al. Antibody-mediated inhibition of MICA and MICB shedding promotes NK cell – driven tumor immunity. Science. 2018;359(6383):1537–42.

178. Doubrovina ES, Doubrovin MM, Vider E, Sisson RB, O'Reilly RJ, Dupont B, et al. Evasion from NK Cell Immunity by MHC Class I Chain-Related Molecules Expressing Colon Adenocarcinoma. J Immunol. 2003;171(12):6891–9.

179. Hanaoka N, Jabri B, Dai Z, Ciszewski C, Stevens AM, Yee C, et al. NKG2D Initiates Caspase-Mediated CD3ζ Degradation and Lymphocyte Receptor Impairments Associated with Human Cancer and Autoimmune Disease. J Immunol. 2010;185(10):5732–42.

180. Wensveen FM, Jelenčić V, Polić B. NKG2D: A master regulator of immune cell responsiveness. Front Immunol. 2018;9(Mar).

181. Tong H V., Toan NL, Song LH, Bock CT, Kremsner PG, Velavan TP. Hepatitis B virus-induced hepatocellular carcinoma: Functional roles of MICA variants. J Viral Hepat. 2013;20(10):687–98.

182. Esteso G, Luzón E, Sarmiento E, Gómez-Caro R, Steinle A, Murphy G, et al. Altered MicroRNA Expression after Infection with Human Cytomegalovirus Leads to TIMP3

Downregulation and Increased Shedding of Metalloprotease Substrates, Including MICA. J Immunol. 2014;193(3):1344–52.

183. Arreygue-Garcia NA, Daneri-Navarro A, del Toro-Arreola A, Cid-Arregui A, Gonzalez-Ramella O, Jave-Suarez LF, et al. Augmented serum level of major histocompatibility complex class I-related chain A (MICA) protein and reduced NKG2D expression on NK and T cells in patients with cervical cancer and precursor lesions. BMC Cancer. 2008;8(16).

184. Kohga K, Takehara T, Tatsumi T, Ohkawa K, Miyagi T, Hiramatsu N, et al. Serum levels of soluble major histocompatibility complex (MHC) class I-related chain A in patients with chronic liver diseases and changes during transcatheter arterial embolization for hepatocellular carcinoma. Cancer Sci. 2008;99(8):1643–9.

185. Holdenrieder S, Stieber P, Peterfi A, Nagel D, Steinle A, Salih HR. Soluble MICA in malignant diseases. Int J Cancer. 2006;118(3):684–7.

186. Jinushi M, Takehara T, Tatsumi T, Hiramatsu N, Sakamori R, Yamaguchi S, et al. Impairment of natural killer cell and dendritic cell functions by the soluble form of MHC class I-related chain A in advanced human hepatocellular carcinomas. J Hepatol. 2005;43(6):1013–20.

187. Kumar V, Yi Lo PH, Sawai H, Kato N, Takahashi A, Deng Z, et al. Soluble MICA and a MICA Variation as Possible Prognostic Biomarkers for HBV-Induced Hepatocellular Carcinoma. PLoS One. 2012;7(9):5–10.

188. Duan X, Deng L, Chen X, Lu Y, Zhang Q, Zhang K, et al. Clinical significance of the immunostimulatory MHC class i chain-related molecule A and NKG2D receptor on NK cells in pancreatic cancer. Med Oncol. 2011;28(2):466–74.

189. Wu JD, Higgins LM, Steinle A, Cosman D, Haugk K, Plymate SR. Prevalent expression of the immunostimulatory MHC class I chain-related molecule is counteracted by shadding in prostate cancer. J Clin Invest. 2004;114(4):560–8.

190. Xing S, Ferrari de Andrade L. NKG2D and MICA/B shedding: a ‘tag game’ between NK cells and malignant cells. Clin Transl Immunol. 2020;9(12):e1230.

191. Curio S, Jonsson G, Marinović S. A summary of current NKG2D-based CAR clinical

trials. Immunother Adv. 2021;1(1):1–8.

192. Peipp M, Klausz K, Boje AS, Zeller T, Zielonka S, Kellner C. Immunotherapeutic targeting of activating natural killer cell receptors and their ligands in cancer. Clin Exp Immunol. 2022;(Mar):22–32.

193. Jones JC, Rustagi S, Dempsey PJ. ADAM Proteases and Gastrointestinal Function. Annu Rev Physiol. 2016;78:243–76.

194. de Almeida LGN, Thode H, Eslambolchi Y, Chopra S, Young D, Gill S, et al. Matrix Metalloproteinases: From Molecular Mechanisms to Physiology, Pathophysiology, and PharmacologyS. Pharmacol Rev. 2022;74(3):712–68.

195. Yamanegi K, Yamane J, Kobayashi K, Ohyama H, Nakasho K, Yamada N, et al. Downregulation of matrix metalloproteinase-9 mRNA by valproic acid plays a role in inhibiting the shedding of MHC class I-related molecules A and B on the surface of human osteosarcoma cells. Oncol Rep. 2012;28(5):1585–90.

196. Shiraishi K, Mimura K, Kua LF, Koh V, Siang LK, Nakajima S, et al. Inhibition of MMP activity can restore NKG2D ligand expression in gastric cancer, leading to improved NK cell susceptibility. J Gastroenterol. 2016;51(12):1101–11.

197. Liu G, Atteridge CL, Wang X, Lundgren AD, Wu JD. Cutting Edge: The Membrane Type Matrix Metalloproteinase MMP14 Mediates Constitutive Shedding of MHC Class I Chain-Related Molecule A Independent of A Disintegrin and Metalloproteinases. J Immunol. 2010;184(7):3346–50.

198. Kohga K, Takehara T, Tatsumi T, Ishida H, Miyagi T, Hosui A, et al. Sorafenib inhibits the shedding of major histocompatibility complex class i-related chain a on hepatocellular carcinoma cells by down-regulating a disintegrin and metalloproteinase 9. Hepatology. 2010;51(4):1264–73.

199. Waldhauer I, Goehlsdorf D, Gieseke F, Weinschenk T, Wittenbrink M, Ludwig A, et al. Tumor-associated MICA is shed by ADAM proteases. Cancer Res. 2008;68(15):6368–76.

200. Chitadze G, Lettau M, Bhat J, Wesch D, Steinle A, Fürst D, et al. Shedding of endogenous MHC class I-related chain molecules A and B from different human tumor

entities: Heterogeneous involvement of the “a disintegrin and metalloproteases” 10 and 17. Int J Cancer. 2013;133(7):1557–66.

201. Kohga K, Takehara T, Tatsumi T, Miyagi T, Ishida H, Ohkawa K, et al. Anticancer chemotherapy inhibits MHC class I-related chain A ectodomain shedding by downregulating ADAM10 expression in hepatocellular carcinoma. Cancer Res. 2009;69(20):8050–7.

202. Khokha R, Murthy A, Weiss A. Metalloproteinases and their natural inhibitors in inflammation and immunity. Nat Rev Immunol. 2013;13(9):649–65.

203. Klein T, Bischoff R. Active metalloproteases of the a disintegrin and metalloprotease (ADAM) family: Biological function and structure. J Proteome Res. 2011;10(1):17–33.

204. Kaiser BK, Yim D, Chow IT, Gonzalez S, Dai Z, Mann HH, et al. Disulphide-isomerase-enabled shedding of tumour-associated NKG2D ligands. Nature. 2007;447(7143):482–6.

205. Wang X, Lundgren AD, Singh P, Goodlett DR, Plymate SR, Wu JD. An six-amino acid motif in the alpha3 domain of MICA is the cancer therapeutic target to inhibit shedding. Biochem Biophys Res Commun. 2009;387(3):476–81.

206. Wu JD, Atteridge CL, Wang X, Seya T, Plymate SR. Obstructing shedding of the immunostimulatory MHC class i chain - Related gene B prevents tumor formation. Clin Cancer Res. 2009;15(2):632–40.

207. Schorey JS, Cheng Y, Singh PP, Smith VL. Exosomes and other extracellular vesicles in host–pathogen interactions. EMBO Rep. 2015;16(1):24–43.

208. Deatheragea BL, Cooksona BT. Membrane vesicle release in bacteria, eukaryotes, and archaea: A conserved yet underappreciated aspect of microbial life. Infect Immun. 2012;80(6):1948–57.

209. Robinson DG, Ding Y, Jiang L. Unconventional protein secretion in plants: a critical assessment. Protoplasma. 2016;253(1):31–43.

210. Colombo M, Raposo G, Théry C. Biogenesis, secretion, and intercellular interactions of exosomes and other extracellular vesicles. Annu Rev Cell Dev Biol. 2014;30:255–

89.

211. Lo Cicero A, Stahl PD, Raposo G. Extracellular vesicles shuffling intercellular messages: For good or for bad. Curr Opin Cell Biol. 2015;35:69–77.

212. Yáñez-Mó M, Siljander PRM, Andreu Z, Zavec AB, Borràs FE, Buzas EI, et al. Biological properties of extracellular vesicles and their physiological functions. J Extracell Vesicles. 2015;4(2015):1–60.

213. Van Niel G, D'Angelo G, Raposo G. Shedding light on the cell biology of extracellular vesicles. Nat Rev Mol Cell Biol. 2018;19(4):213–28.

214. Doyle LM, Zhuo Wang M. Overview of Extracellular Vesicles, Their Origin, Composition, Purpose, and Methods for Exosome Isolation and Analysis. Cells. 2019;8(7):41–68.

215. Ashiru O, López-Cobo S, Fernández-Messina L, Pontes-Quero S, Pandolfi R, Reyburn HT, et al. A GPI anchor explains the unique biological features of the common NKG2D-ligand allele MICA*008. Biochem J. 2013;454(2):295–302.

216. Petersdorf EW, Shuler KB, Longton GM, Spies T, Hansen JA. Population study of allelic diversity in the human MHC class I-related MIC-A gene. Immunogenetics. 1999;49(7–8):605–12.

217. Komatsu-Wakui M, Tokunaga K, Ishikawa Y, Kashiwase K, Moriyama S, Tsuchiya N, et al. MIC-A polymorphism in Japanese and a MIC-A-MIC-B null haplotype. Immunogenetics. 1999;49(7–8):620–8.

218. Pyo CW, Hur SS, Kim YK, Choi HB, Kim TY, Kim TG. Distribution of MICA alleles and haplotypes associated with HLA in the Korean population. Hum Immunol. 2003;64(3):378–84.

219. Fernández-Messina L, Reyburn HT, Valés-Gómez M. Human NKG2D-ligands: Cell biology strategies to ensure immune recognition. Front Immunol. 2012;3(Sep).

220. Seidel E, Le VTK, Bar-On Y, Tsukerman P, Enk J, Yamin R, et al. Dynamic Co-evolution of Host and Pathogen: HCMV Downregulates the Prevalent Allele MICA*008 to Escape Elimination by NK Cells. Cell Rep. 2015;10(6):968–82.

221. Frigoul A, Lefranc M-P. MICA: Standardized IMGT allele nomenclature, polymorphisms and diseases. Recent Res Devel Hum Genet. 2005;3:95–145.

222. Hernández C, Toledo-Stuardo K, García-González P, Garrido-Tapia M, Kramm K, Rodríguez-Siza JA, et al. Heat-killed Helicobacter pylori upregulates NKG2D ligands expression on gastric adenocarcinoma cells via Toll-like receptor 4. Helicobacter. 2021;26(4):1–14.

223. Montalban-Arques A, Wurm P, Trajanoski S, Schauer S, Kienesberger S, Halwachs B, et al. Propionibacterium acnes overabundance and natural killer group 2 member D system activation in corpus-dominant lymphocytic gastritis. J Pathol. 2016;240(4):425–36.

224. Cutler AF, Havstad S, Ma CK, Blaser MJ, Perez-Perez GI, Schubert TT. Accuracy of invasive and noninvasive tests to diagnose Helicobacter pylori infection. Gastroenterology. 1995;109(1):136–41.

225. Pfaffl MW. A new mathematical model for relative quantification in real-time RT–PCR. Nucleic Acids Res. 2001;29(9):e45.

226. Demaison C, Parsley K, Brouns G, Scherr M, Battmer K, Kinnon C, et al. High-level transduction and gene expression in hematopoietic repopulating cells using a human imunodeficiency virus type 1-based lentiviral vector containing an internal spleen focus forming virus promoter. Hum Gene Ther. 2002 May 1;13(7):803–13.

227. Poppe M, Feller SM, Römer G, Wessler S. Phosphorylation of Helicobacter pylori CagA by c-Abl leads to cell motility. Oncogene. 2007 May 24;26(24):3462–72.

228. Schmitt W, Haas R. Genetic analysis of the Helicobacter pylori vacuoiating cytotoxin: structural similarities with the IgA protease type of exported protein. Mol Microbiol. 1994;12(2):307–19.

229. Zhang C, Wang Y, Zhou Z, Zhang J, Tian Z. Sodium butyrate upregulates expression of NKG2D ligand MICA/B in HeLa and HepG2 cell lines and increases their susceptibility to NK lysis. Cancer Immunol Immunother. 2009;58(8):1275–85.

230. Atherton JC, Cao P, Peek RM, Tummuru MKR, Blaser MJ, Cover TL. Mosaicism in vacuolating cytotoxin alleles of helicobacter pylori. Association of specific vacA types

with cytotoxin production and peptic ulceration. J Biol Chem. 1995;270(30):17771–7.

231. Atherton JC, Cover TL, Twells RJ, Morales MR, Hawkey CJ, Blaser MJ. Simple and accurate PCR-based system for typing vacuolating cytotoxin alleles of Helicobacter pylori. J Clin Microbiol. 1999;37(9):2979–82.

232. Chisholm SA, Teare EL, Patel B, Owen RJ. Determination of Helicobacter pylori vacA allelic types by single-step multiplex PCR. Lett Appl Microbiol. 2002;35(1):42–6.

233. López-Cobo S, Pieper N, Campos-Silva C, García-Cuesta EM, Reyburn HT, Paschen A, et al. Impaired NK cell recognition of vemurafenib-treated melanoma cells is overcome by simultaneous application of histone deacetylase inhibitors. Oncoimmunology. 2018;7(2):1–13.

234. Gonzalez S, Martinez-Borra J, Torre-Alonso JC, Gonzalez-Roces S, Sanchez Del Río J, Rodriguez Pérez A, et al. The MICA-A9 triplet repeat polymorphism in the transmembrane region confers additional susceptibility to the development of psoriatic arthritis and is independent of the association of Cw*0602 in psoriasis. Arthritis Rheum. 1999 May;42(5):1010–6.

235. Raposo G, Nijman HW, Stoorvogel W, Leijendekker R, Harding C V., Melief CJM, et al. B lymphocytes secrete antigen-presenting vesicles. J Exp Med. 1996;183(3):1161–72.

236. Fernández-Messina L, Ashiru O, Boutet P, Agüera-González S, Skepper JN, Reyburn HT, et al. Differential mechanisms of shedding of the glycosylphosphatidylinositol (GPI)-anchored NKG2D ligands. J Biol Chem. 2010;285(12):8543–51.

237. Rodríguez-Rodero S, González S, Rodrigo L, Fernández-Morera JL, Martínez-Borra J, López-Vázquez A, et al. Transcriptional regulation of MICA and MICB: A novel polymorphism in MICB promoter alters transcriptional regulation by Sp1. Eur J Immunol. 2007 Jul;37(7):1938–53.

238. Li Z, Groh V, Strong RK, Spies T. A single amino acid substitution causes loss of expression of a MICA allele. Immunogenetics. 2000;51(3):246–8.

239. Zhang C, Zhang J, Niu J, Zhang J, Tian Z. Interleukin-15 improves cytotoxicity of natural killer cells via up-regulating NKG2D and cytotoxic effector molecule

expression as well as STAT1 and ERK1/2 phosphorylation. Cytokine. 2008;42(1):128–36.

240. Duan S, Guo W, Xu Z, He Y, Liang C, Mo Y, et al. Natural killer group 2D receptor and its ligands in cancer immune escape. Mol Cancer. 2019;18(1):1–14.

241. Allegretti YL, Bondar C, Guzman L, Cueto Rua E, Chopita N, Fuertes M, et al. Broad MICA/B Expression in the Small Bowel Mucosa: A Link between Cellular Stress and Celiac Disease. PLoS One. 2013;8(9).

242. Hüe S, Mention JJ, Monteiro RC, Zhang SL, Cellier C, Schmitz J, et al. A direct role for NKG2D/MICA interaction in villous atrophy during celiac disease. Immunity. 2004;21(3):367–77.

243. Allez M, Tieng V, Nakazawa A, Treton X, Pacault V, Dulphy N, et al. CD4+NKG2D+ T Cells in Crohn's Disease Mediate Inflammatory and Cytotoxic Responses Through MICA Interactions. Gastroenterology. 2007 Jun 16;132(7):2346–58.

244. Poggi A, Benelli R, Venè R, Costa D, Ferrari N, Tosetti F, et al. Human gut-associated natural killer cells in health and disease. Front Immunol. 2019;10(May):1–18.

245. Ma H, Tao W, Zhu S. T lymphocytes in the intestinal mucosa: defense and tolerance. Cell Mol Immunol. 2019;16(3):216–24.

246. Roda-Navarro P, Vales-Gomes M, Chisholm SE, Reyburn HT. Transfer of NKG2D and MICB at the cytotoxic NK cell immune synapse correlates with a reduction in NK cell cytotoxic function. Proc Natl Acad Sci U S A. 2006;103(30):11258–63.

247. Boissel N, Rea D, Tieng V, Dulphy N, Brun M, Cayuela J-M, et al. BCR/ABL Oncogene Directly Controls MHC Class I Chain-Related Molecule A Expression in Chronic Myelogenous Leukemia. J Immunol. 2006;176(8):5108–16.

248. Jimenez-Perez MI, Jave-Suarez LF, Ortiz-Lazareno PC, Bravo-Cuellar A, Gonzalez-Ramella O, Aguilar-Lemarroy A, et al. Cervical cancer cell lines expressing NKG2D-ligands are able to down-modulate the NKG2D receptor on NKL cells with functional implications. BMC Immunol. 2012;13(7).

249. Chen X, Trivedi PP, Ge B, Krzewski K, Strominger JL. Many NK cell receptors

activate ERK2 and JNK1 to trigger microtubule organizing center and granule polarization and cytotoxicity. Proc Natl Acad Sci U S A. 2007;104(15):6329–34.

250. Alter G, Malenfant JM, Altfeld M. CD107a as a functional marker for the identification of natural killer cell activity. J Immunol Methods [Internet]. 2004 Nov [cited 2024 Apr 24];294(1–2):15–22. Available from: https://pubmed.ncbi.nlm.nih.gov/15604012/

251. Chitadze G, Bhat J, Lettau M, Janssen O, Kabelitz D. Generation of Soluble NKG2D Ligands: Proteolytic Cleavage, Exosome Secretion and Functional Implications. Scand J Immunol. 2013;78(2):120–9.

252. Zhang Y, Lazaro AM, Lavingia B, Stastny P. Typing for all known MICA alleles by group-specific PRC and SSOP. Hum Immunol. 2001;62(6):620–31.

253. Tang YT, Huang YY, Zheng L, Qin SH, Xu XP, An TX, et al. Comparison of isolation methods of exosomes and exosomal RNA from cell culture medium and serum. Int J Mol Med. 2017;40(3):834–44.

254. Jeppesen DK, Fenix AM, Franklin JL, Higginbotham JN, Zhang Q, Zimmerman LJ, et al. Reassessment of Exosome Composition. Cell. 2019;177(2):428-445.e18.

255. Gavlovsky P-J, Tonnerre P, Gérard N, Nedellec S, Daman AW, McFarland BJ, et al. Alternative Splice Transcripts for MHC Class I–like MICA Encode Novel NKG2D Ligands with Agonist or Antagonist Functions. J Immunol. 2016;197(3):736–46.

256. Orsini B, Vivas JR, Ottanelli B, Amedei A, Surrenti E, Galli A, et al. Human gastric epithelium produces IL-4 and IL-4δ2 isoform only upon Helicobacter pylori infection. Int J Immunopathol Pharmacol. 2007;20(4):809–18.

257. Sun D, Wang X, Zhang H, Deng L, Zhang Y. MMP9 mediates MICA shedding in human osteosarcomas. Cell Biol Int. 2011;35(6):569–74.

258. Hoy B, Löwer M, Weydig C, Carra G, Tegtmeyer N, Geppert T, et al. Helicobacter pylori HtrA is a new secreted virulence factor that cleaves E-cadherin to disrupt intercellular adhesion. EMBO Rep. 2010;11(10):798–804.

259. McClurg UL, Danjo K, King HO, Scott GB, Robinson PA, Crabtree JE. Epithelial cell ADAM17 activation by Helicobacter pylori: Role of ADAM17 C-terminus and

Threonine-735 phosphorylation. Microbes Infect. 2015;17(3):205–14.

260. Mori N, Sato H, Hayashibara T, Senba M, Geleziunas R, Wada A, et al. Helicobacter pylori induces matrix metalloproteinase-9 through activation of nuclear factor κB. Gastroenterology. 2003;124(4):983–92.

261. Oliveira MJ, Costa AC, Costa AM, Henriques L, Suriano G, Atherton JC, et al. Helicobacter pylori induces gastric epithelial cell invasion in a c-Met and type IV secretion system-dependent manner. J Biol Chem. 2006;281(46):34888–96.

262. McGowan PM, Ryan BM, Hill ADK, McDermott E, O'Higgins N, Duffy MJ. ADAM-17 expression in breast cancer correlates with variables of tumor progression. Clin Cancer Res. 2007;13(8):2335–43.

263. Grötzinger J, Lorenzen I, Düsterhöft S. Molecular insights into the multilayered regulation of ADAM17: The role of the extracellular region. Biochim Biophys Acta - Mol Cell Res. 2017;1864(11):2088–95.

264. Cheng Y, Lin L, Li X, Lu A, Hou C, Wu Q, et al. ADAM10 is involved in the oncogenic process and chemo-resistance of triple-negative breast cancer via regulating Notch1 signaling pathway, CD44 and PrPc. Cancer Cell Int. 2021;21(1).

265. Reyburn H, Esteso G, Ashiru O, Vales-Gomez M. Viral strategies to modulate NKG2D-ligand expression in Human Cytomegalovirus infection. New Horizons Transl Med. 2015;2(6–7):159–66.

266. Doubrovina ES, Doubrovin MM, Vider E, Sisson RB, O'Reilly RJ, Dupont B, et al. Evasion from NK Cell Immunity by MHC Class I Chain-Related Molecules Expressing Colon Adenocarcinoma. J Immunol. 2003;171(12):6891–9.

267. De Andrade LF, En Tay R, Pan D, Luoma AM, Ito Y, Badrinath S, et al. Antibody-mediated inhibition of MICA and MICB shedding promotes NK cell-driven tumor immunity. Science. 2018;359(6383):1537–42.

268. Mandell L, Moran AP, Cocchiarella A, Houghton JM, Taylor N, Fox JG, et al. Intact gram-negative Helicobacter pylori, Helicobacter felis, and Helicobacter hepaticus bacteria activate innate immunity via toll-like receptor 2 but not toll-like receptor 4. Infect Immun. 2004;72(11):6446–54.

269. Palframan SL, Kwok T, Gabriel K. Vacuolating cytotoxin A (VacA), a key toxin for Helicobacter pylori pathogenesis. Front Cell Infect Microbiol. 2012;2(92).

270. Yamamoto K, Fujiyama Y, Andoh A, Bamba T, Okabe H. Oxidative stress increases MICA and MICB gene expression in the human colon carcinoma cell line (CaCo-2). Biochim Biophys Acta - Gen Subj. 2001;1526(1):10–2.

271. Kim JM, Kim JS, Yoo DY, Ko SH, Kim N, Kim H, et al. Stimulation of dendritic cells with Helicobacter pylori vacuolating cytotoxin negatively regulates their maturation via the restoration of E2F1. Clin Exp Immunol. 2011;166(1):34–45.

272. Matsumoto A, Isomoto H, Nakayama M, Hisatsune J, Nishi Y, Nakashima Y, et al. Helicobacter pylori VacA reduces the cellular expression of STAT3 and pro-survival Bcl-2 family proteins, Bcl-2 and Bcl-X L, leading to apoptosis in gastric epithelial cells. Dig Dis Sci. 2011 Apr;56(4):999–1006.

273. Saha A, Backert S, Hammond CE, Gooz M, Smolka AJ. Helicobacter pylori CagL activates ADAM17 to induce repression of the gastric H, K-ATPase alpha subunit. Gastroenterology. 2010;139(1):239–48.

274. Salih HR, Rammensee H-G, Steinle A. Cutting Edge: Down-Regulation of MICA on Human Tumors by Proteolytic Shedding. J Immunol. 2002;169(8):4098–102.

275. Posselt G, Crabtree JE, Wessler S. Proteolysis in helicobacter pylori-induced gastric cancer. Toxins (Basel). 2017;9(4):134.

276. Bernegger S, Vidmar R, Fonovic M, Posselt G, Turk B, Wessler S. Identification of Desmoglein-2 as a novel target of Helicobacter pylori HtrA in epithelial cells. Cell Commun Signal. 2021;19(1):108.

277. Agüera-González S, Boutet P, Reyburn HT, Valés-Gómez M. Brief Residence at the Plasma Membrane of the MHC Class I-Related Chain B Is Due to Clathrin-Mediated Cholesterol-Dependent Endocytosis and Shedding. J Immunol. 2009;182(8):4800–8.

278. Agüera-González S, Gross CC, Fernández-Messina L, Ashiru O, Esteso G, Hang HC, et al. Palmitoylation of MICA, a ligand for NKG2D, mediates its recruitment to membrane microdomains and promotes its shedding. Eur J Immunol. 2011;41(12):3667–76.

279. Brown DA, London E. Functions of lipid rafts in biological membranes. Annu Rev Cell Dev Biol. 1998;14:111–36.

280. Tellier E, Canault M, Rebsomen L, Bonardo B, Juhan-Vague I, Nalbone G, et al. The shedding activity of ADAM17 is sequestered in lipid rafts. Exp Cell Res. 2006;312(20):3969–80.

281. Annabi B, Lachambre M, Bousquet-Gagnon NP, Pagé M, Gingras D, Béliveau R. Localization of membrane-type 1 matrix metalloproteinase in caveolae membrane domains. Biochem J. 2001;353(3):547–53.

282. Matthews V, Schuster B, Schütze S, Bussmeyer I, Ludwig A, Hundhausen C, et al. Cellular cholesterol depletion triggers shedding of the human interleukin-6 receptor by ADAM10 and ADAM17 (TACE). J Biol Chem. 2003;278(40):38829–39.

283. Tsutsumi R, Fukata Y, Fukata M. Discovery of protein-palmitoylating enzymes. Pflugers Arch Eur J Physiol. 2008;456(6):1199–206.

284. Wunder C, Churin Y, Winau F, Warnecke D, Vieth M, Lindner B, et al. Cholesterol glucosylation promotes immune evasion by Helicobacter pylori. Nat Med. 2006;12(9):1030–8.

285. Wang HJ, Cheng WC, Cheng HH, Lai CH, Wang WC. Helicobacter pylori cholesteryl glucosides interfere with host membrane phase and affect type IV secretion system function during infection in AGS cells. Mol Microbiol. 2012;83(1):67–84.

286. Schmidt S, Ullrich E, Bochennek K, Zimmermann SY, Lehrnbecher T. Role of natural killer cells in antibacterial immunity. Expert Rev Hematol. 2016;9(12):1119–27.

287. Lu C-C, Wu T-S, Hsu Y-J, Chang C-J, Lin C-S, Chia J-H, et al. NK cells kill mycobacteria directly by releasing perforin and granulysin. J Leukoc Biol. 2014;96(6):1119–29.

288. Feehan DD, Jamil K, Polyak MJ, Ogbomo H, Hasell M, Li SS, et al. Natural killer cells kill extracellular Pseudomonas aeruginosa using contact-dependent release of granzymes B and H. PLoS Pathog. 2022;18(2):1–28.

289. Ribot JC, Lopes N, Silva-Santos B. γδ T cells in tissue physiology and surveillance.

Nat Rev Immunol. 2021;21(4):221–32.

290. Holdenrieder S, Stieber P, Peterfi A, Nagel D, Steinle A, Salih HR. Soluble MICB in malignant diseases: Analysis of diagnostic significance and correlation with soluble MICA. Cancer Immunol Immunother. 2006;55(12):1584–9.

291. Huang CF, Huang CY, Yeh ML, Wang SC, Chen KY, Ko YM, et al. Genetics Variants and Serum Levels of MHC Class I Chain-related A in Predicting Hepatocellular Carcinoma Development in Chronic Hepatitis C Patients Post Antiviral Treatment. EBioMedicine [Internet]. 2017;15:81–9. Available from: http://dx.doi.org/10.1016/j.ebiom.2016.11.031

292. Zumla A, Rao M, Wallis RS, Kaufmann SHE, Rustomjee R, Mwaba P, et al. Host-directed therapies for infectious diseases: Current status, recent progress, and future prospects. Lancet Infect Dis. 2016 Apr 1;16(4):e47–63.

293. Zhang M. High antibiotic resistance rate: A difficult issue for Helicobacter pylori eradication treatment. World J Gastroenterol. 2015;21(48):13432–7.

294. Vadstrup K, Bendtsen F. Anti-NKG2D mAb: A new treatment for crohn's disease? Int J Mol Sci. 2017;18(9).

295. Toledo-Stuardo K, Ribeiro CH, Canals A, Morales M, Gárate V, Rodríguez-Siza J, et al. Major Histocompatibility Complex Class I-Related Chain A (MICA) Allelic Variants Associate With Susceptibility and Prognosis of Gastric Cancer. Front Immunol. 2021;12(March).

296. Mizuki N, Ota M, Kimura M, Ohno S, Ando H, Katsuyama Y, et al. Triplet repeat polymorphism in the transmembrane region of the MICA gene: A strong association of six GCT repetitions with Behçet disease. Proc Natl Acad Sci U S A. 1997;94(4):1298–303.

297. Zou Y, Bresnahan W, Taylor RT, Stastny P. Effect of Human Cytomegalovirus on Expression of MHC Class I-Related Chains A. J Immunol. 2005;174(5):3098–104.

298. Etemadi A, Safiri S, Sepanlou SG, Ikuta K, Bisignano C, Shakeri R, et al. The global, regional, and national burden of stomach cancer in 195 countries, 1990–2017: a systematic analysis for the Global Burden of Disease study 2017. Lancet Gastroenterol

Hepatol. 2020;5(1):42–54.

299. Wang J, Zhang Q, Liu Y, Han J, Ma X, Luo Y, et al. Association between HLA-IIgene polymorphism and Helicobacter pylori infection in Asian and European population: A meta-analysis. Microb Pathog. 2015;82:15–26.

300. Fernández-Messina L, Ashiru O, Agüera-González S, Reyburn HT, Valés-Gómez M. The human NKG2D ligand ULBP2 can be expressed at the cell surface with or without a GPI anchor and both forms can activate NK cells. J Cell Sci. 2011;124(3):321–7.

301. Kim J, Phan MTT, Kweon SH, Yu HB, Park J, Kim KH, et al. A Flow Cytometry-Based Whole Blood Natural Killer Cell Cytotoxicity Assay Using Overnight Cytokine Activation. Front Immunol. 2020;11(August):1–9.

302. Kandarian F, Sunga GM, Arango-Saenz D, Rossetti M. A flow cytometry-based cytotoxicity assay for the assessment of human NK cell activity. J Vis Exp. 2017;2017(126):1–8.

7. Appendix

Appendix 1: Human samples used in this study

Sample ID	Location	Condition	Immunohistochemistry staining					qPCR		
			MICA/B	CD8	CD45	CD56	NKp46	Proteases, MICA, MICB	CD8A and NK cell Markers	NKG2D
16807/21	Antrum	normal	x	x	x	x	x			
16808/21	Corpus	normal	x	x	x	x				
5536/21	Corpus/Antrum	normal	x	x	x	x	x	x	x	
6093/21	Antrum	normal	x	x	x	x	x			
6094/21	Corpus	normal	x	x	x	x				
72804/21	Antrum	normal	x	x	x	x				
72805/21	Corpus	normal	x	x	x	x				
74033/20	Corpus/Antrum	normal	x	x	x	x	x			
74238/20	Antrum	normal	x	x	x	x	x	x		
74239/20	Corpus	normal	x	x	x	x		x		
74242/20	Antrum	normal	x	x	x	x	x	x	x	
74243/20	Corpus	normal	x	x	x	x		x	x	
74245/20	Antrum	normal	x	x	x	x		x	x	
74246/20	Corpus	normal	x	x	x	x		x	x	
74623/20	Antrum	normal	x	x	x	x	x		x	
74624/20	Corpus	normal	x	x	x	x	x	x		
75238/20	Antrum	normal	x	x	x	x		x	x	
75239/20	Corpus	normal	x	x	x	x	x		x	
75240/20	Antrum	normal	x	x	x	x				
75241/20	Corpus	normal	x	x	x	x		x		
75247/20	Antrum	normal	x	x	x	x		x		
75248/20	Corpus	normal	x	x	x	x			x	
75264/20	Antrum	normal	x	x	x	x		x		
75265/20	Corpus	normal	x	x	x	x		x	x	
87843/21	Antrum	normal				x	x			
87849/21	Antrum	normal				x	x			
102441/14	Corpus/Antrum	HpG	x			x		x	x	
102920/14	Antrum/Corpus	HpG	x		x	x		x	x	
102921/14	Antrum	HpG								
103875/14	Corpus/Antrum	HpG	x		x	x		x	x	
107411/14	Corpus/Antrum	HpG	x		x	x			x	
14063/15	Corpus/Antrum	HpG	x	x	x	x	x	x	x	
43303/21	Stomach	HpG	x	x		x				
43887/14	Corpus/Antrum	HpG	x		x	x	x	x	x	
49126/14	Corpus/Antrum	HpG								
49127/14	Corpus/Fundus	HpG								

5532/21	Corpus/Antrum	HpG	x	x	x	x	x			
5920/21	Corpus	HpG	x	x	x	x				
5921/21	Corpus/Antrum	HpG	x	x	x	x	x			
60077/14	Corpus	HpG	x	x	x	x		x	x	
60078/14	Antrum	HpG	x	x	x	x				
65645/14	Corpus/Antrum	HpG	x	x	x	x		x	x	
69201/14	Corpus/Antrum	HpG	x	x	x	x		x	x	
70594/14	Antrum	HpG	x	x	x	x			x	
70595/14	Corpus	HpG	x	x	x	x	x	x	x	
71377/14	Antrum	HpG	x	x	x	x	x	x	x	
71378/14	Corpus	HpG	x	x	x	x		x	x	
72819/20	Corpus/Antrum	HpG	x	x	x	x				
74026/20	Corpus/Antrum	HpG	x		x	x				
74028/20	Corpus/Antrum	HpG	x	x	x	x	x			
74736/20	Antrum	HpG	x	x	x	x	x			
74737/20	Corpus	HpG	x	x	x	x				
7582/21	Antrum	HpG	x	x	x	x				
7583/21	Corpus	HpG	x	x	x	x				
86316/14	Corpus/Antrum	HpG	x	x	x	x	x	x	x	
86356/14	Corpus/Antrum	HpG	x	x	x	x		x	x	
91197/14	Corpus/Antrum	HpG			x			x	x	
86776/21	Antrum	HpG				x	x			
86752/21	Antrum	HpG				x	x			
20920/21	Antrum	Cancer	x	x	x	x	x	x	x	x
96266/21	Corpus/Antrum	Cancer	x	x	x	x	x	x	x	x
1002/21	Corpus	Cancer	x	x	x	x		x	x	x
85595/21	Corpus/Antrum	Cancer	x	x	x	x	x			
22109/21	Corpus	Cancer	x	x	x	x				
91987/21	Antrum	Cancer + HP	x	x	x	x	x	x	x	x
75510/21	Cardia	Cancer + HP	x	x	x	x		x	x	x
47744/21	Stomach	Cancer	x	x	x			x	x	x
85585/21	Stomach	Cancer						x	x	x
78906/21	Stomach	Cancer	x	x	x			x		x
60274-21	Stomach	Cancer	x	x	x				x	
55132-21	Stomach	Cancer							x	
91358/12	Corpus	HpG		x						
26023/13	Stomach	HpG		x						
20688/13	Corpus	HpG		x						
27499/13	Corpus	HpG		x						
85917/11	Stomach	HpG		x						
27799/13	Corpus	HpG		x						
73775/11	Stomach	HpG		x						
15770/11	Corpus	normal		x						
86250/11	Stomach	normal		x						
16011/11	Corpus	normal		x						
15721/11	Corpus	normal		x						
80342/11	Stomach	normal		x						

17337/13	Corpus	normal		x						
unknown	Stomach	HpG								x
unknown	Stomach	normal								x
unknown	Stomach	normal								x
22318/13	Corpus	normal								x
22687/13	Corpus	normal								x
H15721/11	Corpus	normal								x
H91358/12	Corpus	HpG								x
H15835/11	Corpus	HpG								x
H6463/13	Corpus	HpG								x
22318/13	Corpus	normal								x
22687/13	Corpus	normal								x
H15721/11	Corpus	normal								x
H16543/11	Corpus	normal								x
H16013/11	Corpus	normal								x
H91358/12	Corpus	HpG								x
H15835/11	Corpus	HpG								x
H6463/13	Corpus	HpG								x
H16013/11	Corpus	HpG								x
H15764/11	Corpus	HpG								x

Appendix 2: Oligonucleotide primers for qPCR used in this study

Gene name	Gene symbol	NCBI Reference Sequence (mRNA)	Primer	Sequence (5' to 3')
Glyceraldehyde 3-phosphate dehydrogenase	GAPDH	NM_002046.7; NM_001256799.3; NM_001289745.3; NM_001289746.2; NM_001357943.2	F	CCCTTCATTGACCTCAACTACATG
			R	TGGGATTTCCATTGATGACAAGC
Beta actin	ACTB	NM_001101.5	F	CGTGCTGCTGACCGAGG
			R	ACAGCCTGGATAGCAACGTAC
Killer cell lectin like receptor K1	KLRK1 (also known as NKG2D)	NM_007360.4	F	TCTAGATCAGGAACTGAGGACA
			R	TCTTGATTCTTGTGGATAAAAGCCT
MHC class I polypeptide-related sequence A	MICA	NM_000247.3; NM_001177519.3; NM_001289153.2; NM_001289152.2; NM_001289154.2	F	CACCTGCTACATGGAACACAGC
			R	ACATGGAATGTCTGCCAATGACT
MHC class I polypeptide-related sequence B	MICB	NM_005931.5; NM_001289160.2; NM_001289161.2	F	CACCTGCTACATGGAACACAGC
			R	TATGGAAAGTCTGTCCGTTGACTCT
matrix metallopeptidase 9	MMP9	NM_004994.3	F	GCCACTACTGTGCCTTTGAGTC
			R	CCCTCAGAGAATCGCCAGTACT
matrix metallopeptidase 14	MMP14	NM_004995.4	F	CACTGCCTACGAGAGGAAGG
			R	GAGCAGCATCAATCTTGTCG
ADAM metallopeptidase domain 9	ADAM9	NM_003816.3	F	CTTGCTGCGAAGGAAGTACCTG
			R	CACTCACTGGTTTTTCCTCGGC
ADAM metallopeptidase domain 10	ADAM10	NM_001110.4; NM_001320570.2	F	CTGCCCAGCATCTGACCCTAA
			R	TTGCCATCAGAACTGGCACAC

ADAM metallopeptidase domain 17	ADAM17	NM_003183.6; NM_001382777.1; NM_001382778.1	F	GTGGATGGTAAAAACGAAAGCG
			R	GGCTAGAACCCTAGAGTCAGG
Interleukin 15 (Isoform 1, also known as 48aa(LSP)-IL15)	IL15	NM_000585.5	F	CATGTCTTCATTTTGGGCTGT
			R	GGGTGAACATCACTTTCCGT
Interleukin 15 (Isoform 2, also known as 21aa(SSP)-IL15)	IL15	NM_172175.3	F	TAGATTTGTGCAGCTGTTTCAGT
			R	GGGTGAACATCACTTTCCGT
UL16 binding protein 1	ULBP1	NM_025218.4	F	TGGTTCAGGTCTGGACTTAGG
			R	GCTTCTGCACCTGCTGTCT
UL16 binding protein 2 and retinoic acid early transcript 1L	ULBP2 and RAET1L (also known as ULBP6)	NM_025217.4; NM_130900.3	F	CAAGTGCAGGAGCACCACTCG
			R	CAGATGCCAGGGAGGATGAAGC
UL16 binding protein 3	ULBP3	NM_024518.3	F	CATGTCTGGGCAAATGAATG
			R	CCGTACCTGCTATTCGACTG
Transforming growth factor beta 1	TGFB1	NM_000660.7	F	TCGCCAGAGTGGTTATCTT
			R	TAGTGAACCCGTTGATGTCC
Macrophage migration inhibitory factor	MIF	NM_002415.2	F	GCCCGGACAGGGTCTACA
			R	CTTAGGCGAAGGTGGAGTTGTT
Natural cytotoxicity triggering receptor 1	NCR1 (also known as NKp46)	NM_004829.7	F	GGGACATACCGATGTTTTGG
		NM_001145457.3		
		NM_001145458.3		
		NM_001242356.3		
		NM_001242357.3		

			R	AGGAAAGGTGGGGTCTTCAG
Cluster of Differentiation 8a	CD8A	NM_001768.7	F	CCCTGAGCAACTCCATCATGT
		NM_171827.4		
		NM_001145873.1		
		NM_001382698.1		
			R	GTGGGCTTCGCTGGCA
killer cell lectin like receptor F1	KLRF1 (also known as NKp80)	NM_016523.3	F	TTCAGTGACGTTGCACTGGT
		NM_001366534.1		
			R	CTCCCTGAGAAACCAACAGGA
killer cell lectin like receptor D1	KLRD1 (also known as CD94)	NM_002262.5	F	TGCTTCAGCTTCAAAACACAGA
		NM_007334.3		
		NM_001114396.3		
		NM_001351060.2		
		NM_001351062.2		
		NM_001351063.2		
			R	GCATTTCCATTTGGATTATACGC
killer cell lectin like receptor C2, killer cell lectin like receptor C3 and killer cell lectin like receptor C4	KLRC2, KLRC3 and KLRC4 (also known as NKG2C, NKG2E and NKG2F)	NM_002260.4	F	ACCGAACAGGAAATATTCCAAGTA
		NM_002261.3		
		NM_007333.2		
		NM_013431.2		
			R	AATGCAAATGATTCCTAGGACCT
CD244 molecule	CD244	NM_016382.4	F	TGTTAGCTGGGAAAGCCACA
		NM_001166663.2		
			R	AAGGGTGCCAAGGAACAGT

Note: F, forward primer; R, reverse primer